Protecting the Great Walls of Saqsaywaman by restoring the original Incan drainage infrastructure

A Thesis

Presented to

the faculty of the School of Engineering and Applied Science

University of Virginia

in partial fulfillment
of the requirements for the degree

Master of Science

by

Helena C. Nicholakos

December 2018

APPROVAL SHEET

This Thesis
is submitted in partial fulfillment of the requirements
for the degree of
Master of Science

Author Signature: Helena Nicholas

This Thesis has been read and approved by the examining committee:

Advisor: Richard Miksad

Committee Member: Jon Goodall

Committee Member: Patricia Wiberg

Committee Member: _____

Committee Member: _____

Committee Member: _____

Accepted for the School of Engineering and Applied Science:

Craig H. Benson, School of Engineering and Applied Science

December 2018

ACKNOWLEDGMENTS

Thank you to all members of the 2016 and 2017 University of Virginia research teams:

Dr. Richard W. Miksad, University of Virginia

Gina O'Neil, Civil Engineering Graduate Student, University of Virginia

Zoë Schmitt, Civil Engineering Graduate Student, Virginia Polytechnic Institute and State University

Teresa Jarriel, Civil Engineering Graduate Student, University of Texas at Austin

Edward Tiernan, Civil Engineering Graduate Student, University of Texas at Austin

Aaron Banasiewicz, Undergraduate Student, Fordham University

Jack Roswell, Undergraduate Student, Brown University

Kyle Mavity, Civil Engineering Graduate, University of Virginia

Kathryn Jaquish, Civil Engineering Graduate Student, University of Virginia

Erica Mutschlernielsen, Architecture Graduate Student, University of Virginia

Marina Escámez Ballesta, Spanish Department, University of Virginia

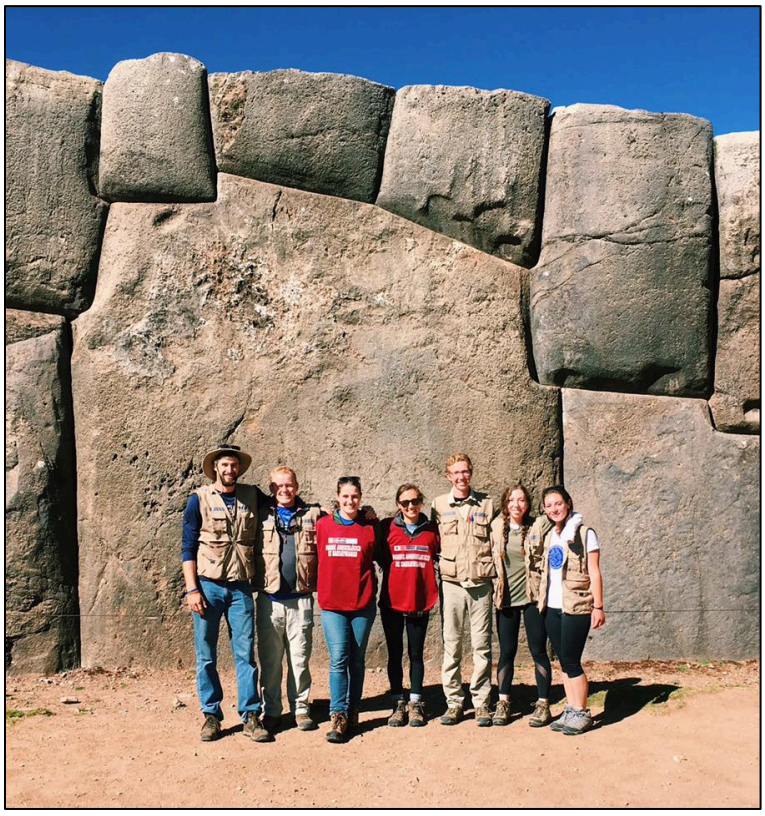

An additional thank you to all of our coworkers, sponsors, and supervisors, without whom, none of this work would be possible:

Sr. Fermin Diaz Angulo, Project Sponsor, Office of Arq. Roberto Zegarra Alfaro, Gobierno Regional Cusco

Dr. Ing. Jorge E. Alva Hurtado, Rector, Universidad Nacional de Ingeniería

Dr. Ing. Leonardo Alcayhuaman, Vice Rector Academico, Universidad Ricardo Palma

Kenneth Wright, Wright Water Engineering, Project Sponsor

Dr. Alexei Vranich, Archeologist

Sara Morrisset, Archeology Graduate Student, University of Cambridge

Carmen Ortiz, Civil Engineering Graduate Researcher, Universidad Nacional de Ingenería, Peru

Álvaro J. Pérez, Civil Engineering Graduate Researcher, Universidad Nacional de Ingenería, Peru

Jorge Soto, Civil Engineering Graduate Researcher, Universidad Nacional de Ingenería, Peru

Lic. Mario Fernando Caller Salas, Project Coordinator, Oficina Central de Cultura UNI, Lima – Peru

Dr. Arminda Gibaja Oviedo, Chief Archeologist, INC at Cusco

Director del Parque Arqueológico de Saqsaywaman

Ing. Jose Antonio Reynoso Palma, Parque de Saqsaywaman

Alejandro Ogato, Trimble

Ben Mallon, Trimble

A special thank you the University of Virginia School of Engineering and Applied Science and Dr. George Cahen for generously contributing funding for this project.

A very special thank you to my advisor and mentor, Dr. Richard W. Miksad. His knowledge and boundless enthusiasm have been invaluable sources of inspiration throughout the duration of this project.

ABSTRACT

The Great Walls of Saqsaywaman, Peru – an ancient Incan archeological site and UNESCO world heritage site – are beginning to show signs of failure after 500 years of remaining structurally sound. Hydrostatic pressure buildup, caused by uncontrolled stormwater runoff, triggered a collapse of one of the walls in 2010. In this thesis, it was hypothesized that restoring the original Incan drainage infrastructure at Saqsaywaman is a potential way to control stormwater runoff in order to protect this cultural icon from further failure. Using field data, investigative engineering analysis, and archeological justification, a possible reconstruction of the original drainage infrastructure was designed. This design consisted of a well-drained terrace system and a surface drainage system of channels and hydraulic drops. Runoff analyses were conducted to validate the efficacy of these possible reconstructions as methods of stormwater control. By implementing the terrace system, it was found that runoff was redirected away from the Great Walls and that surface runoff was reduced by 51% for a hundred-year storm. By implementing the surface drainage system, it was found that most of the remaining 49% of surface runoff from the hundred-year storm was directed out of the site in a controlled manner. In conclusion, the results of the runoff analyses confirm the hypothesis that restoring the site to its original Incan drainage infrastructure is a potential solution to effectively protect the Great Walls from further runoff-induced damage.

The Great Walls of Saqsaywaman (Mavity et al., 2017)

TABLE OF CONTENTS

I. INTRODUCTION ……1

A. A Cultural Treasure in Danger ……...1

B. Restoration is a Solution ……..4

II. HISTORICAL BACKGROUND ……5

A. Saqsaywaman in the Inca Empire (1440 – 1532) ……...6

B. Discovery and Destruction of Saqsaywaman (1532 – 1600) …….9

C. Recent Excavations of Saqsaywaman (1933 – present) ……..10

III. STUDYING THE ENGINEERING OF SAQSAYWAMAN ……13

A. Previous Work ……14

B. Objective of Current Study ……...17

IV. DATA ……...17

A. Above-Ground Data Collection ……18

B. Limits of Above-Ground Data ……..19

C. Sub-Surface Data Collection ……21

D. Limits of Sub-Surface Data ……...22

V. ANALYSIS OF A POTENTIAL ORIGINAL TERRACE SYSTEM ...24

A. Reconstructing a Potential Original Terrace System …….24

1. Methods of Terrace System Reconstruction …….24

2. Filling in Gaps in the Data ……27

3. Proposed Terrace System Reconstruction ……35

B. Topographic Model of the Proposed Terrace System Reconstruction …..37

C. Analysis of Possible Terrace System Drainage Methods ……42

1. Multi-Layered Draining Terrace Backfill ……42
2. Buried Gravel Drainage Network ……45

VI. ANALYSIS OF A POTENTIAL SURFACE DRAINAGE SYSTEM ...47
A. Reconstructing a Potential Original Surface Drainage System ……48
1. Hydraulic Drops ……..48
2. Surface Channels ……54
3. Proposed Surface Drainage System Reconstruction ……...55
B. Hydraulic Analysis of Proposed Surface Drainage System ……58

VII. RUNOFF ANALYSIS ……65
A. Design Storm from Historic Climate Data ……...65
B. Runoff Curve Number Method ……68
1. Land Cover Classification ……..70
2. Hydrologic Soil Type Classification ……..75
3. Assigning Curve Numbers ……76
4. Runoff Curve Number Method Results ……78
C. Mapping Runoff Flow Paths ……78
D. Effect of Proposed Terrace System Drainage Methods on Runoff ……87
E. Effect of Proposed Surface Drainage System on Runoff ……91
F. Discussion of Runoff Analysis ……...95

VIII. CONCLUSIONS ……97

IX. RECOMMENDATIONS ……...98

X. REFERENCES ……100

XI. APPENDICES ……..103

A. R Code Used to Create Transects in Mirador Area ……..103

B. R Code Used to Calculate Storm Statistics ……105

C. NRCS Runoff Curve Number Reference Tables ……...106

List of Figures

Figure 1.1: Overhead view of Saqsaywaman (Mavity et al., 2017) ……...1
Figure 1.2: The three Great Walls of Saqsaywaman (O'Neil, 2016) ……..……2
Figure 1.3: Collapsed section of the third Great Wall (Wildfire et al., 2011) ……....2
Figure 1.4: A megalithic boulder in the Great Walls (Jarriel, 2016) ……..3
Figure 2.1: a) Map of Cusco and Saqsaywaman in 1536 (MacQuarrie, 2007); b) View of the historic district of Cusco from Saqsaywaman in 2017 ……6
Figure 2.2: Digital reconstructions of the towers sector and the north and south terrace profiles at Saqsaywaman (Mar & Beltran-Caballero, 2014) ……..……7
Figure 2.3: Three-dimensional digital reconstruction of the towers sector at Saqsaywaman (Mar & Beltran-Caballero, 2014) ……..……8
Figure 2.4: Incan stones used in colonial buildings in Cusco in: a) 1906 (MacQuarrie, 2007); b) 2016 (Mavity et al., 2017) ……9
Figure 2.5: Unexcavated Saqsaywaman in 1930 (Bauer, 2004) ……...11
Figure 2.6: Saqsaywaman in 1956 (Lohr, 2014) ……...11
Figure 2.7: Saqsaywaman in 2002 (Lohr, 2014) ……...12
Figure 2.8: Saqsaywaman in 2011 (Lohr, 2014) ……...12
Figure 2.9: Impermeable clay cover above the third wall (Miksad) ……13
Figure 3.1: Physical evidence of damage to the third Great Wall due to hydrostatic pressure build-up: a) Support structures needed for bulging walls; b) Separation of stones; c) Vertical shearing (Miksad) ……15
Figure 3.2: Examples of drainage ports in the second Great Wall (Miksad) ……15
Figure 3.3: a) Runoff patterns on Saqsaywaman's 2013 topography; b) Runoff patterns after implenting the terrace system proposed by Gasparini & Margolies (Lohr, 2014) ….16
Figure 4.1: All topographic data points collected at Saqsaywaman between 2014 and 2017 …..18
Figure 4.2: Visible Structural Remains at Saqsaywaman ……19
Figure 4.3: Examples of terrace walls missing several stones at Saqsaywaman ……..20
Figure 4.4: All GPR and SR anomalies discovered at Saqsaywaman ……..20
Figure 4.5: Examples of stray stones near terrace remains at Saqsaywaman ……...23
Figure 5.1: Visible remains and GPR and SR anomalies at Saqsaywaman ……..26
Figure 5.2: Areas at Saqsaywaman lacking clear evidence of terrace remains ……27
Figure 5.3: Northern hillslope of the Mirador area (Miksad) ……...28
Figure 5.4: Potential locations of original terraces on the northern hillslope of the Mirador area, outlined by dashed yellow lines ……..29
Figure 5.5: Locations of transect lines (in blue) in the Mirador area ……...30
Figure 5.6: Mirador area transects, with red lines indicating approximate convex inflection points and blue lines indicating approximate concave inflection points ……...31
Figure 5.7: Convex inflection points on Mirador area transects ……...33
Figure 5.8: Proposed reconstruction of the original Incan terrace system ……35

Figure 5.9: Proposed reconstruction of the original Incan terrace system, overlaying the data used to inform reconstruction ……..36
Figure 5.10: Other possible locations of buried terraces (Alva et al., 2018) ……37
Figure 5.11: Three-dimensional continuous surface model of the proposed terrace system reconstruction ……..……39
Figure 5.12: Three-dimensional continuous surface model of the proposed terrace system reconstruction, with 5-meter contour elevations labeled ……39
Figure 5.13: Three-dimensional continuous surface model of the current topography of Saqsaywaman ……..40
Figure 5.14: Three-dimensional continuous surface model of the current topography of Saqsaywaman, with 5-meter contour elevations labeled ……40
Figure 5.15: Cuts and fills needed to restore the proposed terrace system reconstruction at Saqsaywaman ……..41
Figure 5.16: Typical subsurface drainage strata of terraces at Machu Picchu (Wright & Zegarra, 2000) ……...43
Figure 5.17: Excavation of a buried gravel drain above the third Great Wall (Palma, 2013) …..46
Figure 5.18: Location and direction of flow of buried gravel drain (Miksad) ……..46
Figure 5.19: General directions of elevation decrease at Saqsaywman after implementation of the proposed terrace system ……..47
Figure 6.1: Examples of different types of Incan hydraulic drops: a) Vertical drops at Tipon (Miksad); b) Fountain at Ollantaytambo (Wright et al., 2016); c) Port in the second Great Wall at Saqsaywaman (Miksad) ……...49
Figure 6.2: Drainage port mechanics (Lohr, 2014) ……...49
Figure 6.3: Examples of Incan staircase channels at: a) Machu Picchu (Wright & Zegarra, 2000); b) Suchuna (O'Neil, 2016); c) Ollantaytambo (Miksad); d) Tipon (Wright et al., 2016) ……...50
Figure 6.4: Locations of all known drainage ports (yellow circles) on the Great Walls (blue lines) (Lohr, 2014) ……..51
Figure 6.5: a) Mirador staircase (Miksad); b) South hill staircase ……...52
Figure 6.6: Locations of all known staircases at Saqsaywaman ……...53
Figure 6.7: Examples of channel remains at Saqsaywaman: a) Channel section discovered in (Valcarcel); b) Reconstructed channel in the tower sector (Morrisset, 2016); c) Partially buried channel on a west hill terrace (Morrisset, 2016)……54
Figure 6.8: a,b) Hydraulic drops and orthogonal channels at Tipon; c) Base channels at Tipon (Wright, 2006) ……55
Figure 6.9: Proposed design of a possible original surface drainage system at Saqsaywaman (with proposed terrace system reconstruction for reference) ……..56
Figure 6.10: Proposed design of a possible original surface drainage system at Saqsaywaman ..57
Figure 6.11: Average slopes of surface base channels across the site 61
Figure 6.12: Woodburn Equation diagram (Lohr, 2014) ……..64

Figure 7.1: Annual maximum precipitation occurring over a 24-hour period in January from 1964 to 2010 in the Cusco-Pisac region (UNSAAC) …….66
Figure 7.2: Annual maximum precipitation occurring over a 24-hour period in January from 1964 to 2010 in the Cusco-Pisac region, sorted from smallest to largest precipitation event ..……..……67
Figure 7.3: Annual maximum precipitation occurring over a 24-hour period in January from 1964 to 2010 in the Cusco-Pisac region, sorted by density of occurrence and fitted with a normal distribution (red line) ……...68
Figure 7.4: Current land cover at Saqsaywaman ……..70
Figure 7.5: Large south-facing port in the second Great Wall …….73
Figure 7.6: Representation of archeological remains in the tower sector (Alfaro et al., 2014) …74
Figure 7.7: Proposed original land cover at Saqsaywaman (overlaid with the proposed original terrace system for reference) ……...75
Figure 7.8: Contributing area map of the current site topography ……79
Figure 7.9: Contributing area map of the terraced site topography ……..80
Figure 7.10: Excess precipitation available as runoff during each time step of the design storm for the current land cover ……81
Figure 7.11: Excess precipitation available as runoff during each time step of the design storm for the Inca-era land cover ……..82
Figure 7.12: Runoff flow rates during each step of the design storm for current land cover …...83
Figure 7.13: Runoff flow rates during each step of the design storm for Inca-era land cover 85
Figure 7.14: Excess precipitation absorbed by non-ceremonial terrace backfill ……..88
Figure 7.15: Runoff flow rates during each step of the design storm after maximum drainage through terrace backfill ……...89
Figure 7.16: Contributing area map of the terraced site topography with the surface drainage system channels implemented …….92
Figure 7.17: Runoff flow rates during each step of the design storm after implementing the surface drainage system ……..93

List of Tables

Table 5.1: Hydraulic conductivities of layers in a typical Incan terrace backfill …….43
Table 6.1: Surface base channel dimensions ……61
Table 6.2: Surface orthogonal channel dimensions ……..62
Table 6.3: Staircase channel dimensions ……..63
Table 6.4: Fountain jet horizontal distances (from base channel flow rates and dimensions) ….64
Table 7.1: Design storm modeled from the Cusco-Pisac region's hundred-year storm ……...68
Table 7.2: Current site curve number assignments ……...76
Table 7.3: Inca-era site curve number assignments ……..77
Table 7.4: Excess precipitation on current site …….78
Table 7.5: Excess precipitation on Inca-era site ……...78
Table 11.1a: Runoff curve numbers for urban areas (USDA, 1986) ……..106
Table 11.1b: Runoff curve numbers for cultivated agricultural lands (USDA, 1986) ……...107
Table 11.1c: Runoff curve numbers for other agricultural lands (USDA, 1986) ……...108

I. INTRODUCTION

I.A. A Cultural Treasure In Danger

Saqsaywaman (Figure 1.1), one of the most impressive Incan archeological sites in Peru, has a major problem. The site's most remarkable features – its three megalithic walls (Figure 1.2) – have begun to fail after five centuries of remaining structurally sound. A section of the third Great Wall collapsed in 2010 due to large volumes of uncontrolled stormwater runoff. The runoff created a hydrostatic pressure buildup behind the wall, and the pressure load caused the wall to overturn (Figure 1.3). The runoff had unintentionally been routed towards the third wall by an impermeable clay cover that was placed above it in 2009. This collapse was unexpected because the Great Walls are constructed of massive, tightly fitted boulders (Figure 1.4), some of which are 15 feet tall and weigh over 200 tons (O'Neil, 2016).

Figure 1.1: Overhead view of Saqsaywaman (Mavity et al., 2017)

Figure 1.2: The three Great Walls of Saqsaywaman (O'Neil, 2016)

Figure 1.3: Collapsed section of the third Great Wall (Wildfire et al., 2011)

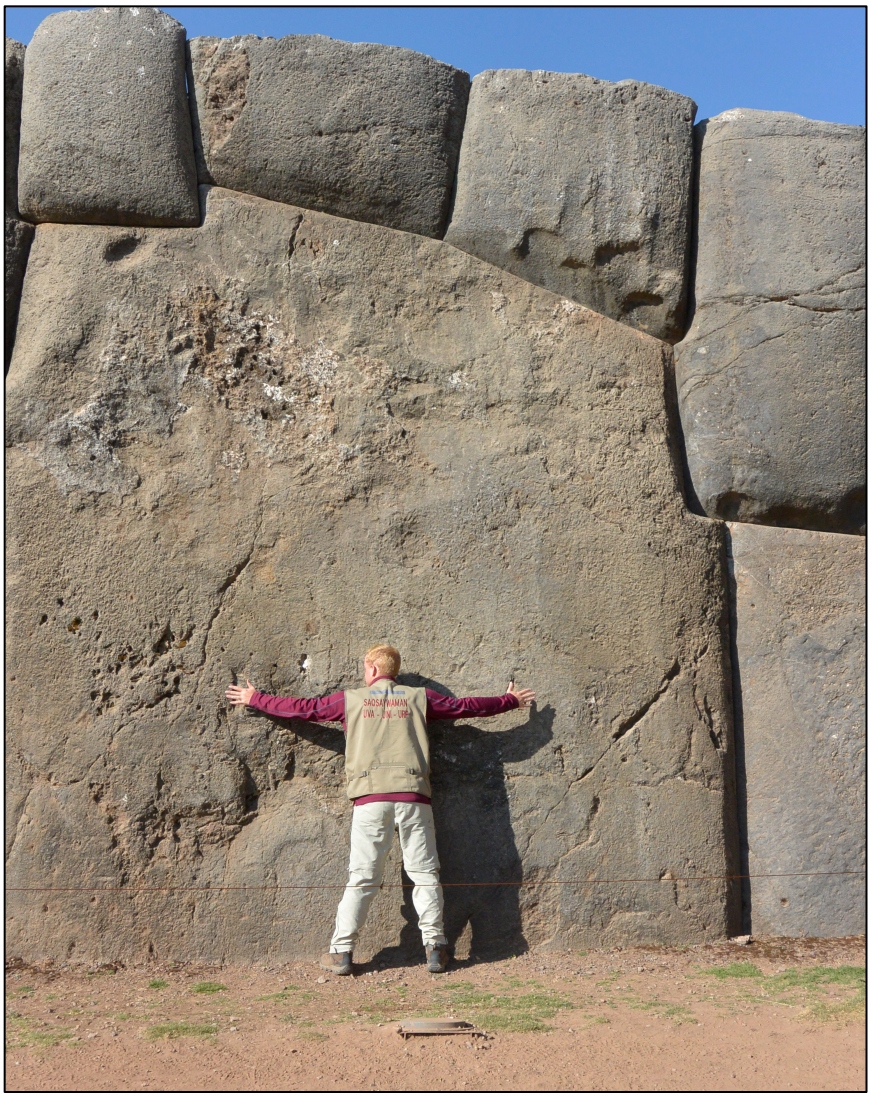

Figure 1.4: A megalithic boulder in the Great Walls (Jarriel, 2016)

Although this collapse was triggered by recent man-made changes in the land cover and topography, it is indicative of a wider problem with the site. Once a marvel of the careful and thorough engineering skills of the Inca, 500 years of damage and abuse have undone their engineering work. Saqsaywaman has not been fully functioning since the early 1500s, and the Great Walls are one of the only original pieces of the site still mostly intact. The Inca were expert civil engineers, and if Saqsaywaman was still operating as they designed it, it is possible that the Great Walls would not be in the danger they are in now.

I.B. Restoration is a Solution

I believe that a potential approach to preventing further damage to the Great Walls is to restore the original Incan drainage infrastructure. Saqsaywaman is a historic cultural icon of Peru and a UNESCO World Heritage site. For this reason, a restoration effort has a responsibility to carefully preserve the archeological authenticity and Incan heritage of the site. This means that the drainage system that is restored should use entirely Incan design techniques. Recently, several half-measures have been implemented in a well-intentioned, but mostly ineffective, attempt to mitigate the runoff flowing towards the Great Walls. These measures include wall bracing structures, thatched roof covers, and ad-hoc clay channels dug above the walls. These are not Incan engineering techniques, and they are also unable to adequately protect the walls. A hydraulic analysis by Wildfire et al. (2011) showed that the ad-hoc clay channels were incapable of diverting the majority of runoff flowing towards the Great Walls, and in some places, even made the problem worse than it was before the channels were implemented. The wall bracing structures and thatched roof cover are preventative at best, and they do not address the true problem of uncontrolled stormwater runoff.

Restoring the original Incan drainage infrastructure at Saqsaywaman is a potential solution that is both authentically Incan in design and capable of controlling stormwater runoff to protect the Great Walls. A major problem with this potential solution, however, is that the exact design of the original drainage infrastructure at Saqsaywaman is largely a mystery. Much of the Incan engineering work has endured extensive destruction and decay since the fall of the Incan Empire. Today, the site contains mostly foundations and scattered remains of its original structures, providing a difficult puzzle for archeologists and engineers alike.

In this study, I will use archeological clues and engineering analysis to determine a possible reconstruction of the original drainage infrastructure at Saqsaywaman for the purpose of protecting the Great Walls. I will show that the infrastructure could have consisted of the following two major pieces: a well-drained system of terraces and a surface drainage system of channels and hydraulic drops. I will then use runoff analyses to evaluate whether this infrastructure design would adequately control stormwater runoff to protect the Great Walls if it were restored at Saqsaywaman. I hope that this study will help display the urgent necessity and feasibility of a full-site restoration of Saqsaywaman, and that the National Institute of Culture of Peru (INC) and the Director of the Archaeological Park of Saqsaywaman will consider initiating a restoration of the original drainage infrastructure.

II. HISTORICAL BACKGROUND

To understand the work needed to restore Saqsaywaman, it is necessary to have a mental image of Saqsaywaman as it was during the Incan Empire, as well as an understanding of the events that brought it to its current state of ruination. Following the end of the Inca Empire Saqsaywaman faced conquest, destruction, erosion, earthquakes, archeological digs, partial reconstructions, and the tourism industry, all of which have drastically altered the site in various ways. The impacts of these alterations are one of the largest obstacles confronting our attempt to reconstruct the original drainage system. When visiting Saqsaywaman in 2018, it is difficult to determine what was originally present at the site that is now gone and what is now present at the site that was originally never there. To help partially illuminate some answers to this dilemma, I will describe the different stages of the life of Saqsaywaman from the Inca era to the 21st century.

II.A. Saqsaywaman in the Inca Empire (1440 – 1532)

Saqsaywaman was built on a hilltop overlooking the city of Cusco (Figure 2.1), the capital of the Incan Empire. It is believed that construction of Saqsaywaman was begun sometime after 1440 by Incan Emperor Pachacuti and was completed in the early 16th century (Dean, 1998). The exact purpose of Saqsaywaman is unknown, but several anthropologists maintain that it was a military fortress as well as a location for religious ceremonies (Dean, 1998; Mar & Beltran-Caballero, 2014; Morrisset, 2016). Although the site now exists as a ruin, we have some idea of what it looked like during the Inca era from the chronicles of Garcilaso de la Vega, who was born in Peru in 1539. As the son of a Spanish nobleman and an Inca princess, de la Vega was in a unique position to learn about the details of Saqsaywaman from his Incan relatives, and he wrote about it in a lengthy chronicle that was published in 1609 (de la Vega, 1966).

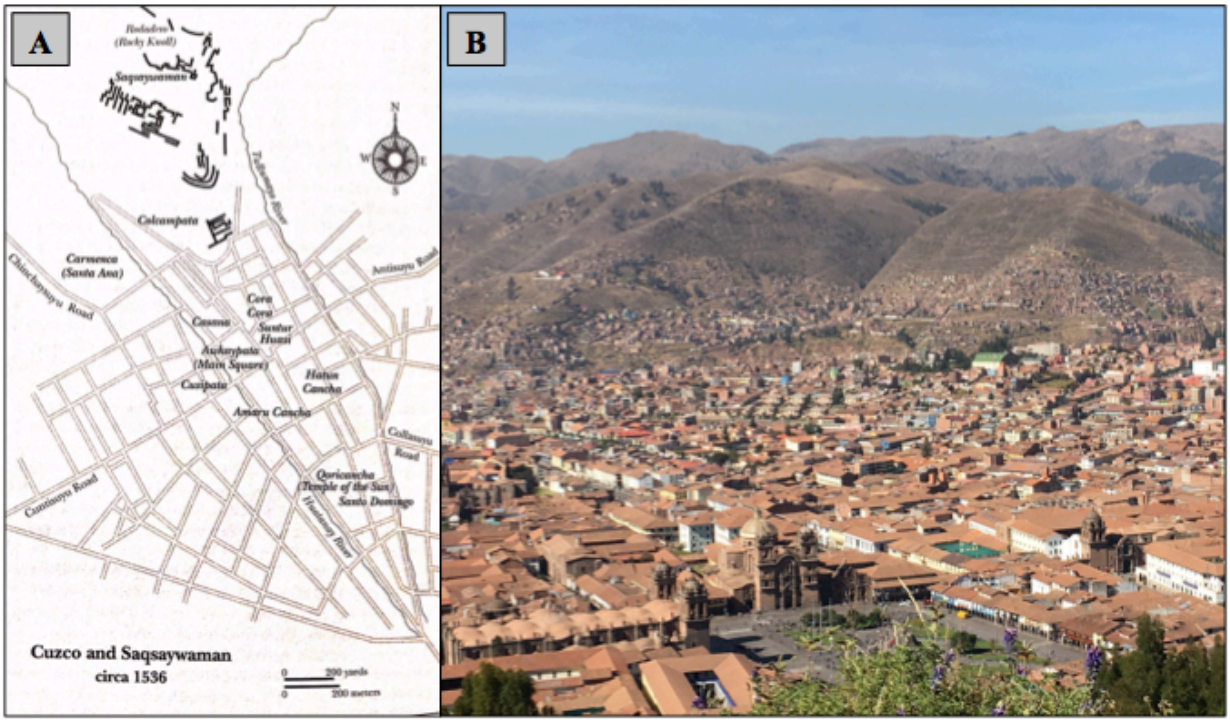

Figure 2.1: a) Map of Cusco and Saqsaywaman in 1536 (MacQuarrie, 2007); b) View of the historic district of Cusco from Saqsaywaman in 2017

In his chronicle, de la Vega described Saqsaywaman as "the greatest and most splendid building erected to show the power and majesty of the Incas." He wrote that it had three "circumvallations," or defensive ramparts, circling the site. These ramparts were constructed of stones of differing sizes, many of which were so large that it seemed impossible that men could have moved them. He also described a "thick freestone wall" on the south hill that was built as the main line of defense against invaders from below.

In describing the area inside of Saqsaywaman's walls, he said "there is a long narrow space containing three strong towers arranged in an elongated triangle…. The chief of these towers, which was in the middle, was called [Muyuqmarka] 'the round fortress'… Within it was a spring with a copious supply of excellent water brought underground for a long distance." (de la Vega, 1966) He explained that this tower was covered in luxurious gold and silver plating, and that only Inca kings were allowed inside of it. The other two towers were square and "contained many rooms for the soldiers on guard." In Figures 2.2 and 2.3 below, Mar & Beltran-Caballero (2014) attempted to bring to life some of the images that de la Vega described at Saqsaywaman.

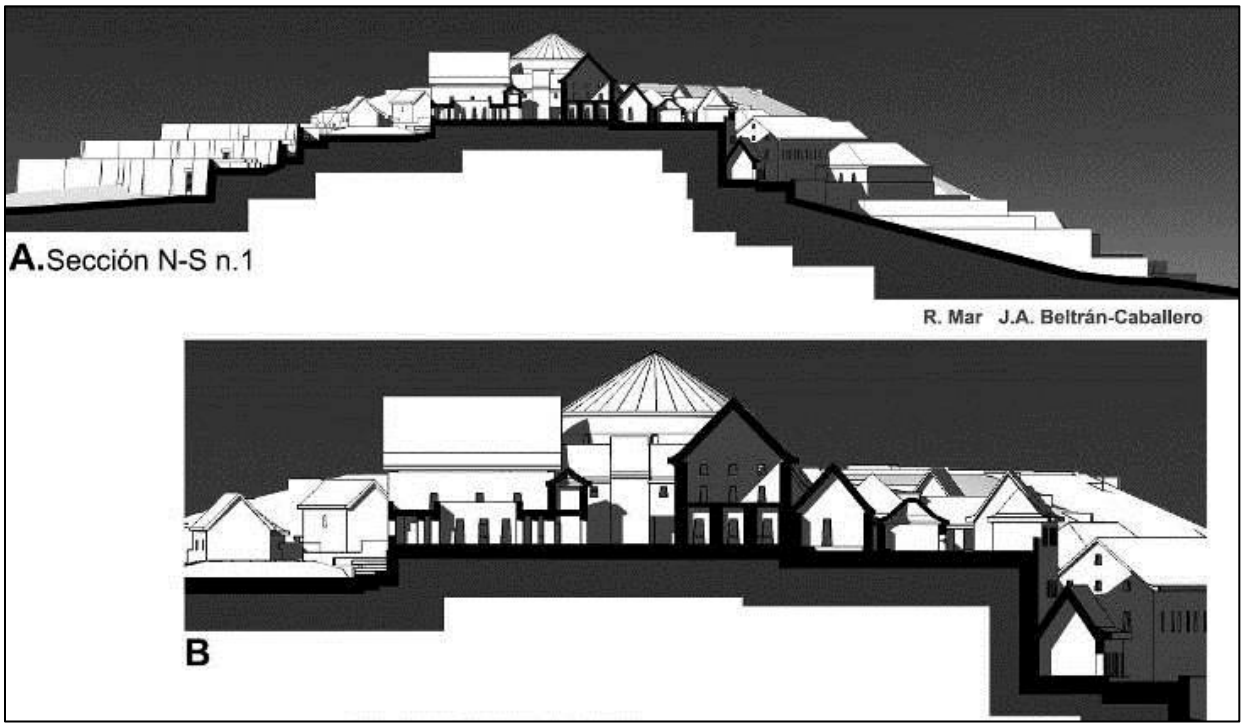

Figure 2.2: Digital reconstructions of the towers sector and the north and south terrace profiles at Saqsaywaman (Mar & Beltran-Caballero, 2014)

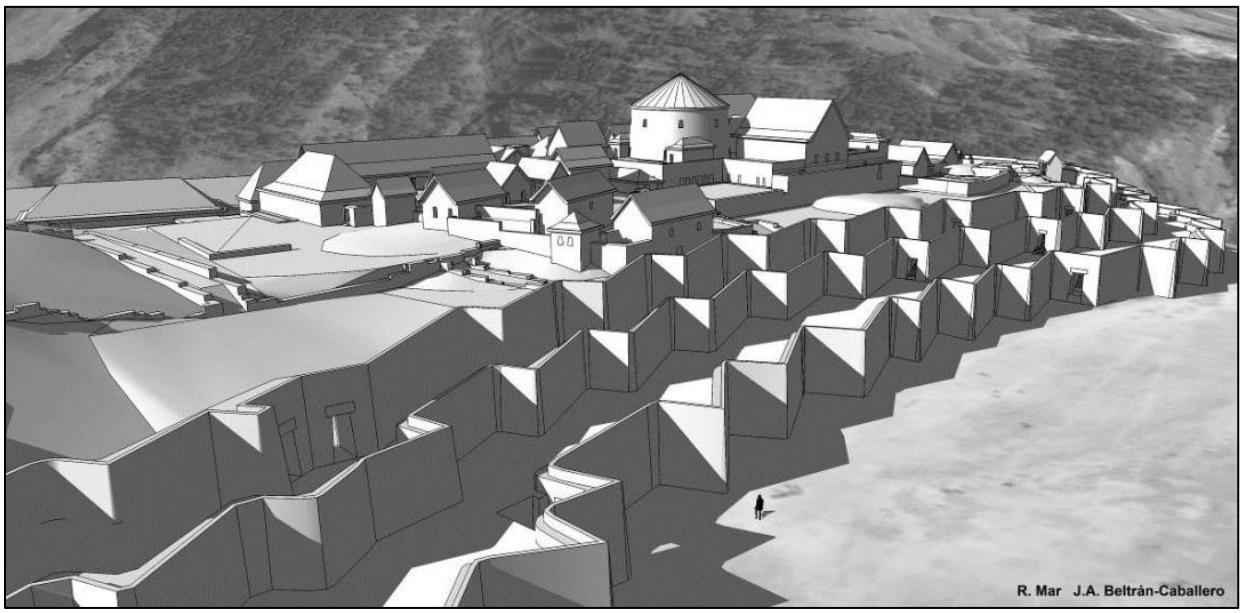

Figure 2.3: Three-dimensional digital reconstruction of the towers sector at Saqsaywaman (Mar & Beltran-Caballero, 2014)

II.B. Discovery and Destruction of Saqsaywaman (1532 – 1600)

Spanish conquistadors invaded the Inca Empire in 1532, and had gained unquestionable control of it by 1572 (MacQuarrie, 2007). During their colonial control of Cusco, the Spanish used Saqsaywaman as a de facto quarry to rebuild the city in a European architectural style (Dean, 1998). Incan stones from Saqsaywaman are still visible in buildings throughout the historic district of Cusco today (Figure 2.4), but no original Incan structures remain in the city. The conquistadors destroyed all Incan buildings because they were considered symbols of the Incas' "pagan" religion, and were therefore threats to Spanish power and the Catholic society they were trying to establish (Morrisset, 2016). For this reason, the destruction of Saqsaywaman served two purposes for the Spanish invaders – a convenient source of readily available construction materials and a means of deconstructing the most prominent symbol of Inca power in Cusco. "[Saqsaywaman] – as a ruin – thus came to symbolize Christian triumph in the Andes."

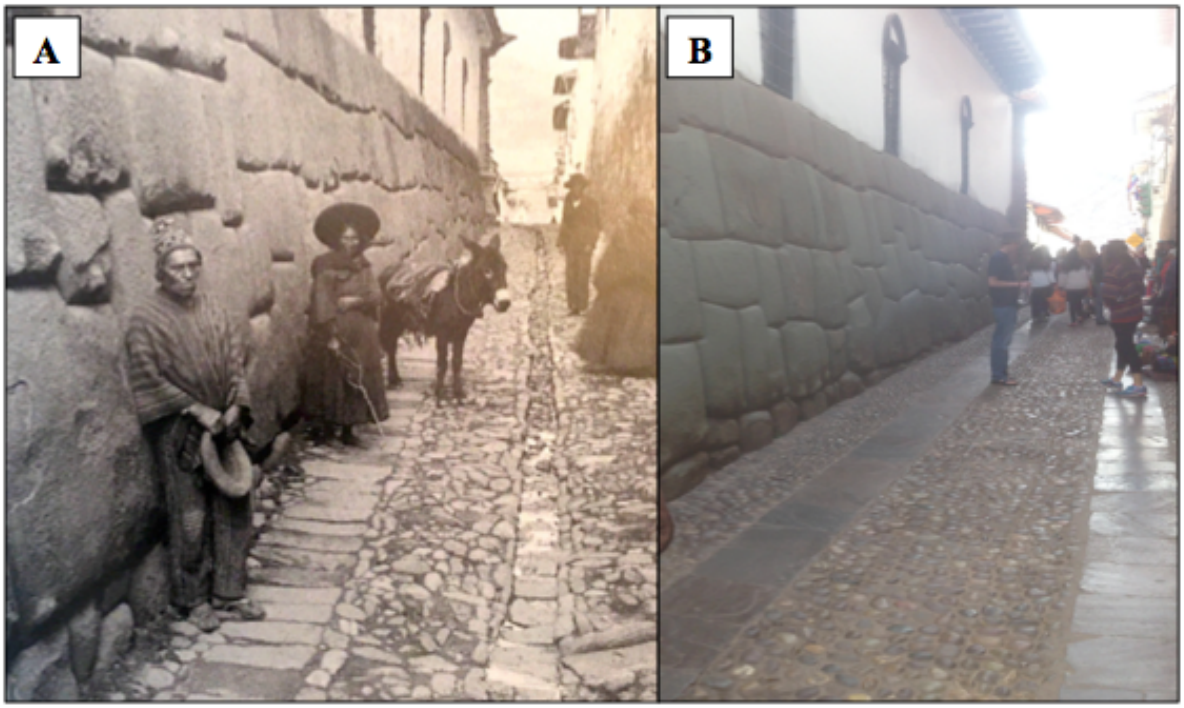

Figure 2.4: Incan stones used in colonial buildings in Cusco in: a) 1906 (MacQuarrie, 2007); b) 2016 (Mavity et al., 2017)

(Dean, 1998) While dismantling Saqsaywaman, all small and easily moveable stones were rolled down the south hill of the site to the city below (Mar & Beltran-Caballero, 2014). All that remained afterwards were the Great Walls and the foundations of the rest of the site (Dean, 1998), which were either too large or too labor-intensive to remove.

II.C. Recent Excavations of Saqsaywaman (1933 – present)

For over three centuries after the conquistadors finished their ruination of Saqsaywaman, the site sat untended and mostly ignored. During these years, erosion and natural processes, including a 7.7 magnitude earthquake in 1650, caused soil to settle over the structural foundations left by the Spanish. The site was littered with debris and stray stones that had been scattered during the dismantling of structures, and until the early 1900s, Saqsaywaman continued to be used as a causal quarry by Cusco residents (Valcarcel, 1934).

The first major excavation of Saqsaywaman was conducted in 1933 by Luis Valcarcel, a preeminent Peruvian anthropologist. When Valcarcel reached Saqsaywaman, the site was mostly covered in soil and debris (Figure 2.5). After his excavations, the tower sector foundations became visible and the west hill terraces were uncovered (Figure 2.6). In the 21st century, the tower sector was further excavated, and archeologists sealed these new excavations with protective cement coverings. Figures 2.7 and 2.8 show Google earth images of the site in 2002 and 2011, respectively. Comparing these images side by side, one can see that the cement covers appear in the tower sector between 2002 and 2011.

In the 1930s, Valcarcel also applied a ‘protective pavement’ to some of his excavations. Using this pavement, he sealed the tops of ramparts on the Great Walls so that he could continue excavating during the rainy season without destabilizing the walls (Valcarcel, 1934). The recent

Figure 2.5: Unexcavated Saqsaywaman in 1930 (Bauer, 2004)

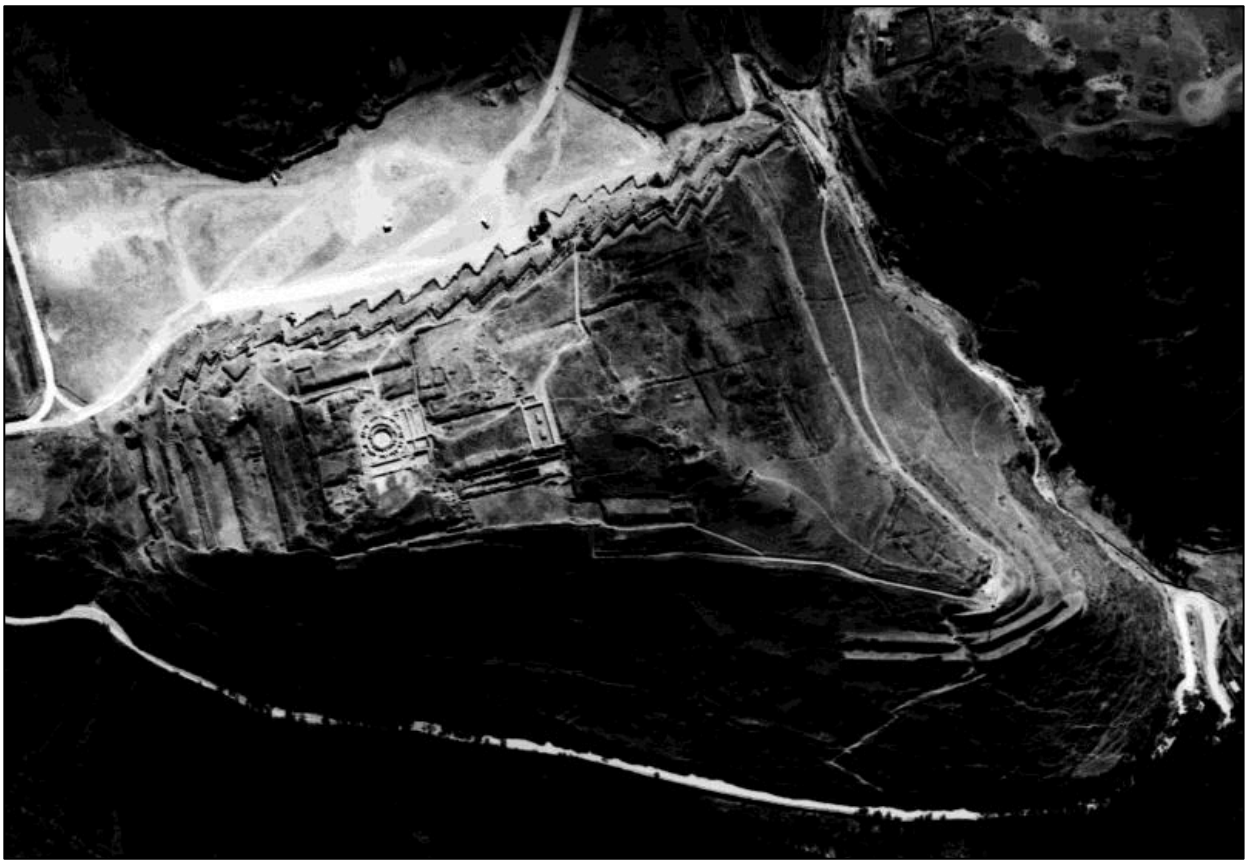

Figure 2.6: Saqsaywaman in 1956 (Lohr, 2014)

Figure 2.7: Saqsaywaman in 2002 (Lohr, 2014)

Figure 2.8: Saqsaywaman in 2011 (Lohr, 2014)

cement covers in the tower sector were put in place for similar reasons – to protect the foundational remains from eroded soil by simply covering the soil with an impermeable pavement. Unfortunately, the new cement covers had the unintended consequence of changing the runoff patterns in the northern area of the site. In particular, the sloped cement cover directly above the center of the Great Walls (Figure 2.9) redirected large volumes of runoff towards the third Great Wall. This eventually caused the collapse of a large section of the third wall after it was no longer able to bear the pressure load from the runoff.

Figure 2.9: Impermeable clay cover above the third wall (Miksad)

III. STUDYING THE ENGINEERING OF SAQSAYWAMAN

Preceding this thesis, there have been several years of work studying the problem of structural failure of the Great Walls and uncontrolled runoff at Saqsaywaman. The third wall's collapse in 2010 inspired a research team from the University of Virginia (UVa), led by Dr. Richard Miksad, to visit Saqsaywaman. Their goal was to determine the cause of the wall's

failure using engineering analysis. Since then, UVa research teams have continued to study Saqsaywaman, in conjunction with research teams from the Universidad Nacional de Ingeniería de Peru and the Universidad de Ricardo Palma, to learn more about the ancient engineering methods implemented in the original Incan design of Saqsaywaman. I was a member of the 2016 and 2017 research teams from UVa. The work preceding this study will be summarized in the following section. Then, the objectives of this study will be discussed.

III.A. Previous Work

In a 2011 study by Wildfire et al., it was determined that the collapse of the third Great Wall was caused by a build-up of hydrostatic pressure behind the wall. This hydrostatic pressure was the result of the introduction of an impermeable cement cover just above the third wall, which had the unintended effect of drastically increasing the volume of stormwater runoff directed towards the wall.

After centuries of the Great Walls remaining relatively stable and unchanged, this unexpected collapse led to the conclusion that the walls were not originally designed to handle large quantities of runoff. This conclusion was further substantiated by examining the choice of backfill materials used in the construction of the third wall (Wildfire et al., 2011). The backfill consisted of a mostly impervious soil and rock mixture, which did not allow water to drain effectively behind the wall. As a result, this backfill trapped any water that drained into it, causing hydrostatic pressure to build up behind the wall during storm events. When the hydrostatic pressure load became too large during the storm in 2010, the structural stability of the walls became compromised and prone to failure. Figure 3.1 below shows evidence of hydrostatic

damage in multiple locations on the third wall. The wall is bulging out in many places, putting it in danger of collapsing in those areas as well.

Besides lacking a porous backfill, the third wall also lacked any drainage ports, which would have provided an outlet for water to flow through after it percolated through the backfill. Porous backfills and drainage ports (Figure 3.2) were both used in the first and second Great Walls, as well as in walls at other Incan sites (Wildfire et al., 2011). The lack of these two characteristics in the third wall justifies the conclusion that it was never designed to handle large quantities of water. If the third wall was not designed to drain water, then the Incan engineers must have utilized some other form of drainage technology to control runoff in that area.

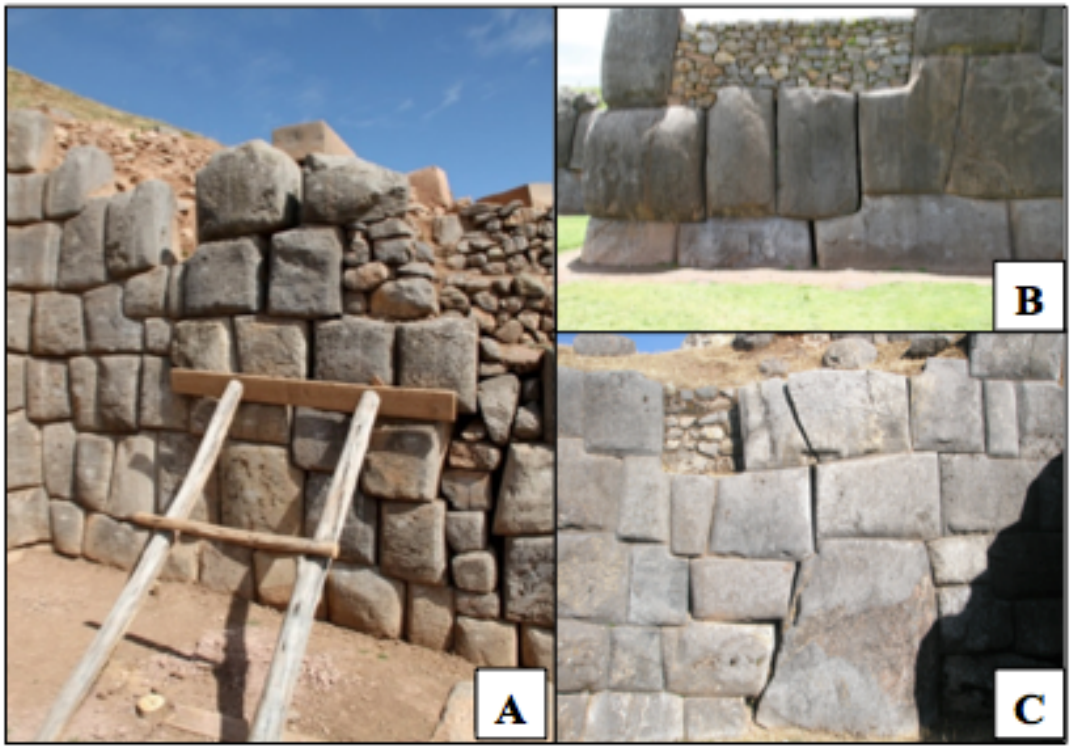

Figure 3.1: Physical evidence of damage to the third Great Wall due to hydrostatic pressure build-up: a) Support structures needed for bulging walls; b) Separation of stones; c) Vertical shearing (Miksad)

Figure 3.2: Examples of drainage ports in the second Great Wall (Miksad)

In a 2014 study, Lohr began to explore other drainage methods that the Incan engineers may have used. He concluded that Saqsaywaman probably had a master drainage system that consisted of multiple different drainage technologies, including terraces, ports, channels, and subsurface gravel drains. There are some remains of all of these drainage methods at Saqsaywaman, but particularly prominent are remains of terrace walls. In a topographic study of Saqsaywaman, Lohr showed that if the site were terraced, runoff behind the third wall would be shed laterally to the east and west instead of straight towards the wall (Figure 3.3). This analysis

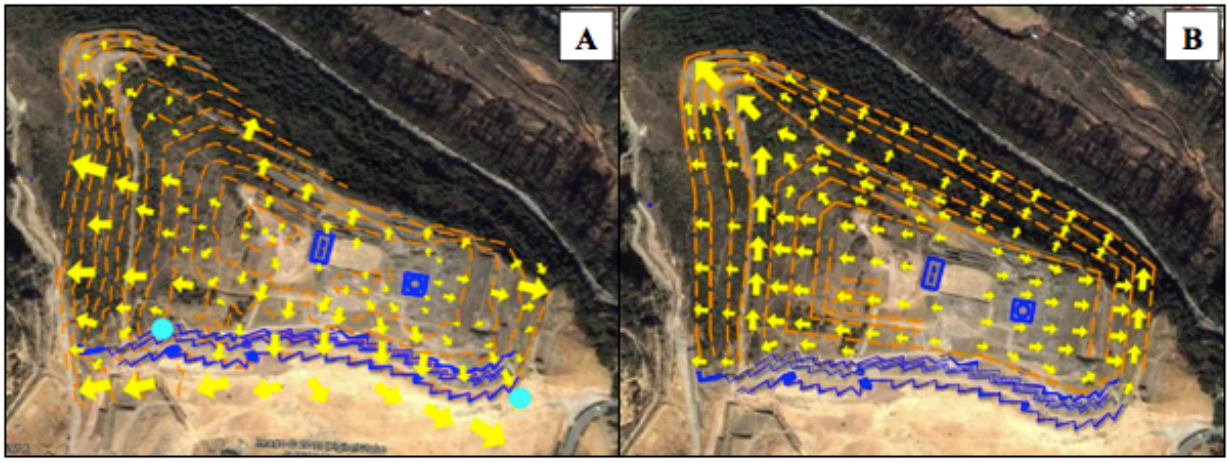

Figure 3.3: a) Runoff patterns on Saqsaywaman's 2013 topography; b) Runoff patterns after implenting the terrace system proposed by Gasparini & Margolies (Lohr, 2014)

was based off of a theoretical terrace model suggested by historians Gasparini and Margolies (1980).

Studies by O'Neil (2016), Jarriel (2016), and Mavity et al. (2017) expanded on Lohr's theory of a full-site terrace system by attempting to locate and model the original Incan terraces at Saqsaywaman. During field studies in summers 2015, 2016, and 2017, extensive surveying was conducted to locate both visible terrace remains and evidence of subsurface terrace remains on site. O'Neil (2016), Jarriel (2016), and Mavity et al. (2017) all began piecing together the original terrace system, but none were able to create a full-site terrace system model.

III.B. Objectives of Current Study

This thesis follows and builds upon the summer 2017 field study. I hypothesized that restoring the original Incan drainage infrastructure at Saqsaywaman is a potential way to control stormwater runoff in order to protect the site from further failure. To reconstruct the original the drainage infrastructure, first, a possible full-site model of the original Incan terrace system will be reconstructed using data collected in field studies. Then, a possible surface drainage system will be reconstructed using engineering analysis and archeological and historical justification. These proposed reconstructions will then be validated using runoff analyses to check whether they are able to control stormwater runoff and protect the Great Walls.

IV. DATA

The major body of empirical data used in this study was collected by UVa research teams over the course of multiple field studies at Saqsaywaman between 2014 and 2017. The data collected was comprised of two main types of information: above-ground data and sub-surface

data. The above-ground data consisted of: 1. Visible evidence of terrace wall remains and other relevant structural remains on site, and 2. Topographic data points used to model the three-dimensional surface of present-day Saqsaywaman. An accurate model of the site's current topography was necessary for the runoff analysis conducted later in this study. The sub-surface data consisted of potential locations of buried terrace remains.

IV.A. Above-Ground Data Collection

Above-ground data was collected using a Topcon GTS-240 NW Series electronic Total Station in 2014 and 2015 (O'Neil, 2016), and a survey-grade Trimble GPS system in 2016 and 2017. These data were collected in the form of northing, easting, and elevation ([N, E, Z]) points. Around 3,600 [N, E, Z] points were collected overall between 2014 and 2017 (Figure 4.1), with a

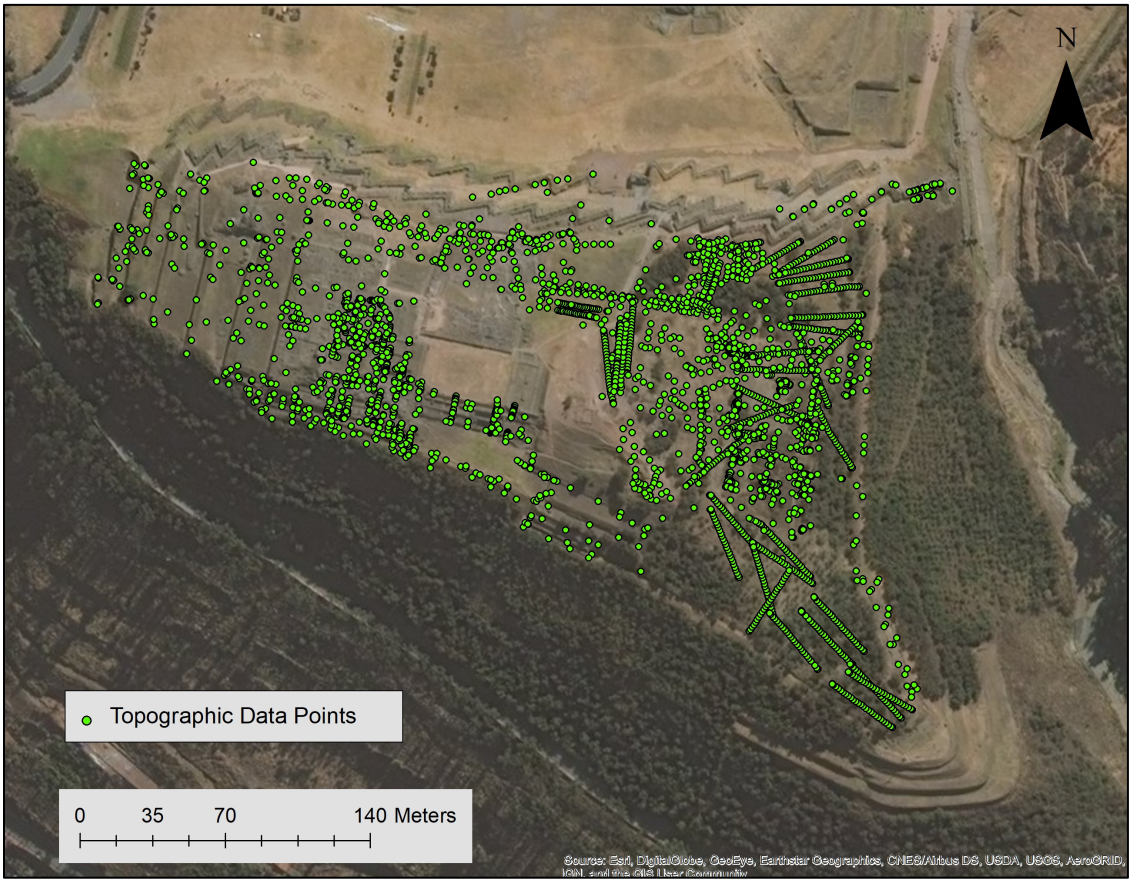

Figure 4.1: All topographic data points collected at Saqsaywaman between 2014 and 2017

focus on collecting points to map the site topography in earlier studies and a focus on collecting points to catalogue visible structural remains in more recent studies. Figure 4.2 shows all visible structural remains at Saqsaywaman, which were digitally mapped using ArcGIS software from the Environmental Systems Research Institute (ESRI). The mapping and modeling of the current site topography will be discussed in detail in Section V.B.

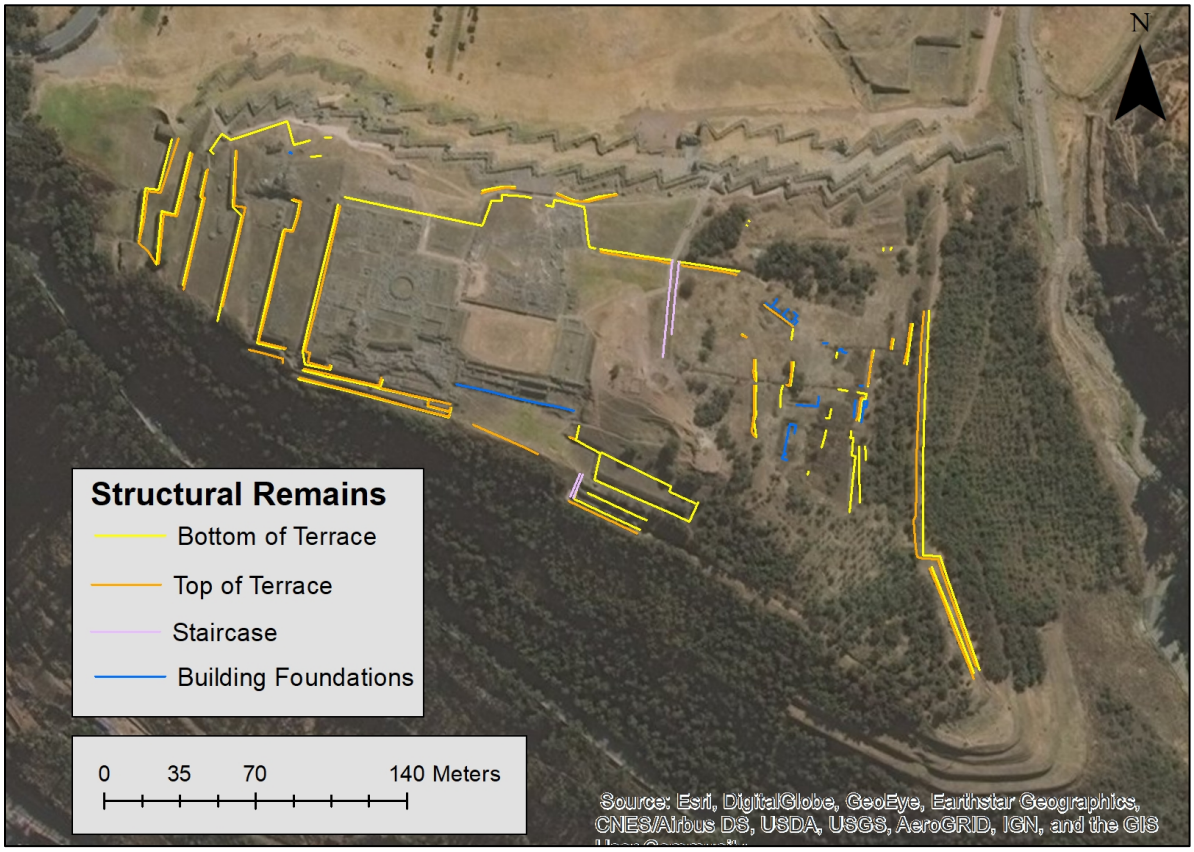

Figure 4.2: Visible Structural Remains at Saqsaywaman

IV.B. Limits of Above-Ground Data

As was discussed in Section II, Saqsaywaman was used as a quarry in the years following the Spanish conquest of the site. All stones that could be easily moved were taken away for use in the rebuilding of the city of Cusco. As a result, the only structural remains left at Saqsaywaman were stones that could *not* be easily moved, which left stones that were either too

large or too tightly packed into the ground to be moved. For this reason, most of the terrace wall remains on site today are missing many of their top-layer stones (Figure 4.3), because they were the easiest stones to pick up and remove.

Without the top layers of stones, it is impossible to know how tall most of the terraces were originally. Lacking the original terrace wall heights, the next best estimate of the original terrace heights was the elevation of the bottoms of the terrace walls behind them. While this provided a better height estimate than trying to guess which, if any, of the remaining top-most stones were originally in the top-most layer of a terrace wall, it was still not a definite indication of the terrace wall heights. The terrace wall bottoms were designed to extend underground to provide extra structural support. However, without the ability to excavate, it was difficult to know whether the junction of a wall and the ground was where the terrace bottom was originally, or if the current height of the terrace platform was a result of erosion or incomplete excavation.

Figure 4.3: Examples of terrace walls missing several stones at Saqsaywaman

IV.C. Sub-Surface Data Collection

The majority of the sub-surface data collection was carried out during the 2015 and 2016 summer field studies. Sub-surface data collection was necessary because several areas on the site remain unexcavated, and based on the theory that a full-site terrace system originally existed, there would have originally been more terrace walls than those that are visible today. From this, we inferred that the rest of the terrace wall remains are probably still buried in unexcavated areas of the site. The goal of the sub-surface data collection was to locate those remains. Saqsaywaman is a working tourist attraction in Cusco, so we were unable to request excavations during our field studies. In lieu of excavating, Ground Penetrating Radar (GPR) and Seismic Refraction (SR) were used to collect sub-surface data without moving any soil.

GPR data was collected using a Quantum Imager Ground Penetrating Radar and SR data was collected using a SmartSeis ST Geometrics model seismograph. GPR collects data by sending radar waves below ground, which are reflected back up to the surface when they reach a high-density material, such as bedrock or stone. The amount of time it takes for a radar wave to resurface provides data about how deep the dense material is underground. At Saqsaywaman, when the time of wave return was much shorter in a certain location than it was in adjacent areas, we estimated that there were stone structural remains buried in that location (Mavity et al., 2017). Similarly, SR collects data by sending compressional waves underground, then by measuring the amount of time it takes for the wave to resurface at a known distance away from the starting point (ASTM International, 2011).

Figure 4.4 shows the location of all GPR and SR “anomalies” detected during the 2015 and 2016 summer field studies. These “anomalies” pinpoint locations where there is a high likelihood of a subsurface structural remnant. The mechanics of GPR and SR, and the use of

GPR and SR in past Saqsaywaman field studies, are explained in greater detail in Jarriel, 2016, O'Neil, 2016, and Mavity et al., 2017.

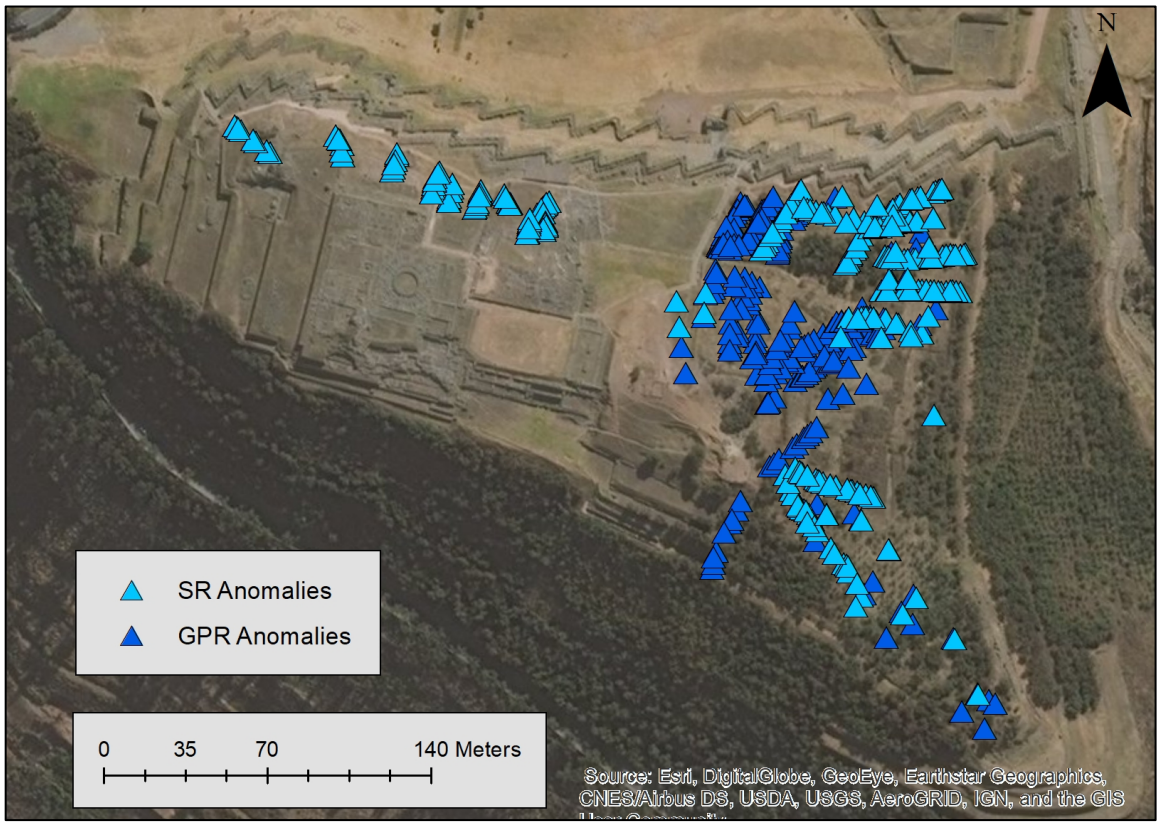

Figure 4.4: All GPR and SR anomalies discovered at Saqsaywaman

IV.D. Limits of Sub-Surface Data

It was impossible to know exactly what objects the GPR and SR anomalies were locating without digging into the ground to check. Without the ability to excavate, all that was known for certain was that each anomaly pinpointed an isolated instance of a material that was significantly denser than the material surrounding it. This led to the reasonable inference that the anomalies showed the locations of pieces of stone that were above-ground at the time of Saqsaywaman's abandonment, but have since been covered by eroded soil. These pieces of stone could be sections of a terrace wall, sections of a building foundation, or could simply be some large stones

that were removed from a structure by Spanish conquerors and left lying on the ground. Today, there are still scattered, lost stones laying on the ground throughout the site (Figure 4.5), so it is reasonable to believe that there were even more misplaced stones lying around amongst the actual terrace remains after Saqsaywaman's initial destruction and abandonment. These scattered stones would have been become buried by erosion just as the terrace remains did, which contributes to our current uncertainty about the true identity of our GPR and SR anomalies.

As was mentioned earlier, excavation was not possible on site during our field studies, so it was not possible to verify the identities of these anomalies. However, we do know that a stray rock would have probably been smaller in size than a section of a terrace wall remain, so a stray

Figure 4.5: Examples of stray stones near terrace remains at Saqsaywaman

rock would have been more difficult to detect during subsurface data collection. GPR is a more sensitive tool than SR, so GPR detected more anomalies than SR. For this reason, the GPR anomalies were considered less trustworthy markers of potential structural remains than the SR anomalies, because GPR was more likely to detect the smaller pieces of inconsequential stone than SR. Therefore, SR anomalies were given higher importance than GPR anomalies when using them to inform terrace system reconstruction.

V. ANALYSIS OF A POTENTIAL ORIGINAL TERRACE SYSTEM

Based off topographic clues and past field studies discussed in Section III.A, I believe that one piece of the original Incan drainage infrastructure at Saqsaywaman could have been a full-site system of terraces. Using the data discussed in Section IV, I will design a potential reconstruction of the original Incan terrace system. Then, I will model the topography of Saqsaywaman with the proposed terrace system reconstruction implemented. Last, I will discuss possible subsurface drainage methods that might have been built into the terraces. Later, in Section VII, I will analyze the efficacy of this proposed terrace system as a means of stormwater management to protect the Great Walls.

V.A. Reconstructing a Potential Original Terrace System

V.A.1. Methods of Terrace System Reconstruction

To design a possible reconstruction of the original Incan terrace system at Saqsaywaman, I fitted my proposed terrace walls to the data discussed in Section IV by "connecting the dots" of the data with the terrace walls. Much of the above-ground data marked known locations of original terrace wall remains, while the sub-surface data marked possible locations of terrace

wall remains. There were several instances of conflicting data points between the different data types, so the proposed terrace walls were fitted first to the most significant data, then to the second-most significant data, and so on. The significance of each data type was based on how certain I was that the data type indicated the locations of original terraces. The data types in order of significance, from most to least significant, are as follows: visible terrace remains, building foundation remains, instances of overlapping SR and GPR anomalies, SR anomalies, and GPR anomalies.

Visible terrace remains were considered the most significant because they are pieces of the original terraces, and therefore show exactly where sections of the original terraces were located. These remains were the starting point from which the rest of the proposed terrace system was reconstructed. In Figure 5.1 below, the yellow and orange lines show the visible terrace remains at Saqsaywaman.

Building foundation remains were considered the second most significant because they showed where terrace walls definitely were *not* located. It was assumed that all buildings would have been built on the flat, horizontal surfaces atop the terraces, so while terrace walls might have run near or adjacent to the foundational remains, they would not have run through them. Foundational remains are shown by the bright green lines in Figure 5.1 below.

Subsurface data was considered less significant than the visible terrace wall and building foundation remains because GPR and SR anomalies showed locations where it was assumed, but not known, that terrace walls might have been located. As was discussed earlier in Section IV.III, it was impossible to know whether a GPR or SR anomaly indicated a section of a buried terrace wall or a stray stone because we were unable to excavate to identify the anomalous objects. We assumed that a SR anomaly was more likely to predict the location of a buried terrace wall

remain than a GPR anomaly. This is because GPR is a more sensitive tool than SR, so we assumed that it was more likely to notice both smaller and larger stone objects, whereas we assumed that SR, being less sensitive in comparison, was more likely to notice only larger stone objects underground, such as terrace wall remains. For this reason, SR anomalies were considered more significant than GPR anomalies.

Instances where there were both a GPR anomaly and a SR anomaly overlapping each other were considered more significant than instances of a SR or GPR anomaly alone. The two types of anomalies in the same place indicated a stone object large enough to have been noticed by both data collection methods, which we assumed was more likely to predict a buried terrace wall remain. The GPR and SR anomalies are shown by the dark blue and light blue triangles, respectively, in Figure 5.1.

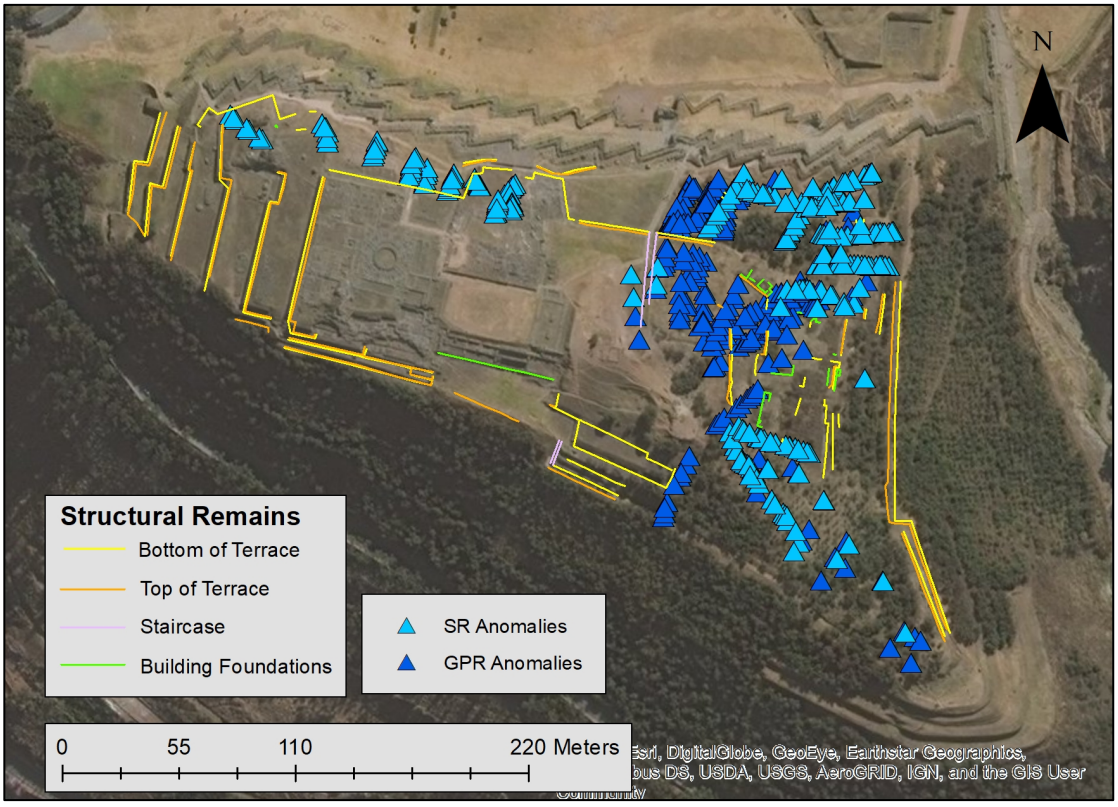

Figure 5.1: Visible remains and GPR and SR anomalies at Saqsaywaman

V.A.2. Filling in Gaps in the Data

Despite the extensive data collection that has been conducted at Saqsaywaman over the last several years, there are still some areas on the site with relatively little conclusive information about terrace wall locations. In particular, the area surrounding the Mirador lookout point (the location of highest elevation at Saqsaywaman), the lower east hill area, and the south hill area lack clear evidence of locations of terrace wall remains. These areas are identified in Figure 5.2 below. The lack of data in these areas is mainly due to the fact that they have not been excavated as thoroughly as other areas of the site. I will attempt to fill in the data gaps by analyzing each area individually to estimate where terraces may have originally been located.

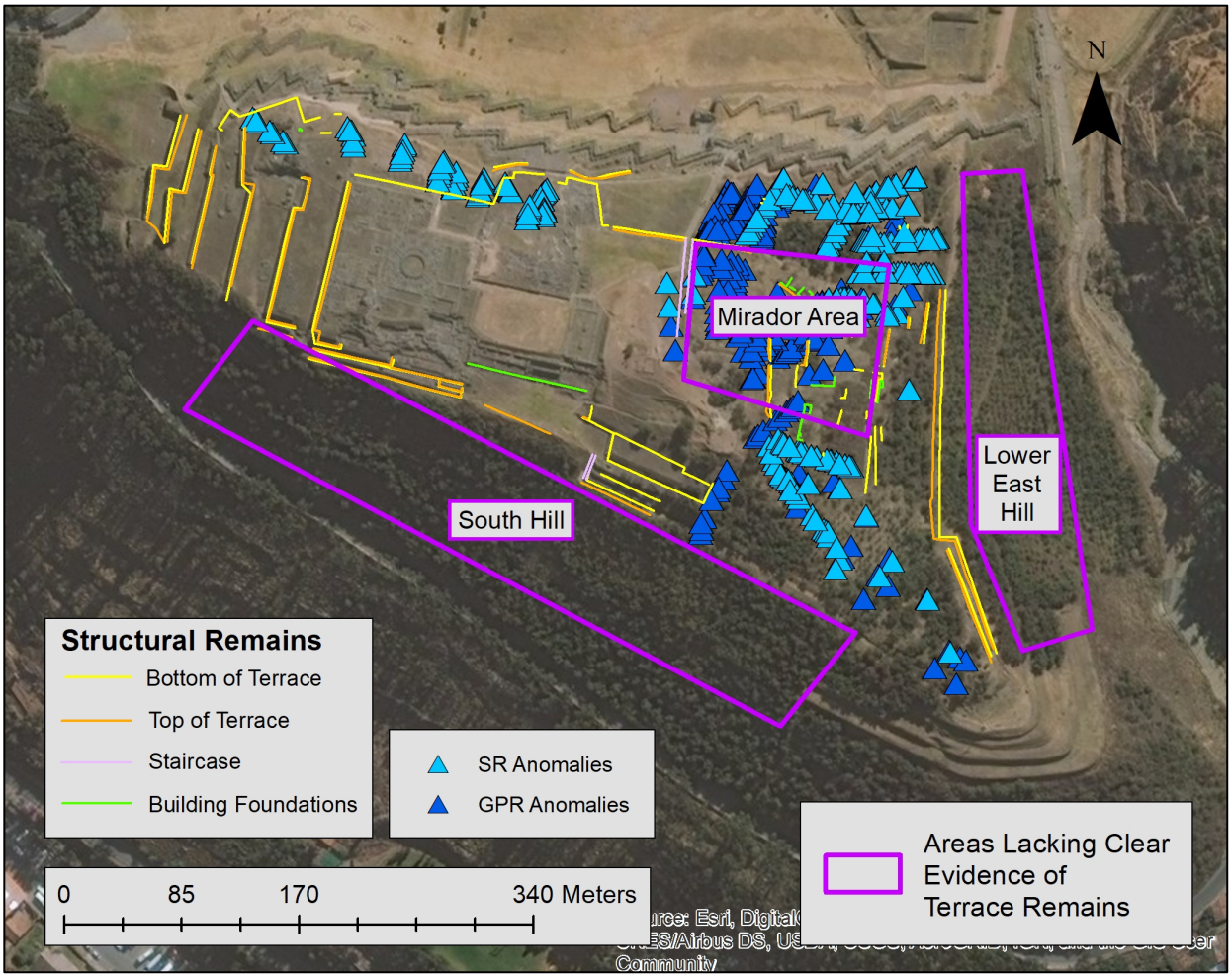

Figure 5.2: Areas at Saqsaywaman lacking clear evidence of terrace remains

Mirador Lookout Point Area

In the case of the Mirador area, there were very few visible terrace remains to guide the reconstruction of possible terrace walls. Just north of the Mirador point, there was a dense cluster of GPR and SR anomalies, but the large number of anomalies in this location made it difficult to tell which of them were significant. This indicated that there were probably many stray stones and debris that became buried by erosion in this area, obscuring the locations of any potential buried terrace wall remains.

The Mirador area is one of the more hydrologically important regions on the site because the northern section of this area (Figure 5.3) slopes down towards the Great Walls at a roughly 30% slope. This slope is dangerous for the walls because as it is currently, it directs runoff straight towards the third wall. In order to protect the Great Walls, I assumed that this area was

Figure 5.3: Northern hillslope of the Mirador area (Miksad)

originally terraced in order to control runoff on this hillslope. The contours present in this area corroborate this assumption because they appear to be smoothed, eroded versions of terraces. These smoothed "terraces" were roughly identified by visual inspection, and are shown by the dashed yellow lines in Figure 5.4 below.

Figure 5.4: Potential locations of original terraces on the northern hillslope of the Mirador area, outlined by dashed yellow lines (Miksad)

I assumed that these smoothed "terraces" represented the rough locations of the original terraces in this area. Based on this assumption, I attempted to empirically identify the locations of the original terraces by analyzing a series of parallel transects of the area's topography. Each transect showed a cross-sections of the curvature of the hillslope in the transect's location. Figure 5.5 shows the location of each transect in the area. Figure 5.6 shows each individual transect, with the inflection points of the contours identified. The transects were created mainly using R

3.5.1 software. The code used can be found in Appendix XI.A, but the general method used will be described here.

First, the three-dimensional surface of the Mirador area was extracted from Saqsaywaman's current topography in ArcGIS (the modeling of this continuous surface will be described later in Section V.II), and it was uploaded into R. Then, seven adjacent parallel lines were drawn from north to south across the Mirador area's surface in R. The transects were created from the curvature of the surface along the length of each line.

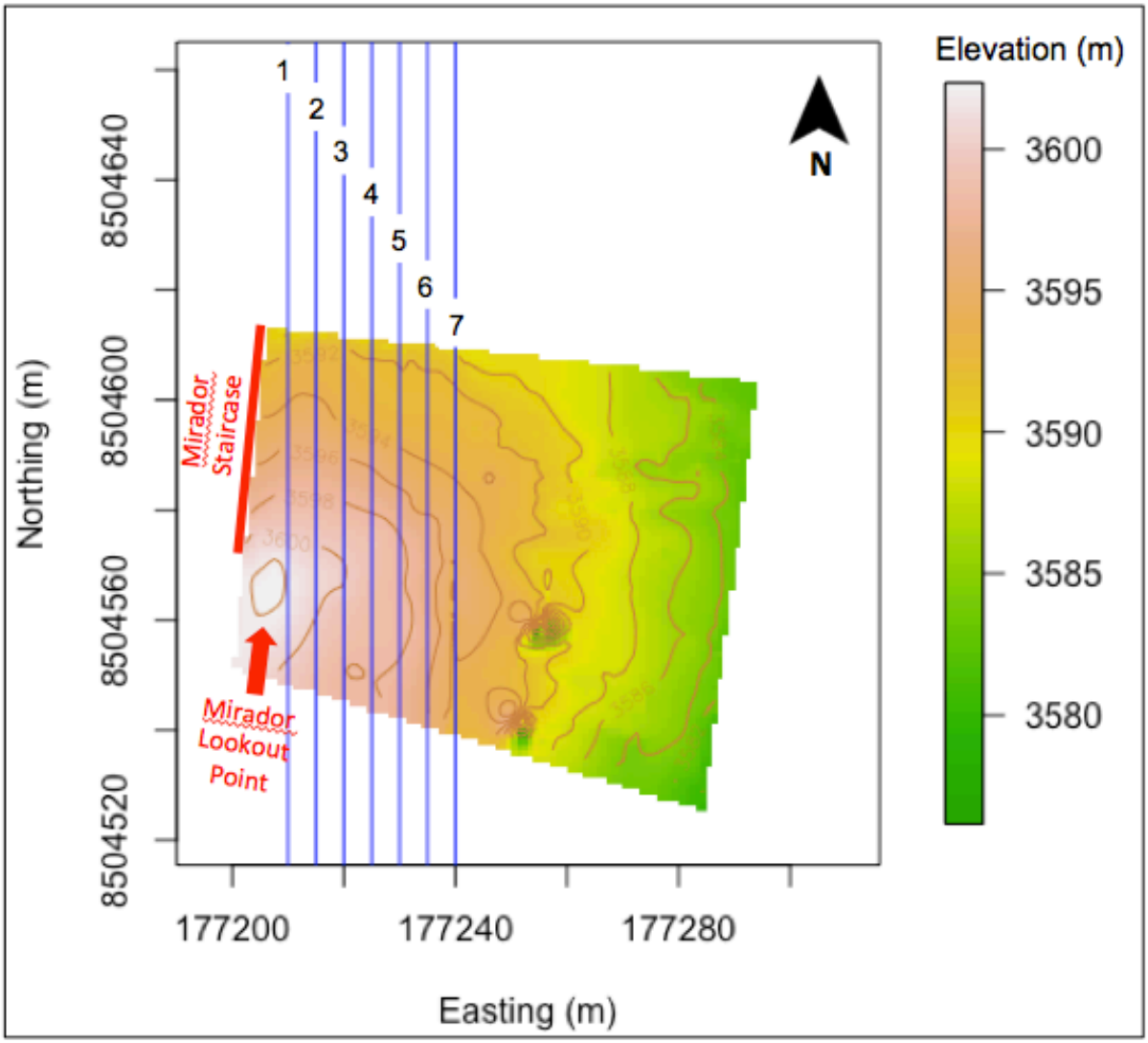

Figure 5.5: Locations of transect lines (in blue) in the Mirador area

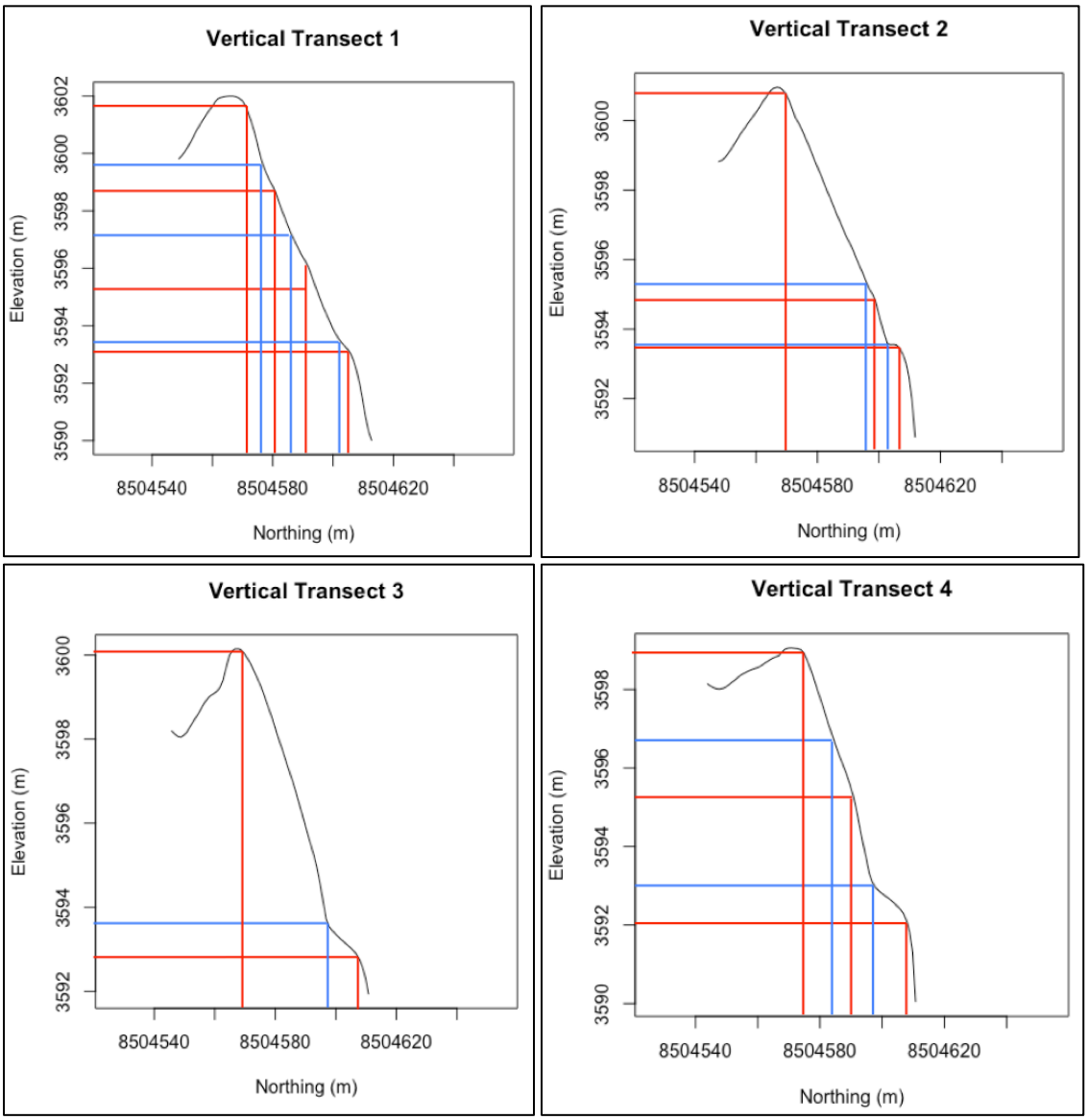

Figure 5.6 (continued on next page): Mirador area transects, with red lines indicating approximate convex inflection points and blue lines indicating approximate concave inflection points

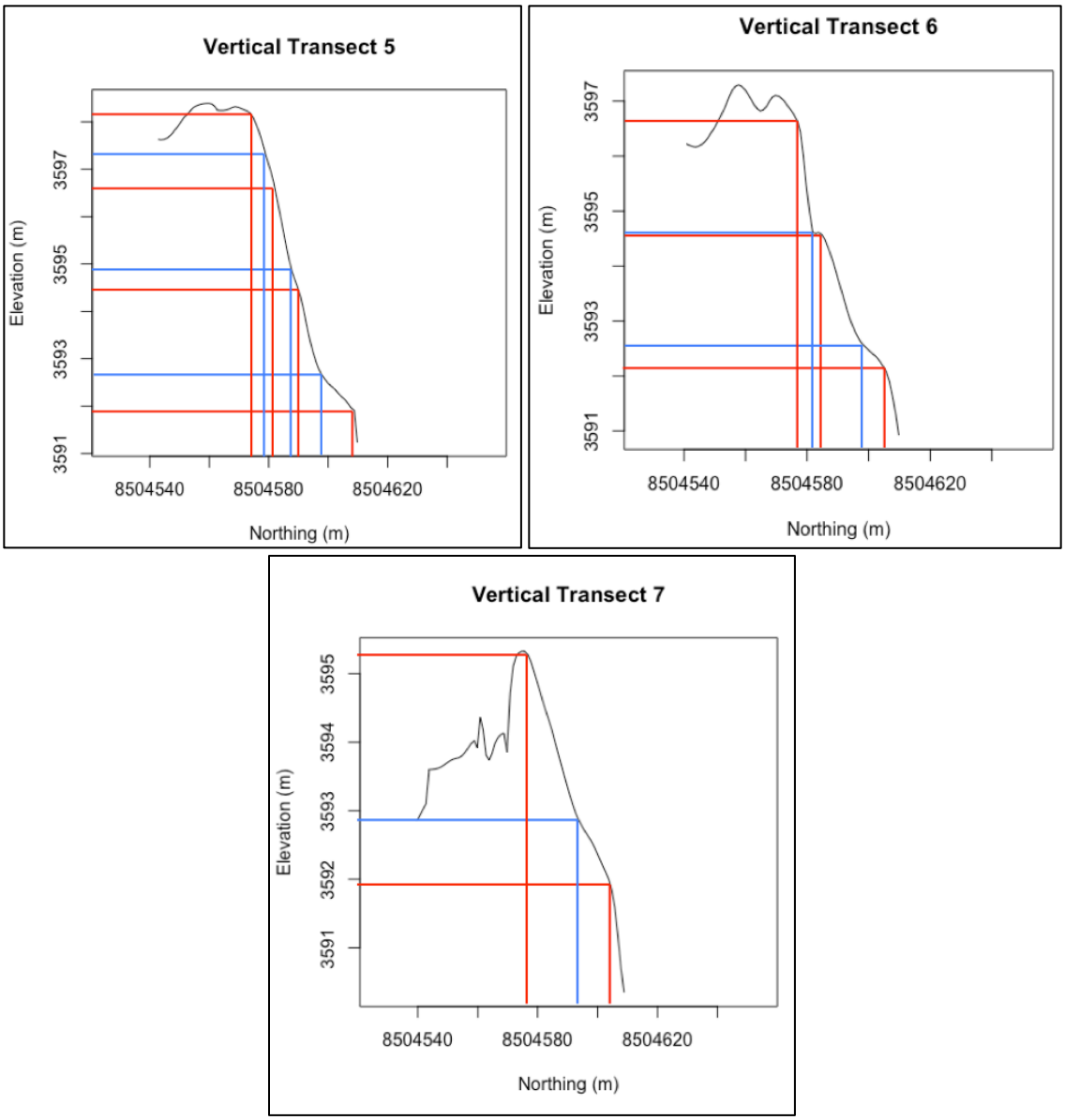

Figure 5.6 (continued from previous page): Mirador area transects, with red lines indicating approximate convex inflection points and blue lines indicating approximate concave inflection points

Next, in order to use these transects to locate potential original terraces, I identified the concave and convex inflection points of the contours on each transect. I assumed that if these inflection points lined up with each other laterally, then their contours indicated the possibility of buried terraces. If the inflection points were somewhat staggered or random, I assumed that the contours were a result of scattered stones that had become buried rather than terrace remains. To

determine whether the contours lined up laterally, I placed the convex inflection points on a map of Saqsaywaman to examine them side by side (Figure 5.7).

Some of the inflection points on the transects were significantly more pronounced than others. For this reason, the inflection points were sorted into categories of "strong" and "weak," with "strong" indicating the more pronounced inflection points and "weak" indicating the fainter ones. In Figure 5.7, the strong inflection points roughly line up laterally in two places, at the north end and the south end of the transect lines, indicating a stronger possibility of buried terraces in those areas. The other inflection points are more staggered and scattered, so they give no indication of possible buried terraces.

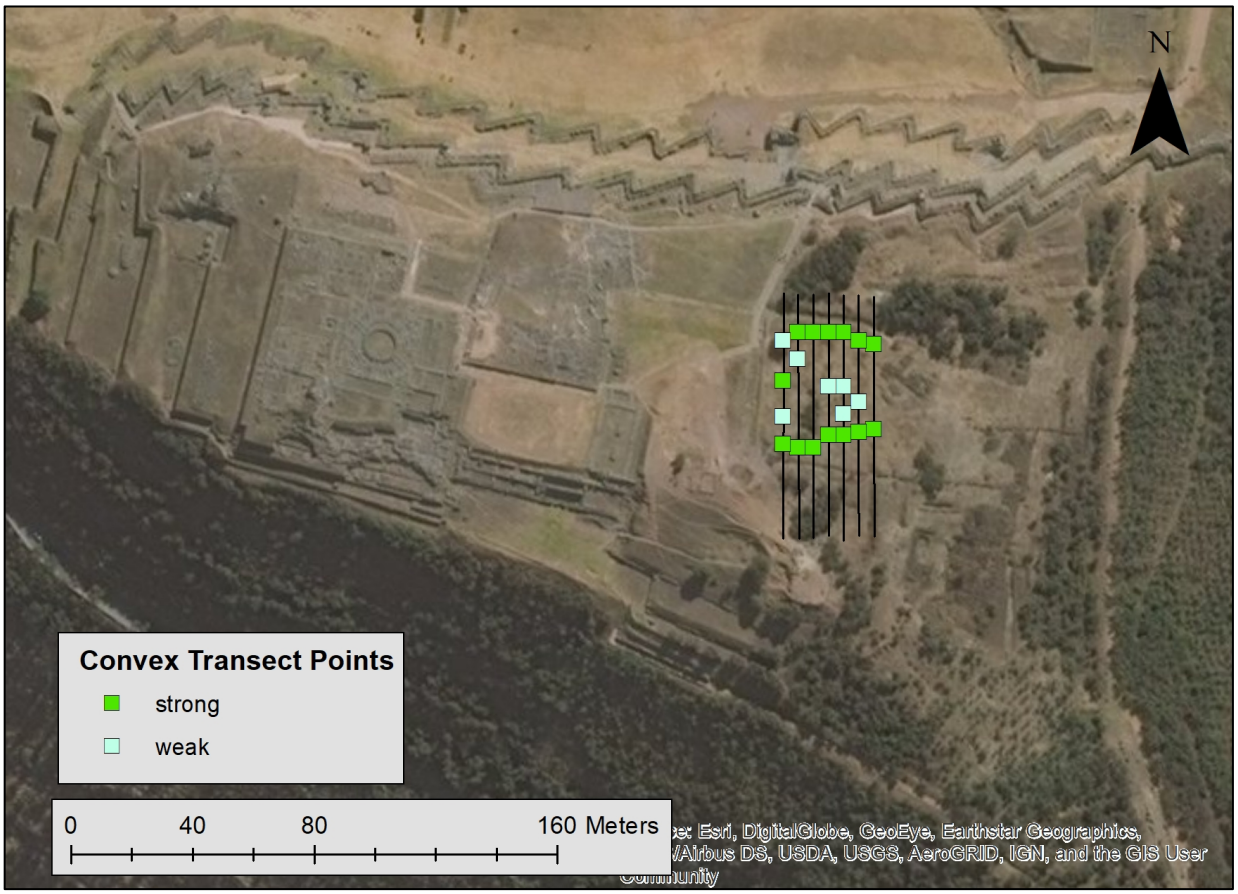

Figure 5.7: Convex inflection points on Mirador area transects

Lower East Hill Area

We were unable to collect data on the east hill further east than the terrace remains shown in Figure 5.1, because the hill became too steep and too densely vegetated for safe data collection below that point. However, E. George Squier, a 19th century Andean explorer, tells us that there were at least three terraces on the lower east hill. In his detailed account of his exploration of Saqsaywaman, he stated that as he ascended the hill along the ravine bordering the site to the east, he saw "long lines of walls, which are the faces of the eastern terraces of the fortress," which "become heavier as we advance until, when we finally reach the level of the plateau, they cease to be simply retaining walls, and rise in massive, independent walls composed of great blocks of limestone." (Squier, 1877) This tells us that three terraces on the lower east hill connected seamlessly to the three Great Walls.

South Hill Area

We were also unable to collect data in the south hill area due to the steep, nearly sheer slope and dense vegetation. There is reason to believe, however, that barely any evidence or stones remain in this area. As was stated earlier in Section II.B, after the Spanish conquest of Saqsaywaman in 1536, the conquistadors rolled stones down the south hill to use them as building materials in the city below. For this reason, any stones on the south hill that were not purposefully sent down to the city would have likely been knocked out of place by other stones being rolled downhill, at which point gravity would have carried the all of the stones downhill together.

As was discussed earlier in Section II.A, the 17th century chronicler Garcilaso de la Vega wrote that Saqsaywaman had a "thick freestone wall" surrounding the site on all sides, so we

know that there was at least one major terrace on the south hill. He also described three defensive ramparts that circle the site. This would require that the south hill had three large terrace walls that connected to the west hill and east hill terraces, completing the full-site "circumvallations" that de la Vega described.

V.A.3. Proposed Terrace System Reconstruction

Using the data, methods, and assumptions discussed in the sections above, the resulting proposed reconstruction of the original Incan terrace system is shown in Figure 5.8. Figure 5.9 shows the proposed terrace system overlaying the data used in reconstruction.

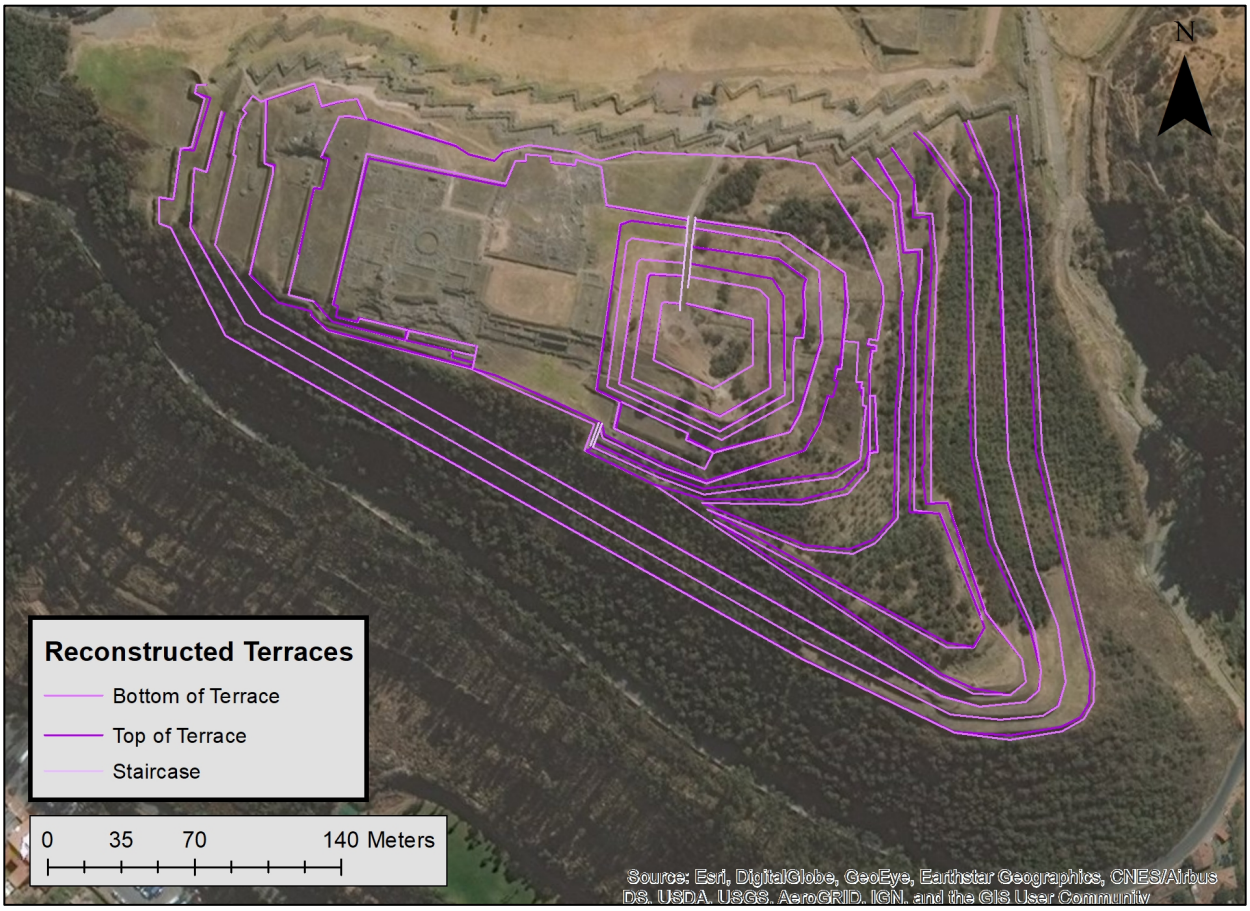

Figure 5.8: Proposed reconstruction of the original Incan terrace system

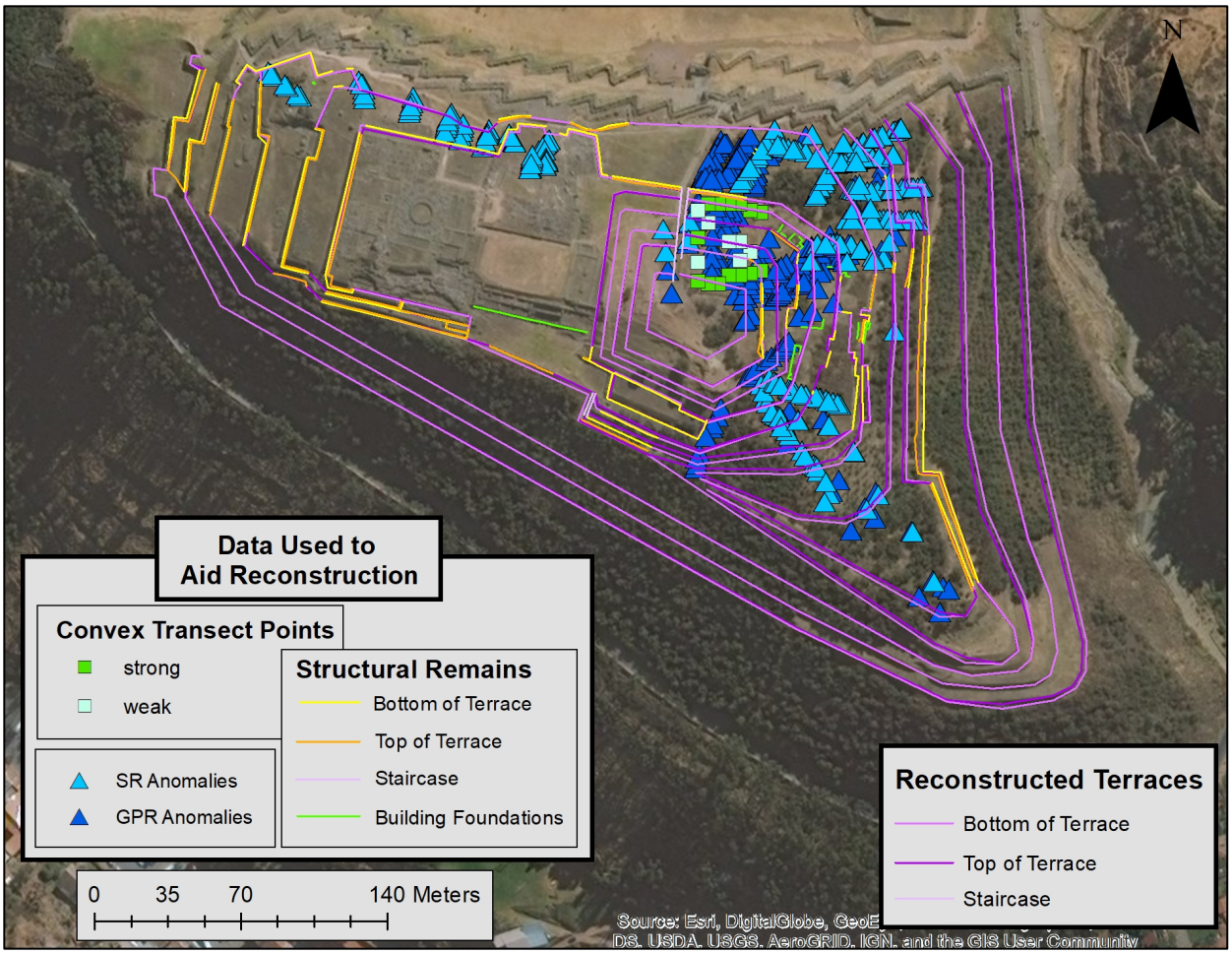

Figure 5.9: Proposed reconstruction of the original Incan terrace system, overlaying the data used to inform reconstruction

This proposed reconstruction is just one possibility of how the original terrace system might have looked during the Incan Empire. Civil engineering researchers Alva et al. from the Universidad Nacional de Ingeniería de Peru have also collected and analyzed extensive sub-surface data at Saqsaywaman for the purpose of locating the original terrace remains. They came to a slightly different conclusion of where some buried terraces could be located (Figure 5.10). It is unclear why the proposed terrace locations of Alva et al. differ from those in my proposed reconstruction, but it shows that more investigation is needed on this subject before we can know with certainty where the original terraces were located.

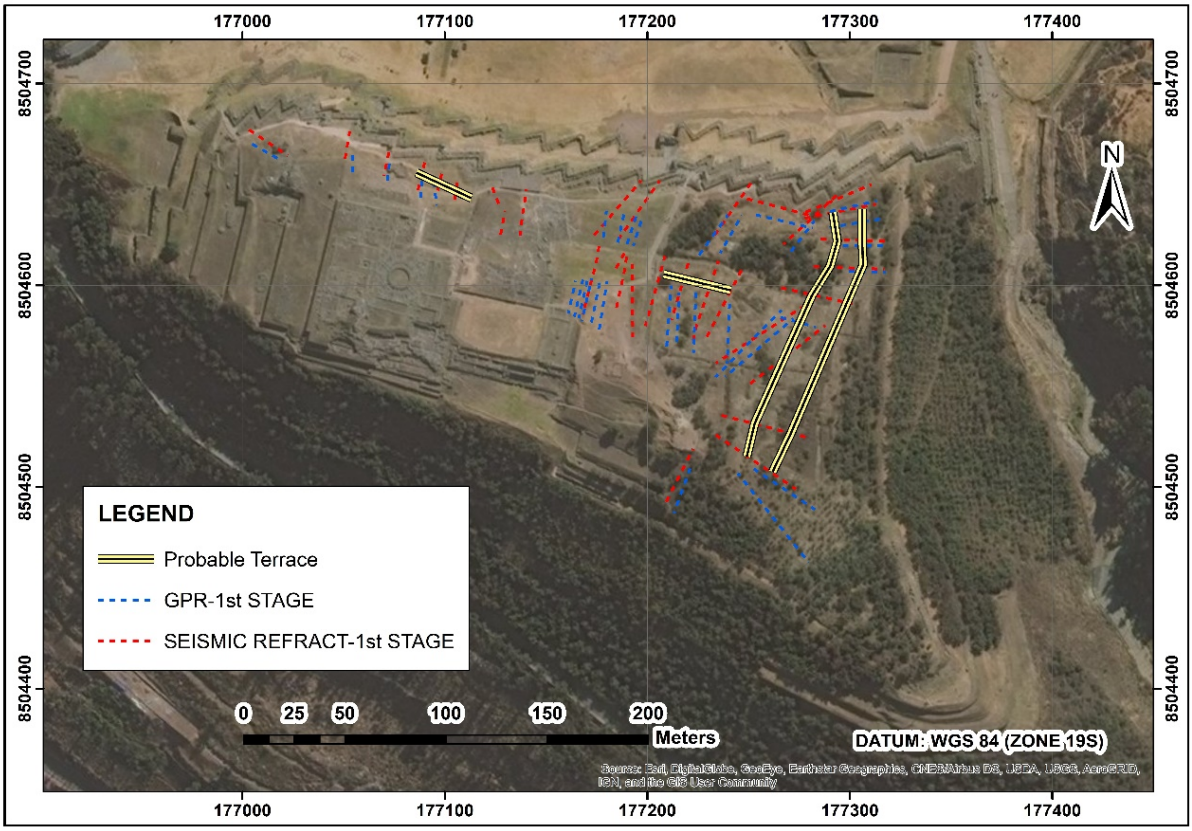

Figure 5.10: Other possible locations of buried terraces (Alva et al., 2018)

V.B. Topographic Model of the Proposed Terrace System Reconstruction

To show the changes that would be made to Saqsaywaman's topography if a restoration were carried out using my proposed terrace system reconstruction, the proposed terraces were modeled as a three-dimensional continuous surface. The current topography of Saqsaywaman was also modeled as a three-dimensional continuous surface for comparison to the terraced surface.

To create these surface models, the Spline with Barriers tool in ArcGIS was used. Spline is a method of interpolation that works by passing an imaginary thin plate of flexible material through a collection of anchor points while minimizing the overall curvature of the plate (Mitas & Mitasova, 1988). The "splined" output surface is a smoothed approximation of the real-life

surface based off of the representative anchor points. It is necessary that the anchor points are accurate to the real-life surface, and ideally, they should be collected from the real-life surface in a field survey.

The Spline tool is limited in that it cannot preserve sharp edges on a surface, such as terrace walls, because the output surface is completely smoothed in the areas between the anchor points. The Spline With Barriers tool overcomes this limitation because it allows the user to add a collection of lines or polygons as "barriers" to interpolation. These "barriers" can represent any sharp-edged features that the user does not want smoothed over in the output surface. The tool preserves the sharp edges by smoothing the surface around the features, but not smoothing the features themselves.

To model the three-dimensional continuous surface of the proposed terrace system reconstruction, the [N, E, Z] points (from Figure 4.1) were used as the anchor points for interpolation and the proposed terrace system reconstruction (from Figure 5.8) was input as a collection of polyline barriers for the Spline with Barriers tool. The resulting model of the terraced surface is shown in Figure 5.11. Figure 5.12 shows the same terraced surface model, but with elevations labeled.

To model the three-dimensional continuous surface of Saqsaywaman's current topography, the same method was used as for the terraced surface model, but the existing structural remains (from Figure 4.2) were input as polyline barriers instead of the proposed terrace system reconstruction. The resulting model of the current surface is shown in Figure 5.13. Figure 5.14 shows the same current surface model, but with elevations labeled.

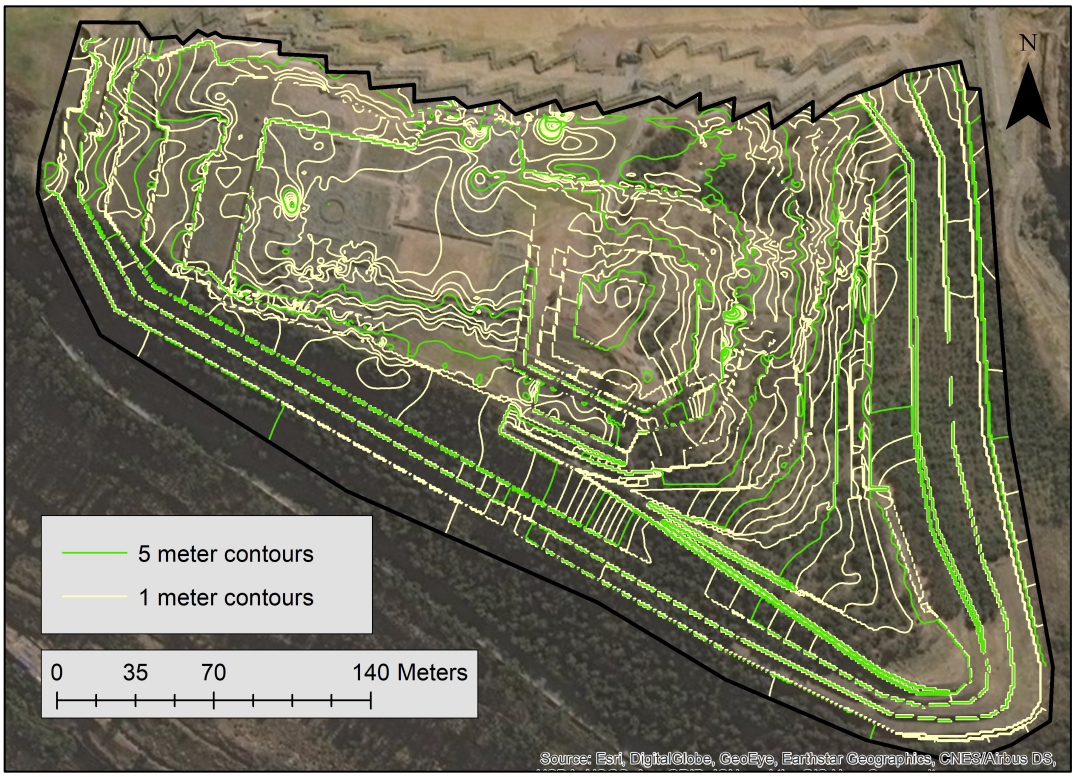

Figure 5.11: Three-dimensional continuous surface model of the proposed terrace system reconstruction

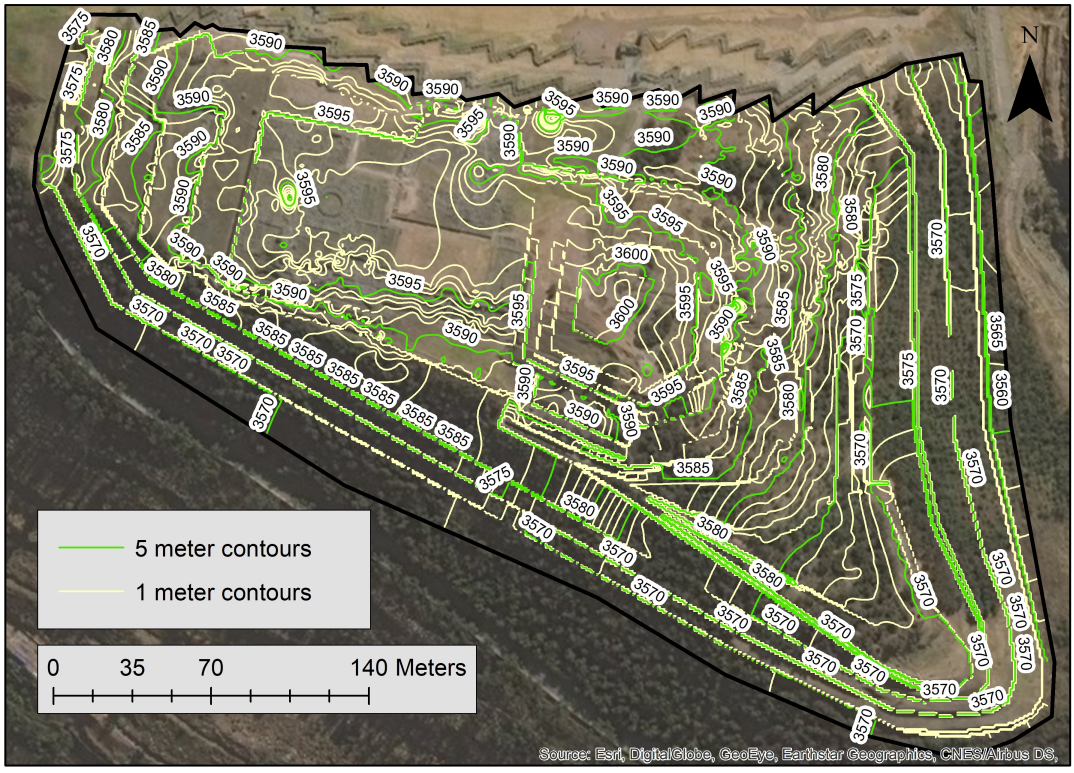

Figure 5.12: Three-dimensional continuous surface model of the proposed terrace system reconstruction, with 5-meter contour elevations labeled

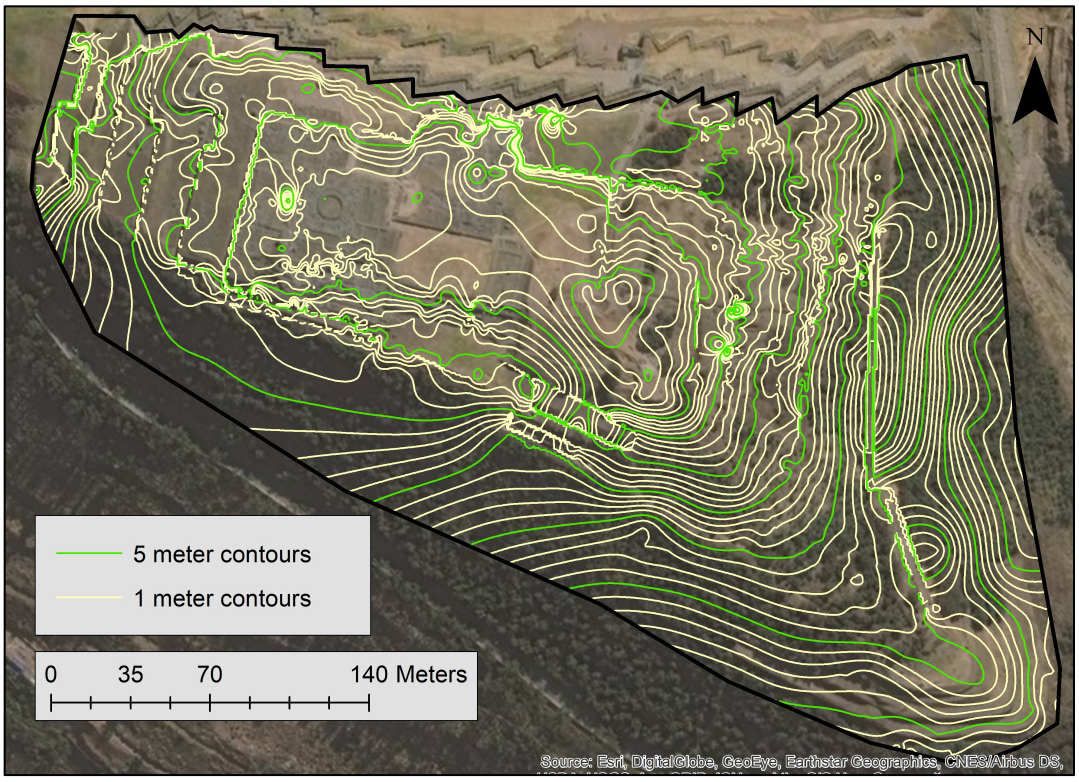

Figure 5.13: Three-dimensional continuous surface model of the current topography of Saqsaywaman

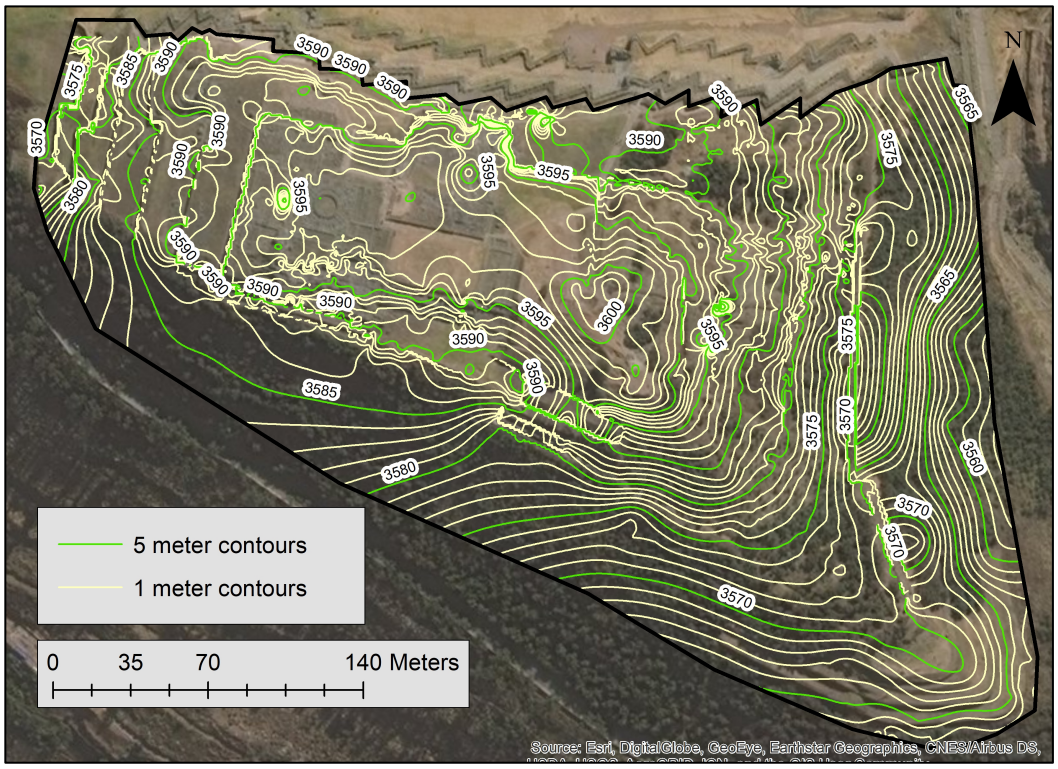

Figure 5.14: Three-dimensional continuous surface model of the current topography of Saqsaywaman, with 5-meter contour elevations labeled

To better display the changes that would be needed for this restoration, a map was created showing the cuts and fills required to change the current topography to look like the proposed terraced topography (Figure 5.15). This map was made by subtracting the current topography from the terraced topography using the raster calculator function in ArcGIS. A raster is an image made up of rows and columns of cells, where each cell contains a value that represents spatially distributed information (ESRI). The two topography maps were raster maps where each cell's value was the elevation of the surface at that cell's location. Subtracting the two maps showed the differences in elevation between the current topography and the proposed terraced topography.

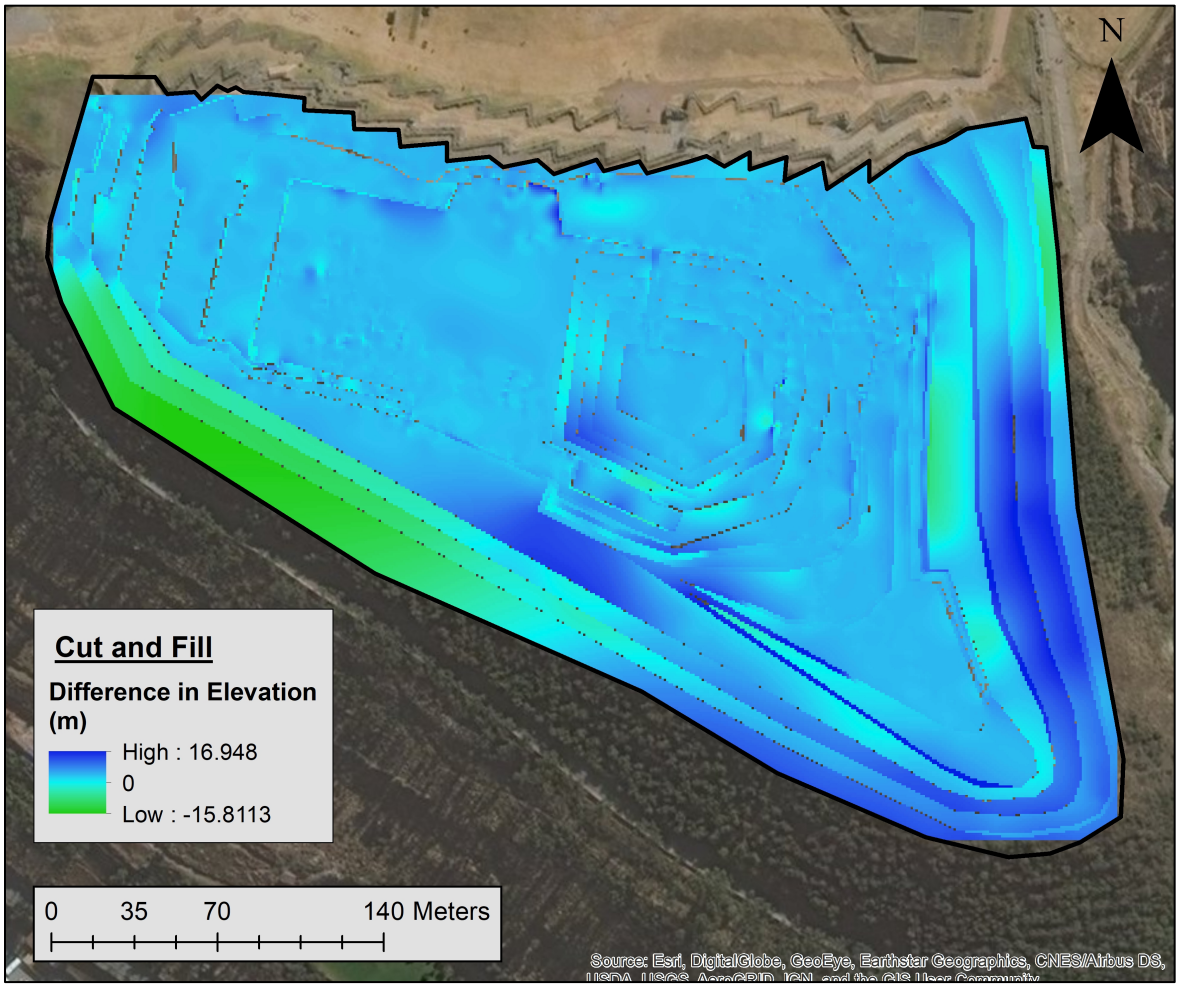

Figure 5.15: Cuts and fills needed to restore the proposed terrace system reconstruction at Saqsaywaman

From Figure 5.15, we can see that most of the site requires fills to construct the proposed terrace system. Most of these fills would be needed to add soil to the tops of terraces that have become smoothed and slanted after centuries of erosion. Some cuts would be needed to restore the fronts of the terraces to a vertical plane. Cuts would also be on the south hill to connect the west and east terraces.

V.C. Analysis of Potential Terrace System Drainage Methods

A system of terraces would provide some stormwater control hydrologically by slowing down or redirecting runoff along the flat, horizontal planes of the terraces. For increased stormwater control, Incan engineers also often incorporated hydraulic drainage methods into their terrace design. Some typical hydraulic features of Incan terraces included: a multi-layer draining backfill, weep holes built into the terrace walls, sub-surface gravel drains, surface channels, and hydraulic drops. Surface channels and hydraulic drops will be discussed in Section VI in regards to their roles in a possible surface drainage system. In this section, I will discuss the other three possible hydraulic drainage techniques and how they might have been implemented at Saqsaywaman.

V.C.1. Multi-Layered Draining Terrace Backfill

I assumed that a multi-layered drainage material was used to backfill the retaining walls of the non-ceremonial terraces at Saqsaywaman. Non-ceremonial terraces were mainly used for purposes of agriculture, drainage, or hillslope stabilization (Hyslop, 1990; Wright et al., 2016), whereas ceremonial terraces were used more for aesthetic purposes. The roles of non-ceremonial terraces required that they be able to drain water efficiently, so many of these terraces had multi-

layered backfills to facilitate sub-surface drainage. Backfills of this nature have been found in the terraces at other Incan sites that were built around the same time as Saqsaywaman, such as Machu Picchu and Ollantaytambo (Wright & Zegarra, 2000; Wright et al., 2016). This led to the assumption that Saqsaywaman may also have employed this drainage method.

This backfill would have facilitated a controlled percolation of water downward behind the terrace walls. At Machu Picchu, it was estimated that "90 percent of the annual water yield from the agricultural terraces occurred as subsurface flow and 10 percent as surface runoff" as a result of this drainage method (Wright & Zegarra, 2000). An example of this backfill is shown in Figure 5.16.

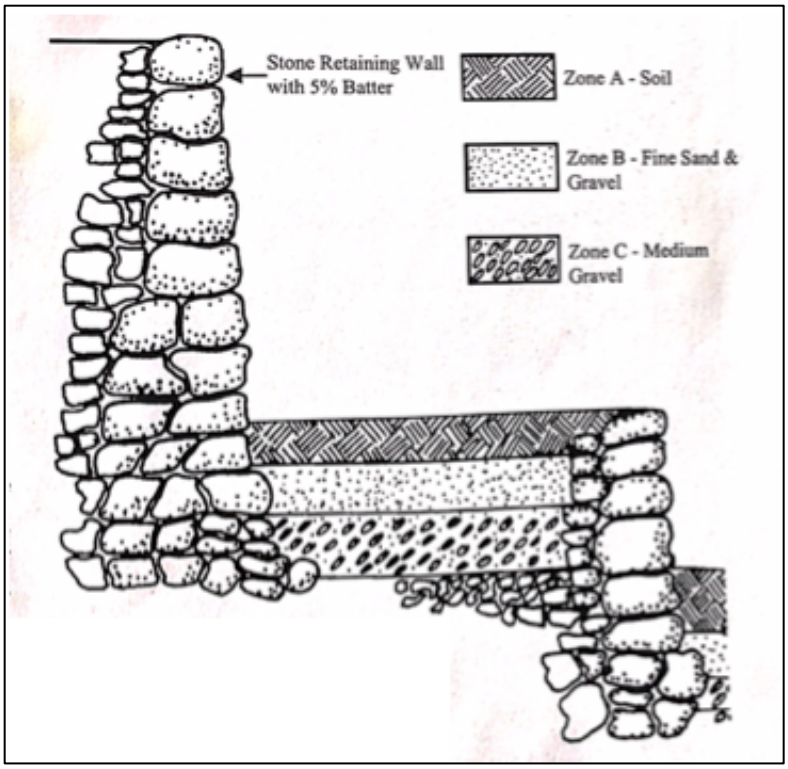

Figure 5.16: Typical subsurface drainage strata of terraces at Machu Picchu (Wright & Zegarra, 2000)

The hydraulic conductivity and subsurface drainage potential of this backfill were calculated. To determine its composite vertical hydraulic conductivity (K_Z), Equation 5.1 was used,

$$K_Z = \frac{d_{total}}{\sum \frac{d_i}{K_i}}$$

Equation 5.1

where d_{total} was the total vertical depth of the backfill, d_i was the depth of each individual layer of the backfill, and K_i was the hydraulic conductivity of each individual layer of backfill. I assumed that the depths of the three backfill layers in Figure 5.16 were about equal (such that $d_1 = d_2 = d_3$). This assumption caused Equation 5.1 to simplify to Equation 5.2 below.

$$K_Z = \frac{3}{\sum \frac{1}{K_i}}$$

Equation 5.2

The hydraulic conductivity of each layer of the backfill was determined from typical hydraulic conductivity values of soil types (Budhu, 2011). These values are listed in Table 5.1.

Table 5.1: Hydraulic conductivities of layers in a typical Incan terrace backfill

Terrace Backfill Layer	**Hydraulic Conductivity (cm/s)**
Soil	10^{-4}
Fine Sand & Gravel	10^{-2}
Medium Gravel	1.0

Using these hydraulic conductivity values and Equation 5.2, it was determined that the composite vertical hydraulic conductivity of the Incan terrace backfill was 3.00 x 10^{-4} cm/s. With this composite vertical hydraulic conductivity, terraces utilizing this backfill would drain water at a rate of 0.425 inches per hour. The impact that this backfill would have on runoff during a storm event at Saqsaywaman is discussed in Section VII.

V.C.2. Buried Gravel Drainage Network

The draining terrace backfill discussed in the previous section would have mitigated surface runoff by allowing water to percolate downwards through the soil strata. After draining through the backfill, runoff would then need a subsurface drainage route to prevent it from building up behind the terrace walls and causing them to collapse. Two possible drainage routes for subsurface runoff are weep holes built into the terrace walls or buried gravel drains. If weep holes were used, evidence of them would probably still be present in visible terrace remains today because they would have been built into the vertical faces of the terrace walls. No weep holes have been found on site, implying two possible conclusions: 1. Any terrace wall remains containing weep holes are still buried, or 2. The Incan engineers never used weep holes at Saqsaywaman.

Although weep holes remain a question, there is evidence of a buried gravel drain at Saqsaywaman. Part of a gravel drain was discovered above the third Great Wall during an excavation in 2013 (Figures 5.17 and 5.18). It was believed that this drain functioned similar to a modern French drain – water would percolate down to the gravel drainage channel, after which it would follow the channel to some outlet point (Lohr, 2014).

A subsurface gravel channel network would have been an efficient choice for the Incan engineers. The bottom-most layer in the typical Incan terrace backfill was gravel, so the infrastructure for the gravel channels would have already been present on much of the site. Recent geophysical investigations by Alva et al. (2018) identified clayey gravel as one of the soil type layers present throughout Saqsywaman, further justifying the possibility of a subsurface gravel network. After percolating into the gravel channels, the natural elevation decreases on site (Figure 5.19) would carry the water through the gravel channels to the natural lowest elevation

Figure 5.17: Excavation of a buried gravel drain above the third Great Wall (Palma, 2013)

Figure 5.18: Location and direction of flow of buried gravel drain (Miksad)

on the site – the southeast corner. At this point, subsurface water could then easily exit the site through an outlet point into the ravine that runs along the east side of the site down towards the city.

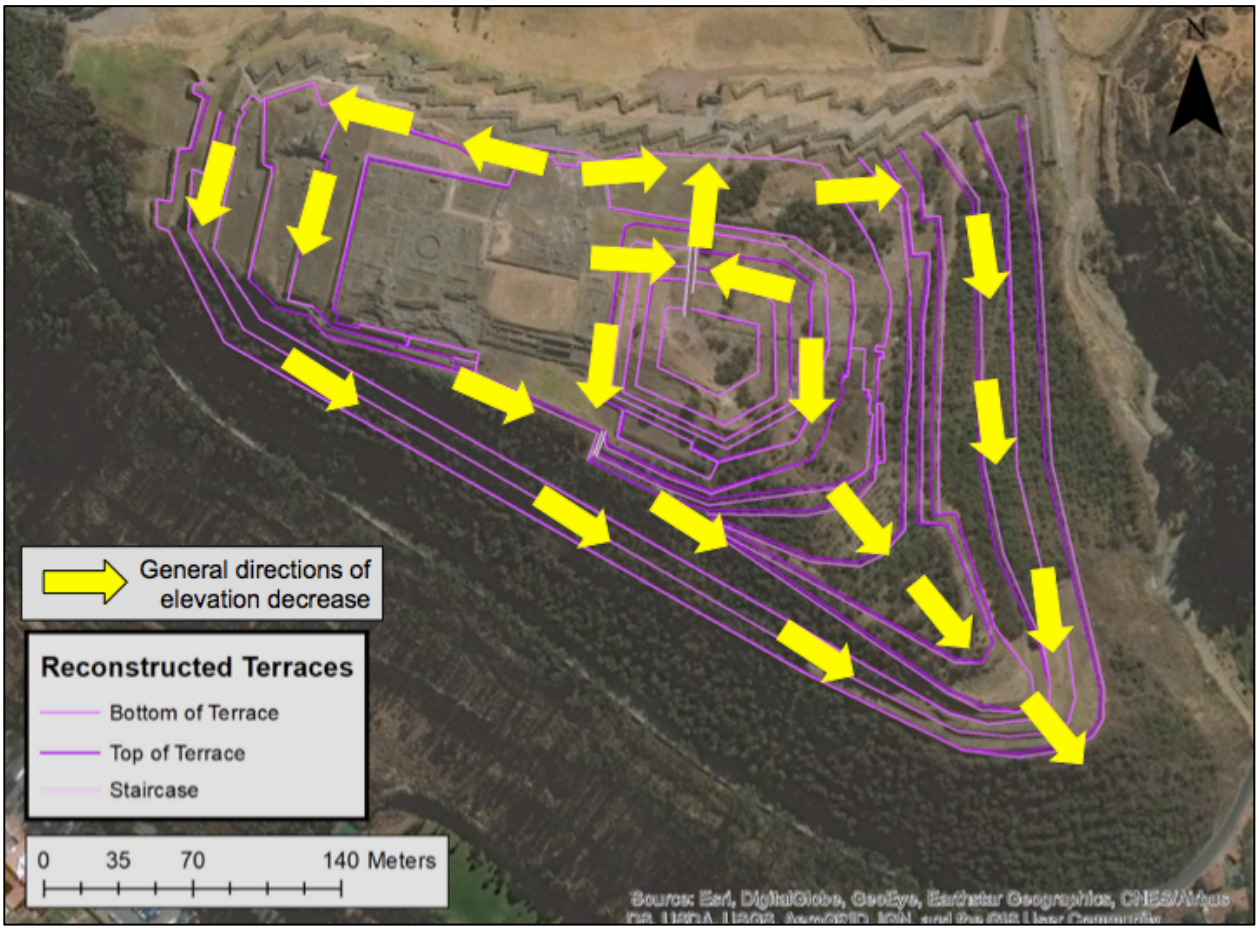

Figure 5.19: General directions of elevation decrease at Saqsaywaman after implementation of the proposed terrace system

VI. ANALYSIS OF A POTENTIAL SURFACE DRAINAGE SYSTEM

In the previous section, I discussed the role of the proposed terrace system in controlling and mitigating surface runoff at Saqsaywaman. While terracing was used at most Incan sites built around the same time as Saqsaywaman, surface drainage systems were also often used in tandem with terracing for further runoff control and cautionary protection. Based on the ubiquity of surface drainage systems in Incan engineering, I assumed that Saqsaywaman also had surface

drainage in place, which would have helped further protect the Great Walls in case of unexpectedly large storms.

Incan surface drainage systems were typically composed of channels and hydraulic drops. Channels were used to control the flow of water along a terrace's surface and hydraulic drops were used to control the flow of water from one terrace to another. Different sites used different versions of these two basic hydraulic features depending on the site's unique needs. At Saqsaywaman, I assumed that most of its hydraulic drops were sloped channels lining the staircases on site. I assumed all other hydraulic drops consisted of ports in the Great Walls and some fountains used in the south and southeast areas of the site. I assumed its surface channels lined the bases of most of the terrace walls and carried water to the hydraulic drops.

In the following sections, I will explain my assumptions. Then, I will use those assumptions to create my proposed design of a possible original surface drainage system at Saqsaywaman.

VI.A. Reconstructing a Potential Original Surface Drainage System

VI.A.1. Hydraulic Drops

There were several different types of hydraulic drops utilized by Incan engineers depending on a site's needs. Four of the most commonly used types included: carved vertical drops, fountains, ports, and staircase channels. Vertical drops were carved like a vertical channel into the entire length of a terrace wall (Figure 6.1a). Fountains were generally carved into the top of a terrace wall, such that water could flow out of it like the spout of a pitcher (Figure 6.1b). Ports were channels that were carved like tunnels through the insides of walls, leading from one

terrace through the backfill material down to the next terrace (Figures 6.1c and 6.2). Staircase channels were sloped channels that bordered the sides of staircases (Figure 6.3).

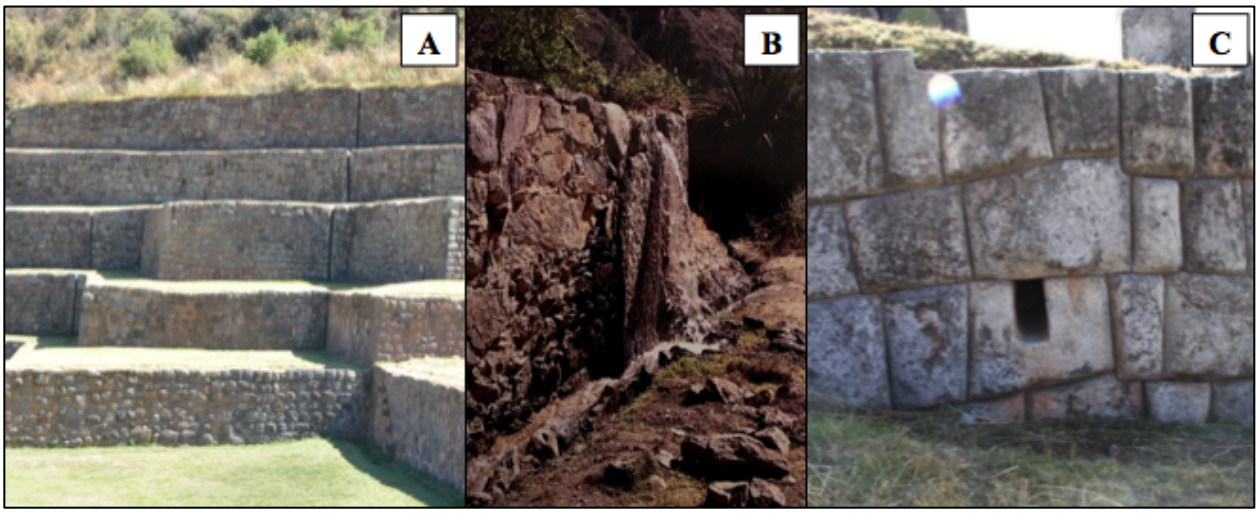

Figure 6.1: Examples of different types of Incan hydraulic drops: a) Vertical drops at Tipon (Miksad); b) Fountain at Ollantaytambo (Wright et al., 2016); c) Port in the second Great Wall at Saqsaywaman (Miksad)

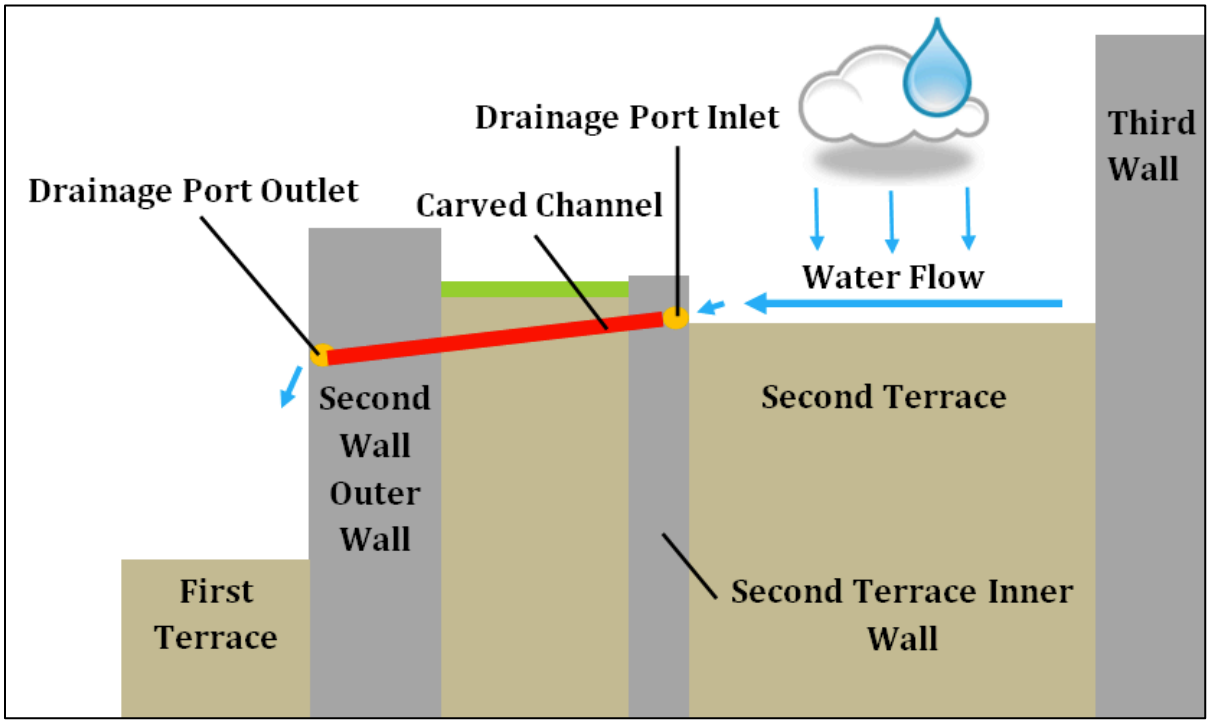

Figure 6.2: Drainage port mechanics (Lohr, 2014)

Figure 6.3: Examples of Incan staircase channels at: a) Machu Picchu (Wright & Zegarra, 2000); b) Suchuna (O'Neil, 2016); c) Ollantaytambo (Miksad); d) Tipon (Wright et al., 2016)

We do not know for sure what the Incan engineers used for hydraulic drops at Saqsaywman, but based on the remains present, I assumed that staircase channels were used to control the bulk of the runoff load, while some fountains were also used in the south and southeast areas of the site. Within the Great Walls, we know that ports were used as hydraulic drops between the walls because there is still evidence of several ports in those walls (Lohr, 2014). The locations of all of the known ports are shown in Figure 6.4.

Figure 6.4: Locations of all known drainage ports (yellow circles) on the Great Walls (blue lines) (Lohr, 2014)

There are two large staircases on site (Figure 6.5) – one in the Mirador area and one on the south hill. The current states of these staircases made it difficult to tell whether they originally had channels lining them. The south hill staircase has been completely rebuilt in a modern way and almost none of the original stones are visible. The Mirador staircase has been modernly rebuilt in the lower part, while the top part is almost completely decayed and is still partially buried. However, because these staircases are the only remaining evidence of paths with controlled elevation changes on site, I assumed that they were originally used as the main hydraulic drops. Channels lining staircases have been found at several other Incan sites built around the same time as Saqsaywama, including at the Suchuna area across the plaza from

Saqsaywaman (Figure 6.3b). The frequency of use of this hydraulic technique in Incan engineering adds further justification to my assumption that they were used at Saqsaywaman.

Besides the Mirador staircase and the south hill staircase in the main part of the site, there are also several staircases within the Great Walls. I assumed that these staircases were also lined with channels, which could have supplemented the ports in the Great Walls with further runoff control. These staircase channels could also have provided a way to route runoff from above the Great Walls – especially from the Mirador staircase channel – safely out of the site. The locations of all of the known staircases on site are shown in Figure 6.6.

There was some evidence of fountains on the south side of the site. While no further evidence of fountains has been found, a lack of evidence of fountains did not necessarily mean they were not used. This is because fountains would have been carved into one of the top-most

Figure 6.5: a) Mirador staircase (Miksad); b) South hill staircase

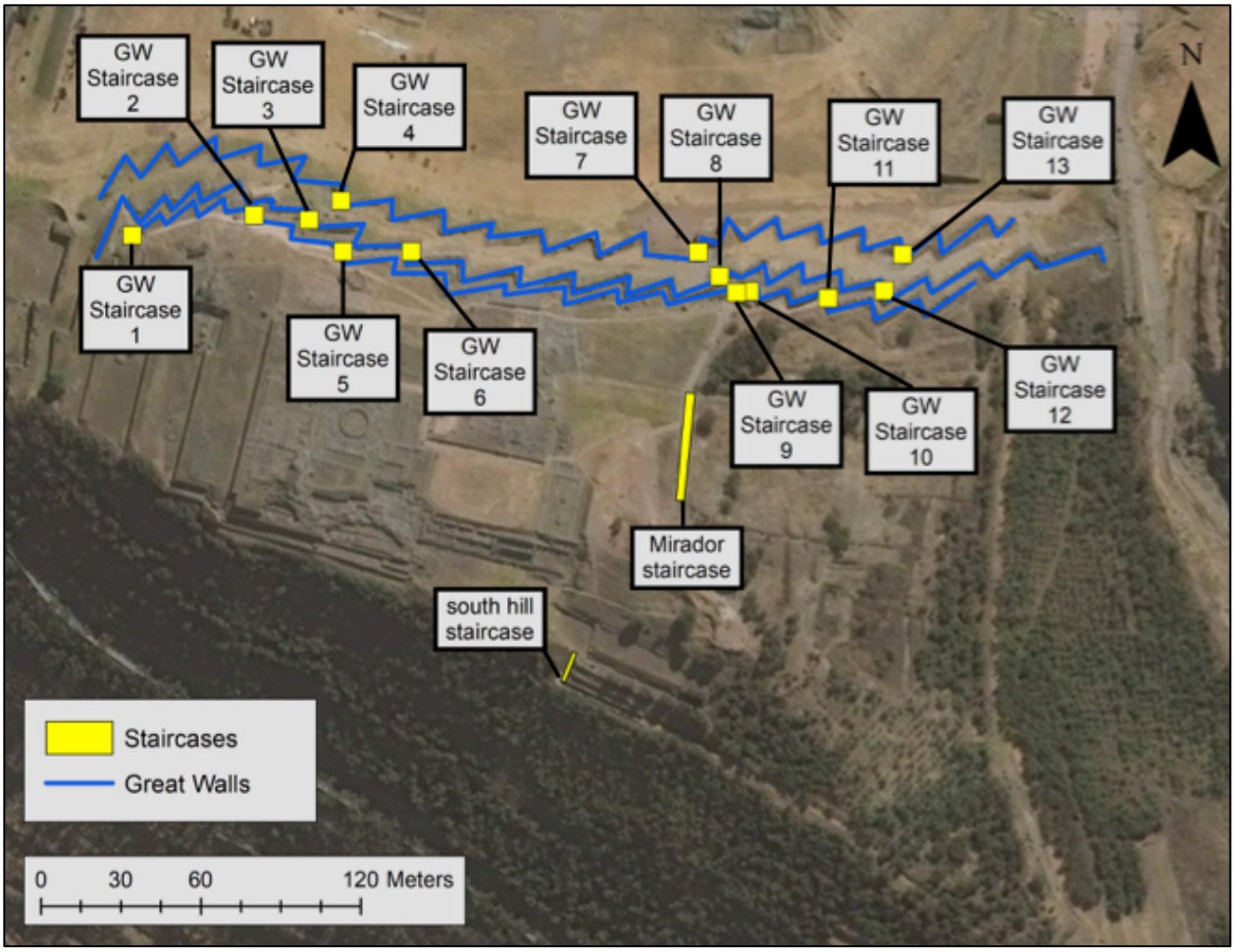

Figure 6.6: Locations of all known staircases at Saqsaywaman

stones of a terrace wall. Most terrace wall remains are currently missing their top layers of stones, leaving it unknown whether or not they originally contained fountains. For this reason, I assumed that fountains could have possibly been used in other areas of the site.

I assumed that no vertical drops were used because there was no evidence of vertical drops on site. If they had been used, evidence would likely still be visible in terrace wall remains because the drops would have been carved into the whole length of the terrace walls.

VI.A.2. Surface Channels

At Saqsaywaman today, some remains of carved channel sections are present (Figure 6.7), implying that there could have been a network of surface channels on site during the Incan era. While some of these channel sections have been restored based on their initial locations, many others are no longer in their original positions (Morrisset, 2016), making it nearly impossible to determine definitively where channels were originally located on site.

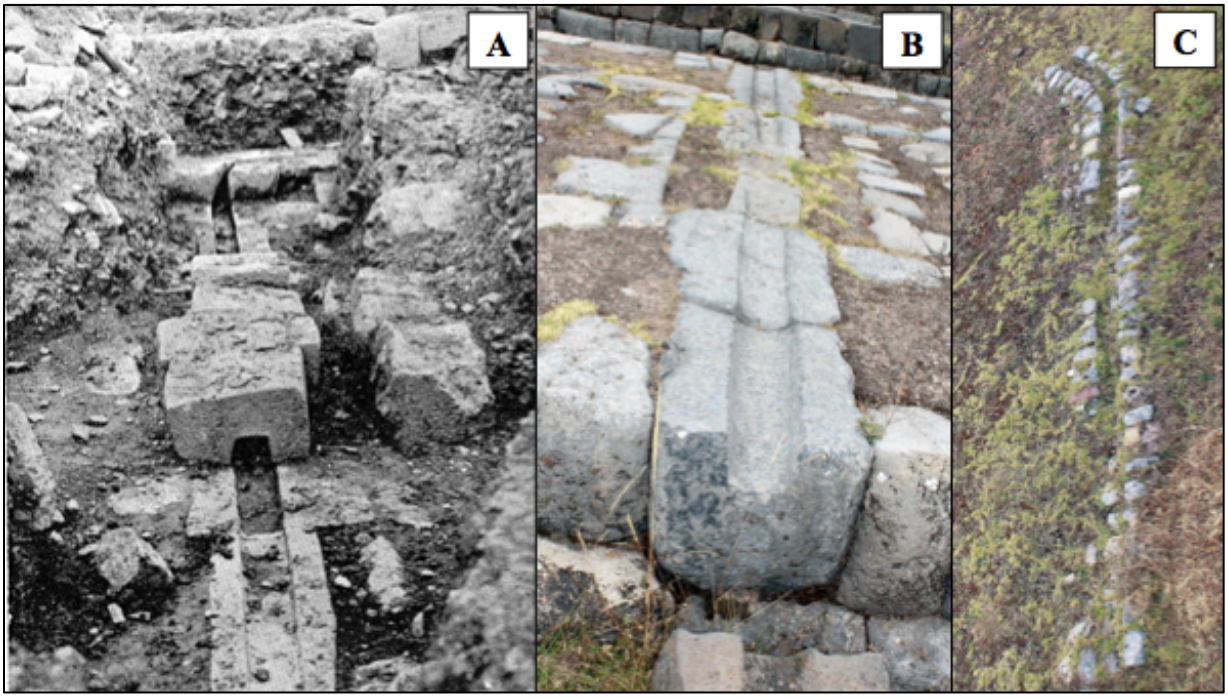

Figure 6.7: Examples of channel remains at Saqsaywaman: a) Channel section discovered in 1934 (Valcarcel); b) Reconstructed channel in the tower sector (Morrisset, 2016); c) Partially buried channel on a west hill terrace (Morrisset, 2016)

At other Incan sites near Saqsaywaman, some surface channels were placed along the bases of terrace walls (I will refer to these as "base" channels), while others ran across the terraces' widths (I will refer to these as "orthogonal" channels). An example of both of these types of channels can be seen at Tipon (Figure 6.8). Orthogonal channels were mostly used to

connect a base channel to a hydraulic drop or to connect two hydraulic drops. Base channels were typically used to carry water along the lengths of terraces.

Based on the hydraulic drops I assumed were present at Saqsaywaman, I assumed that base channels made up the majority of the channels on site because they could have carried surface water from anywhere on the terraces directly to the staircase channels. I also assumed that some orthogonal channels were used to connect base channels and fountains in the south and southeast areas of Saqsaywaman.

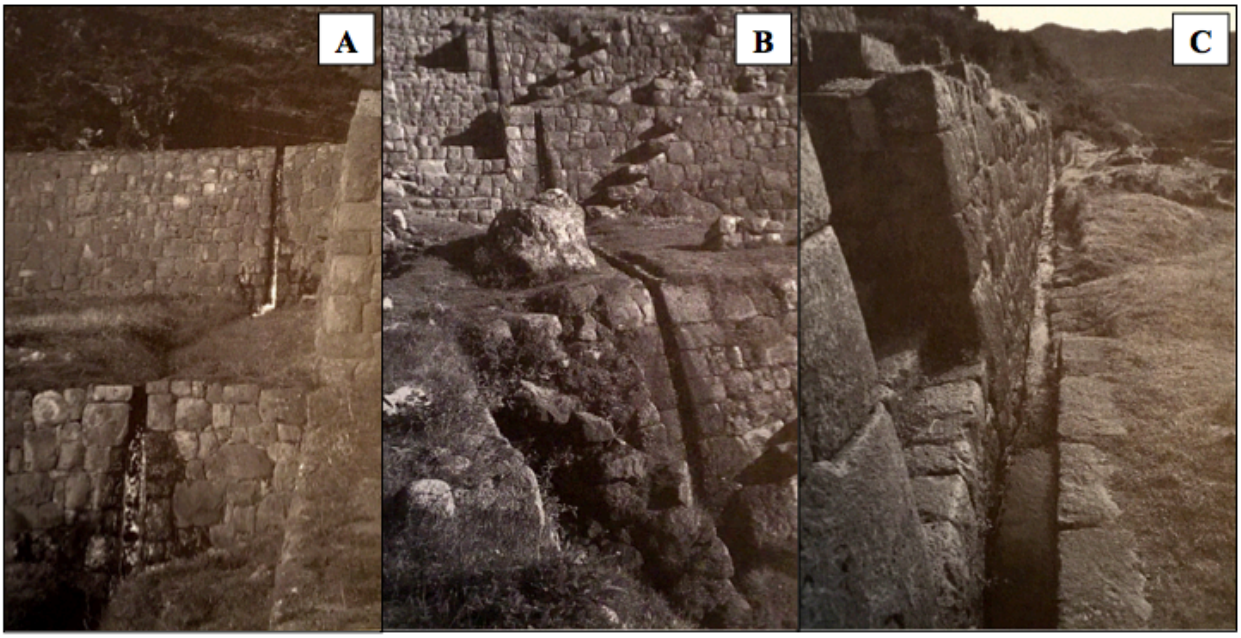

Figure 6.8: a,b) Hydraulic drops and orthogonal channels at Tipon; c) Base channel at Tipon (Wright, 2006)

VI.A.3. Proposed Surface Drainage System Reconstruction

From the drainage features discussed in the previous sections, I designed a possible surface drainage system that could have been built by the Incan engineers at Saqsaywaman (Figures 6.9 and 6.10). The site did not have much remaining evidence of surface drainage features to guide the design, so it was based mostly on meeting the site's perceived hydraulic needs while staying within the confines of typical Incan design techniques. Figure 6.9 shows the

design with my proposed terrace system reconstruction included for reference. Figure 6.10 shows the system without the referential terrace system so that the proposed surface drainage system can be viewed more easily.

I assumed every staircase on site was lined with a channel that functioned as a hydraulic drop. I assumed that the tops of all terraces were flat planes that sloped laterally in the directions of natural elevation decrease that were outlined in Figure 5.19. I also assumed the tops of terraces sloped slightly inward orthogonally so that water landing on the terraces would flow into

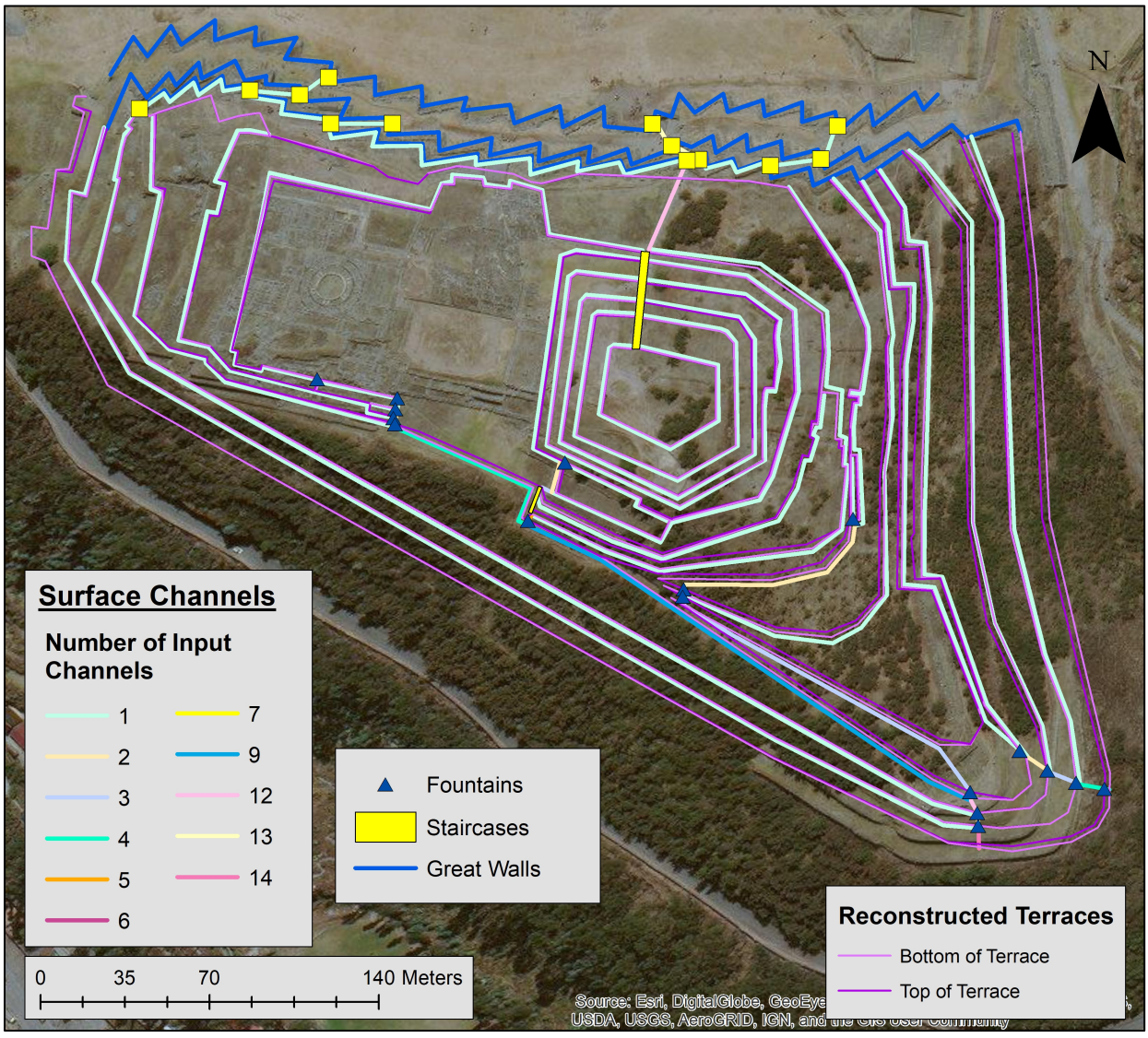

Figure 6.9: Proposed design of a possible original surface drainage system at Saqsaywaman (with proposed terrace system reconstruction for reference)

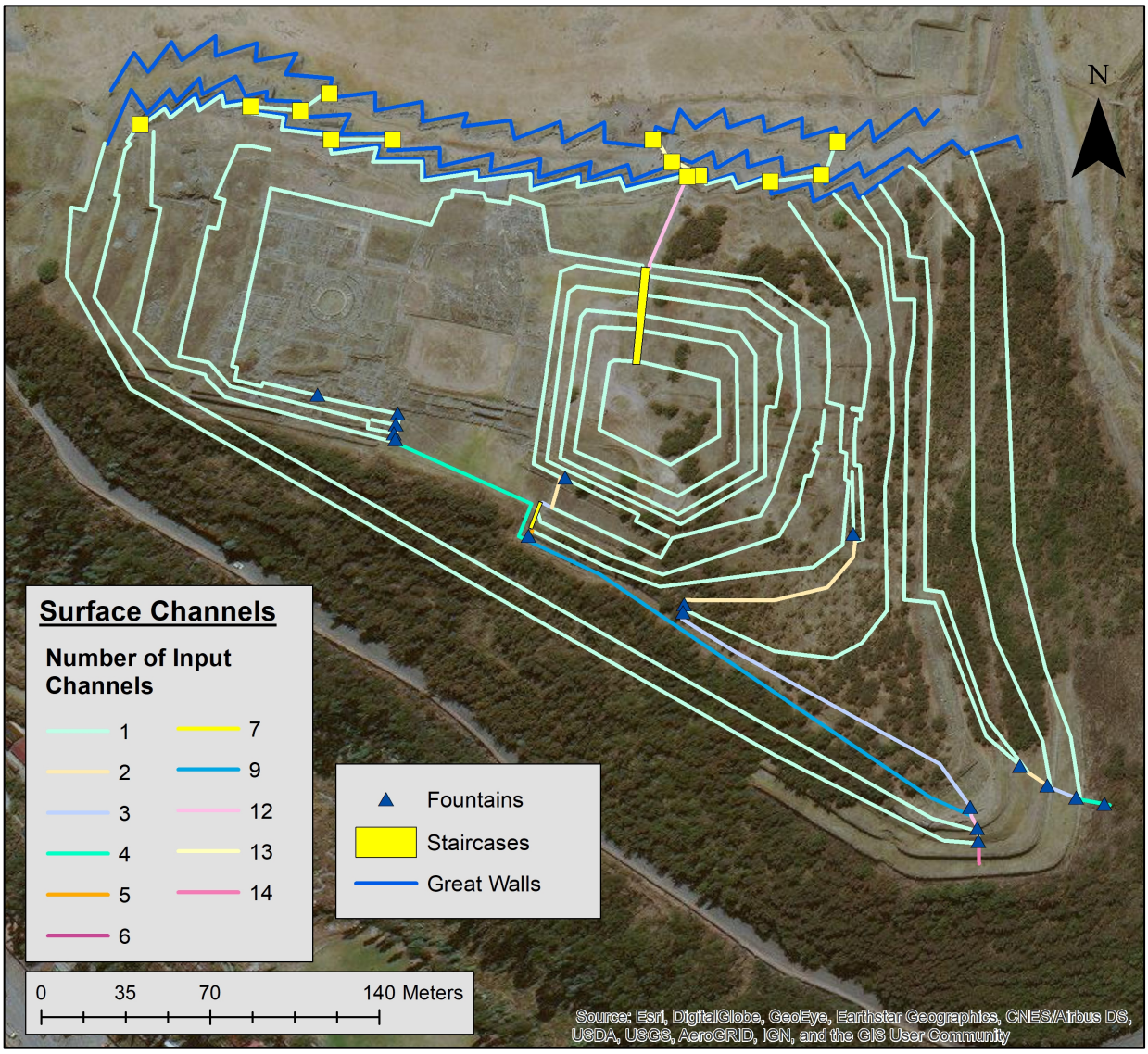

Figure 6.10: Proposed design of a possible original surface drainage system at Saqsaywaman

the base channels rather than flowing over the edges of the terraces. I assumed that each surface channel was gravity-fed, with the channel slopes following the rough directions of elevation from Figure 5.19.

In Figures 6.9 and 6.10, the surface channels were color-coded to show the number of input channels feeding into each of the channels. The surface channels connected to the staircase channels wherever possible to move water down and out of the site. In locations where the surface channels could not reach the staircase channels, fountains were used as hydraulic drops.

To direct water out of the site, most water would drain out of the southeast corner into the ravine, or onto the plaza north of the site. I assumed that the northern plaza had a subterranean layer of chipped rock and gravel so that the plaza could "receive and infiltrate" runoff. This same technique was also used in the plaza at Machu Picchu to collect and disperse runoff from the terraces without flooding the plaza area (Wright & Zegarra, 2000).

VI.D. Hydraulic Analysis of Proposed Surface Drainage System

To validate the efficacy of my proposed surface drainage system as a means of stormwater control, I analyzed what flow capacities these features could potentially handle. First, I determined the flow rates that the surface channels would need to be able to receive. Then, I calculated the dimensions of the surface channels from these flow rates. Last, I calculated what size the hydraulic drops would need to be to receive the flow from the surface channels.

Lacking adequate evidence of original channel dimensions at Saqsaywaman, I used flow measurements from surface channels at Tipon as a starting point for calculating my design surface channel dimensions. At Tipon, it was found that the central terrace channels carried a discharge of about 820 L/min, or 0.0137 m^3/s (Wright, 2006). For surface channels with more than one input channel, I assumed that their maximum flow rates were 0.0137 m^3/s multiplied by the number of input channels.

To determine the dimensions needed for the surface channels to carry these flow rates, Manning's equation (equation 6.1) for open channel flow was used,

$$Q = \left(\frac{k}{n}\right) A_W R_H^{\frac{2}{3}} S^{\frac{1}{2}}$$

Equation 6.1

where Q is the volumetric flow rate through the channel in units of m^3/s, n is a dimensionless roughness coefficient determined by the roughness of the channel materials, k is 1.0 for SI units, A_W is the cross-sectional area of flow (or "wetted" cross-sectional area) in units of m^2, R_H is the hydraulic radius (which is calculated from equation 6.2) in units of m, and S is the slope of the channel in the direction of flow in units of m/m. Hydraulic radius (R_H) is the ratio of the wetted cross-sectional area (A_W) to the wetted perimeter in a channel (P_W). Hydraulic radius is calculated in equation 6.2 below.

$$R_H = \frac{A_W}{P_W}$$

Equation 6.2

I assumed channels utilized the "best" hydraulic section rule for uniform flow, which states that a channel's depth should be half the length of its width. Following this rule provides the maximum flow rate for a given cross-sectional area by minimizing the wetted perimeter and therefore minimizing frictional forces on flow (Elger et al., 2013). This rule is represented by equation 6.3.

$$d = \frac{1}{2}w \quad OR \quad w = 2d$$

Equation 6.3

Substituting the relationship described by equation 6.3, A_W is shown by equation 6.4 and P_W is shown by equation 6.5.

$$A_W = dw = 2d^2$$

Equation 6.4

$$P_W = 2d + w = 4d$$

Equation 6.5

Substituting equations 6.4 and 6.5 into equation 6.2, R_H is simplified to equation 6.6.

$$R_H = \frac{2d^2}{4d} = \frac{1}{2}d$$

Equation 6.6

Substituting equations 6.4 and 6.6 into equation 6.1, the design depth of flow can be calculated using equation 6.7.

$$d = 0.917\left[\left(\frac{n}{k}\right)\frac{Q}{S^{1/2}}\right]^{3/8}$$

Equation 6.7

After finding the design depth of flow, the design channel width can be found using equation 6.3.

Manning's roughness coefficient *n* was considered to be 0.02 for the stone-lined canals at Machu Picchu (Wright & Zegarra, 2000) and Tipon (Wright, 2006), so 0.02 was also used for Manning's *n* at Saqsaywaman.

The directions of the slopes of the surface base channels were determined from the general decreases of elevation outlined in Figure 5.19. I calculated a rough average slope for each general region of the site (Figure 6.11), and used those slopes in my base channel calculations. The calculated surface base channel dimensions are shown in Table 6.1.

Orthogonal channel slopes could not follow the topographic elevation changes because, as I discussed in Section VI.A.3, I assumed that the tops of terraces sloped slightly inward orthogonally to ensure water would get to the base channels. I wanted water in the orthogonal channels to flow outward, not inward, so I assumed that each orthogonal channel had a slope of about 0.020 m/m in the desired direction of flow. The calculated orthogonal channel dimensions are shown in Table 6.2.

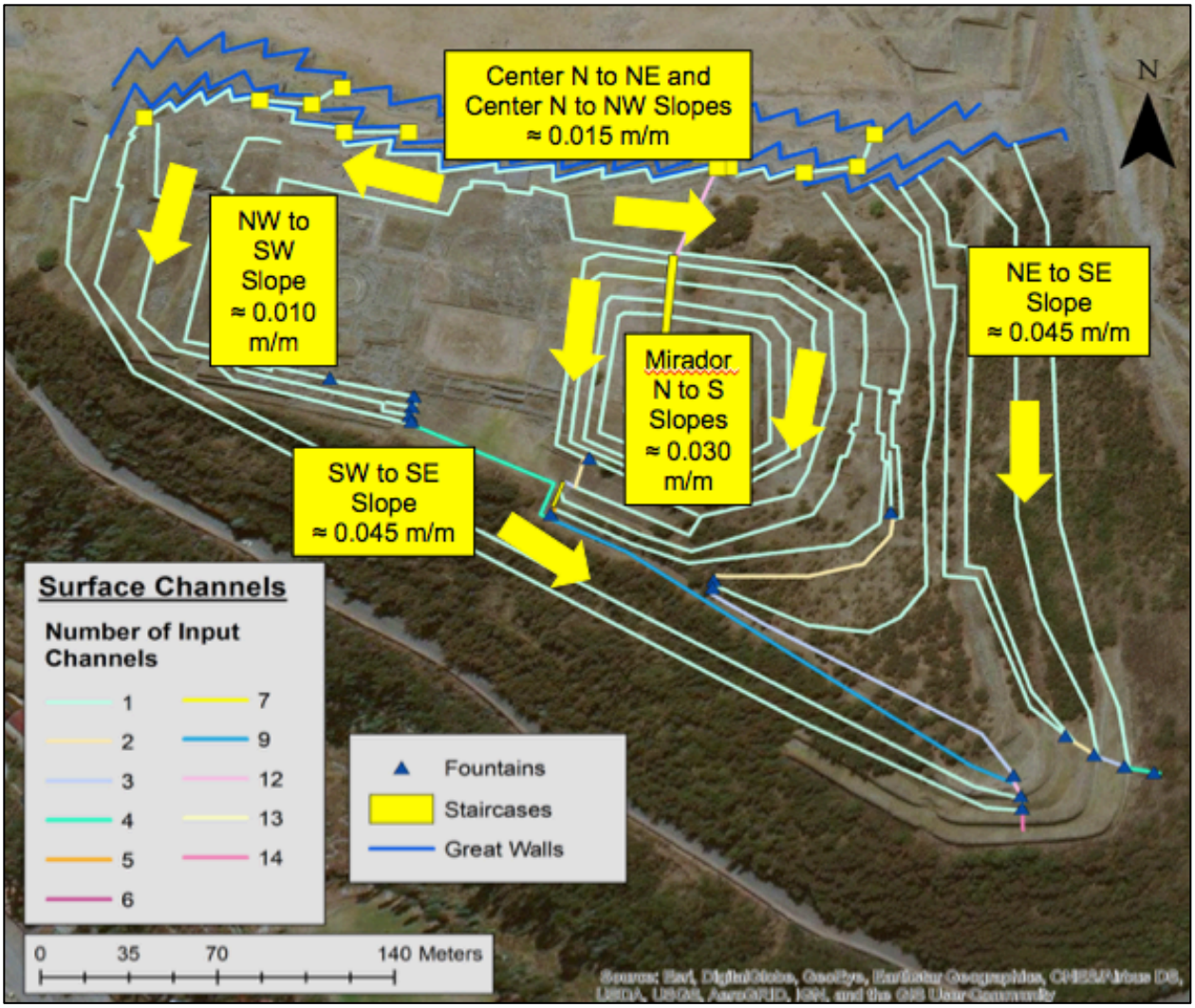

Figure 6.11: Average slopes of surface base channels across the site

Table 6.1: Surface base channel dimensions

Channel #	Region	Number of Input Channels	Q (m^3/s)	S (m/m)	d (cm)	w (cm)
1	NW to SW	1	0.0137	0.010	10.04	20.07
2	SW to SE	1	0.0137	0.045	7.57	15.14
3		4	0.0548	0.045	12.73	25.46
4		9	0.1233	0.045	17.25	34.51
5	NE to SE	1	0.0137	0.045	7.57	15.14
6		2	0.0274	0.045	9.82	19.63
7	Mirador N to S	1	0.0137	0.030	8.17	16.33
8		2	0.0274	0.030	10.59	21.18
9	N	1	0.0137	0.015	9.30	18.60

Table 6.2: Surface orthogonal channel dimensions

Number of Input Channels	Q (m^3/s)	d (cm)	w (cm)
1	0.0137	8.81	17.62
2	0.0274	11.43	22.86
3	0.0411	13.30	26.61
4	0.0548	14.82	29.64
5	0.0685	16.11	32.23
6	0.0822	17.25	34.51
7	0.0959	18.28	36.56
8	0.1096	19.22	38.44
9	0.1233	20.09	40.17
10	0.137	20.90	41.79
11	0.1507	21.66	43.31
12	0.1644	22.38	44.75
13	0.1781	23.06	46.11
14	0.1918	23.71	47.41

Next, I calculated the dimensions needed for the staircase channels to receive the surface channel flows using Equations 6.7 and 6.3. I assumed the maximum flow volume received by each staircase channel was the sum of the flow volumes of all of the surface channels that input into the staircase channel. The calculated staircase channel dimensions are shown in Table 6.3.

Within the Great Walls, the staircase channels were not the only means of runoff control. There were also many ports present. The flow capacities of the ports were analyzed by Joseph Torp and Kenneth Lohr in 2014, and were found to be able to handle a total of 0.2318 m^3/s and an average of 0.0052 m^3/s per port when operating at maximum capacity.

I assumed that the fountains had the same dimensions as the channels feeding into them. The jet of water flowing out of a fountain would travel a certain horizontal distance away from the fountain before landing on the terrace below it. It is useful to know the horizontal jet distance for fountains that outlet into base channels so that the base channels can be placed the correct horizontal distance away from the fountain to receive the jet. For fountains that outlet into ortho-

Table 6.3: Staircase channel dimensions

Staircase	Number of input channels	Q (m^3/s)	S (m/m)	d (cm)	w (cm)
Mirador	12	0.1644	0.29	13.54	27.08
South Hill	4	0.0548	0.51	7.24	14.49
GW1	1	0.0137	0.60	4.66	9.31
GW2	1	0.0137	1.00	4.27	8.53
GW3	1	0.0137	1.20	4.12	8.25
GW4	1	0.0137	1.20	4.12	8.25
GW5	1	0.0137	1.80	3.82	7.64
GW6	1	0.0137	0.80	4.45	8.90
GW7	13	0.1781	1.20	10.69	21.38
GW8	13	0.1781	1.00	11.07	22.14
GW9	6	0.0822	2.40	7.24	14.49
GW10	7	0.0959	2.40	7.24	14.49
GW11	1	0.0137	1.60	3.91	7.81
GW12	1	0.0137	2.00	3.75	7.49
GW13	1	0.0137	1.20	4.12	8.25

gonal channels, it is less important to know the horizontal jet distance because the orientation of the orthogonal channel in relation to the fountain will cause it to necessarily lie in the jet's path. The horizontal jet distance can be calculated using the Woodburn Equation (Equation 6.8),

$$x = \sqrt{\frac{2v^2}{g}\Delta y}$$

Equation 6.8

where x is the horizontal distance traveled by the jet in units of m, y is the vertical distance traveled by the jet in units of m, v is the velocity of the jet in units of m/s, and g is the gravitational constant of 9.81 m/s^2. The Woodburn Equation is shown visually in Figure 6.12.

The jet velocity, v, can be calculated using Equation 6.9,

$$v = \frac{Q}{d * w}$$

Equation 6.9

where Q is the volumetric flow rate of the jet in units of m^3/s, d is the fountain depth in units of m, and w is the fountain width in units of m.

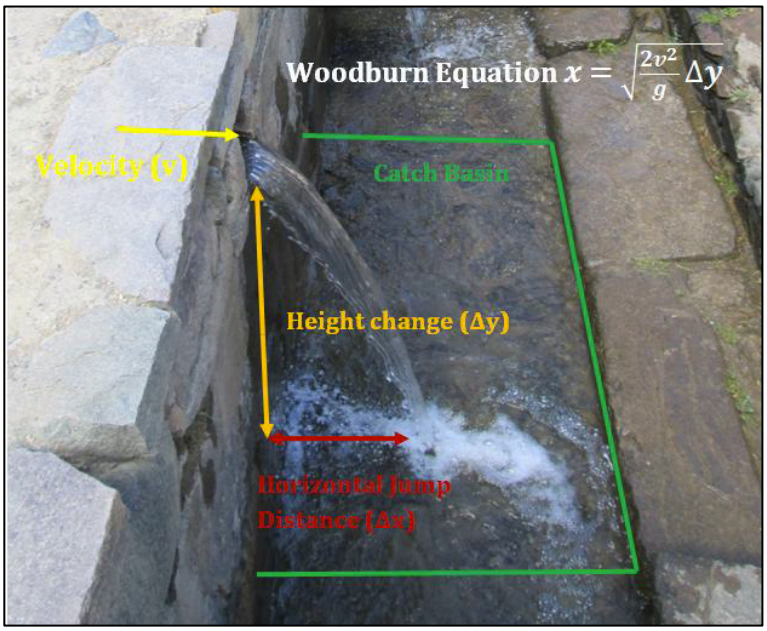

Figure 6.12: Woodburn Equation diagram (Lohr, 2014)

The horizontal jet distance, x, was calculated using Equations 6.8 and 6.9 from the surface base channel flow rates and dimensions in Table 6.1. The average terrace height was about 2.5 m, so 2.5 m was used as the vertical jet distance in the calculations. The jet calculations are shown in Table 6.4.

Table 6.4: Fountain jet horizontal distances (from base channel flow rates and dimensions)

Channel #	***Q*** **(m^3/s)**	***d*** **(m)**	***w*** **(m)**	***v*** **(m/s)**	***x*** **(m)**
1	0.0137	0.100	0.201	0.680	0.486
2	0.0137	0.076	0.151	1.196	0.854
3	0.0548	0.127	0.255	1.691	1.207
4	0.1233	0.173	0.345	2.071	1.478
5	0.0137	0.076	0.151	1.196	0.854
6	0.0274	0.098	0.196	1.422	1.015
7	0.0137	0.082	0.163	1.027	0.733
8	0.0274	0.106	0.212	1.221	0.872
9	0.0137	0.093	0.186	0.792	0.565

VII. RUNOFF ANALYSIS

A runoff analysis was conducted to show how the proposed reconstruction of the original Incan drainage infrastructure would perform during a storm event. For this analysis, first, a design storm was created using historical precipitation data from the Cusco-Pisac region of Peru. Next, the National Resources Conservation Service (NRCS) Runoff Curve Number method (USDA, 1986) was used to calculate the quantity of runoff generated by the design storm. This calculation was done twice – first, for Saqsaywaman's current land cover, and second, for its assumed Inca-era land cover. From this, the flow paths of the generated runoff were mapped onto the site. Then, the effects of the proposed original drainage infrastructure on runoff were calculated and discussed. These methods of analysis are described in greater detail in the following sections. ArcGIS was a major tool used in these analyses.

VII.A. Design Storm from Historic Climate Data

The Inca were masterful civil engineers for many reasons, one of which being that they designed their drainage infrastructure to handle even unexpectedly large storms. For this reason, a hundred-year storm was chosen as the design storm to use for runoff analyses of Saqsaywaman. A hundred-year storm is a precipitation event that is statistically likely to occur only once in every one hundred years. Scientists are able to estimate the size of future hundred-year storms from statistical calculations of historical climate records.

Historical precipitation data (from the Universidad Nacional de San Antonia Abad del Cusco (UNSAAC)) was available for the Cusco-Pisac region from 1964 to 2010 (Figure 7.1). This data shows the annual maximum rainfall that occurred within a twenty-four hour period in

the month of January, which is mid-way through Cusco's three-month-long rainy season. Half of Cusco's mean annual precipitation occurs during this season (Perry et al., 2014).

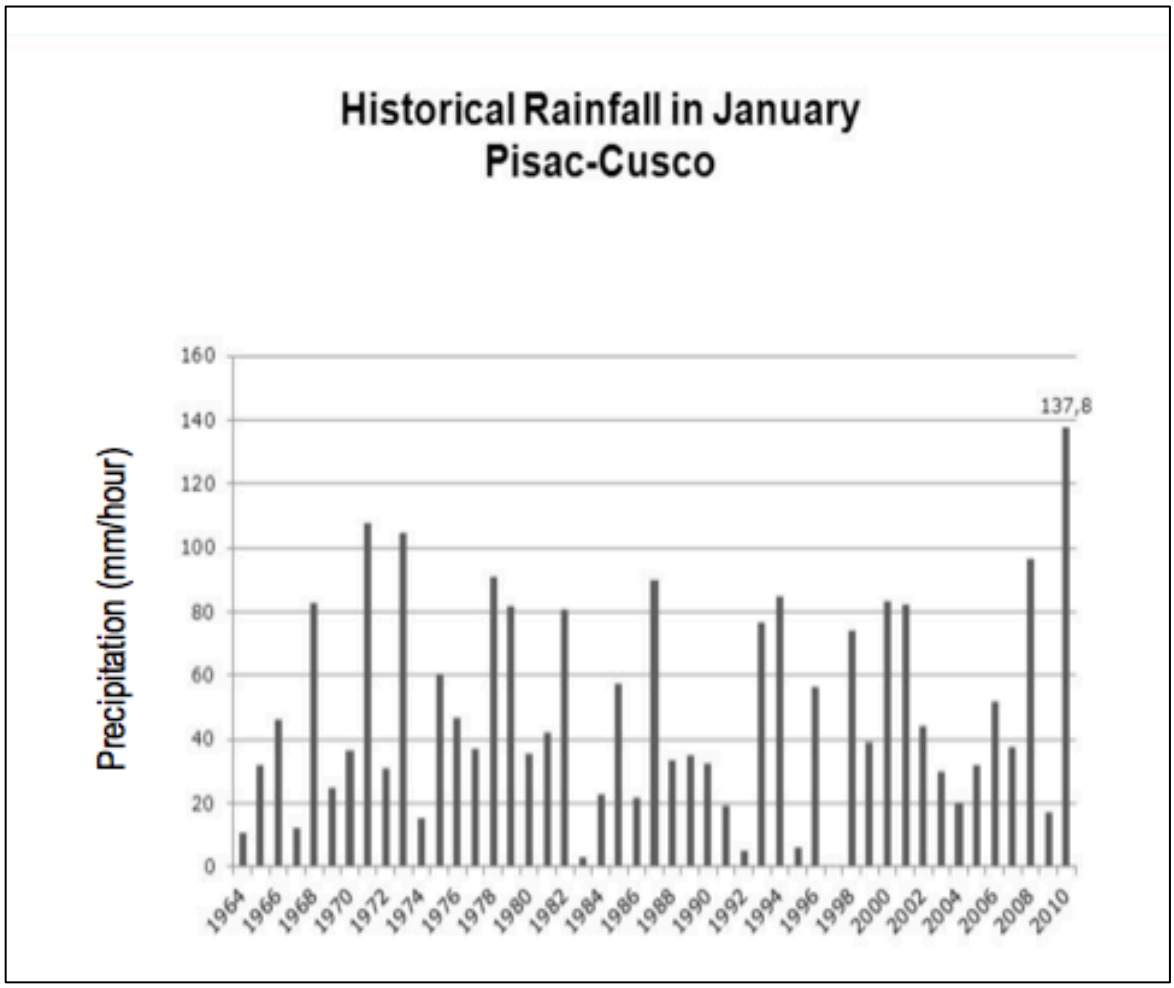

Figure 7.1: Annual maximum precipitation occurring over a 24-hour period in January from 1964 to 2010 in the Cusco-Pisac region (UNSAAC)

A method described by Tom Di Liberto for NOAA explains how statistical forecasting can be used to estimate a hundred-year storm when one hundred years of climate data are not available. This method was recreated to determine the hundred-year storm for the Cusco-Pisac region from the data in Figure 7.1 above. All statistical calculations were done using R 3.5.1 software (see Appendix XI.B for the R code used).

First, the data was sorted in order of smallest to largest precipitation event (Figure 7.2).

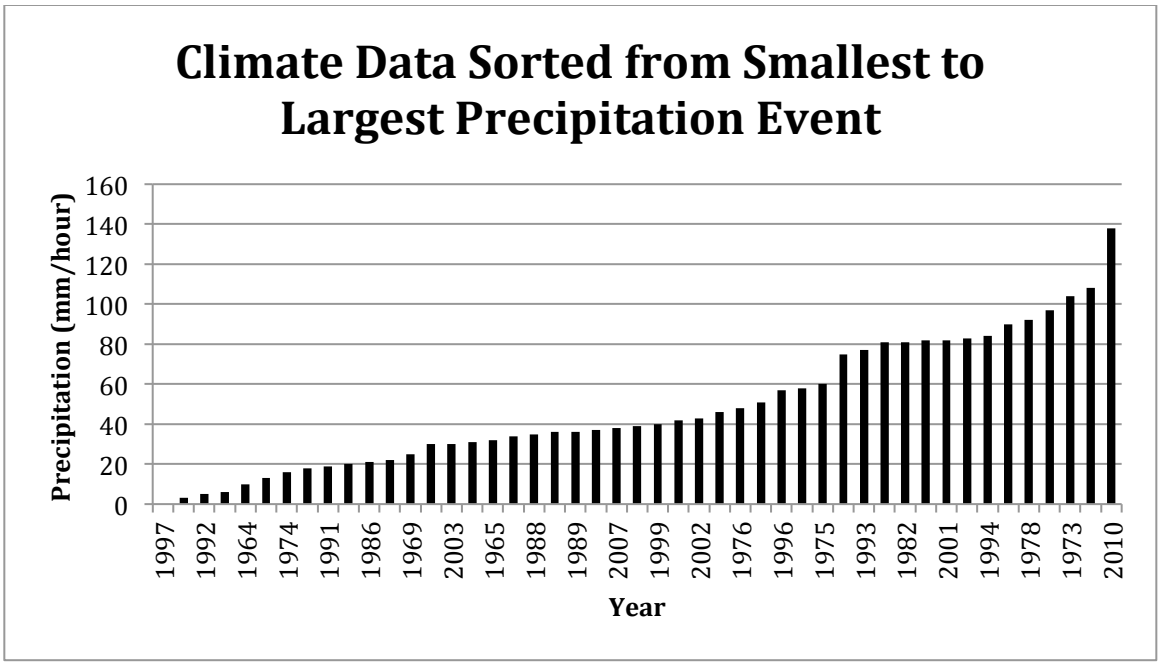

Figure 7.2: Annual maximum precipitation occurring over a 24-hour period in January from 1964 to 2010 in the Cusco-Pisac region, sorted from smallest to largest precipitation event

Next, the precipitation was sorted into "bins", with a "bin" for 0 to 5 mm/hour of rainfall, 6 to 10 mm/hour of rainfall, et cetera, which grouped the years by density of occurrence of storm sizes. Density of storm occurrence was plotted as a histogram, and a normal distribution curve was fitted to the histogram (Figure 7.3). The quality of the fit of the normal distribution to the histogram is directly correlated with the amount of historical data available – the more years of data used, the closer the normal distribution should fit the histogram. For the histogram in Figure 7.3, the mean storm size was 48.4 millimeters per hour (1.91 inches per hour), and the standard deviation was 32.4 millimeters per hour (1.28 inches per hour).

After the normal distribution curve was generated, the hundred-year storm was determined by finding the area under 99% of the curve. The hundred-year storm for the Cusco-Pisac region was found to be 123.7 inches per hour, or 4.87 inches per hour. This was used to create an hour-long design storm with fifteen-minute intervals (Table 7.1).

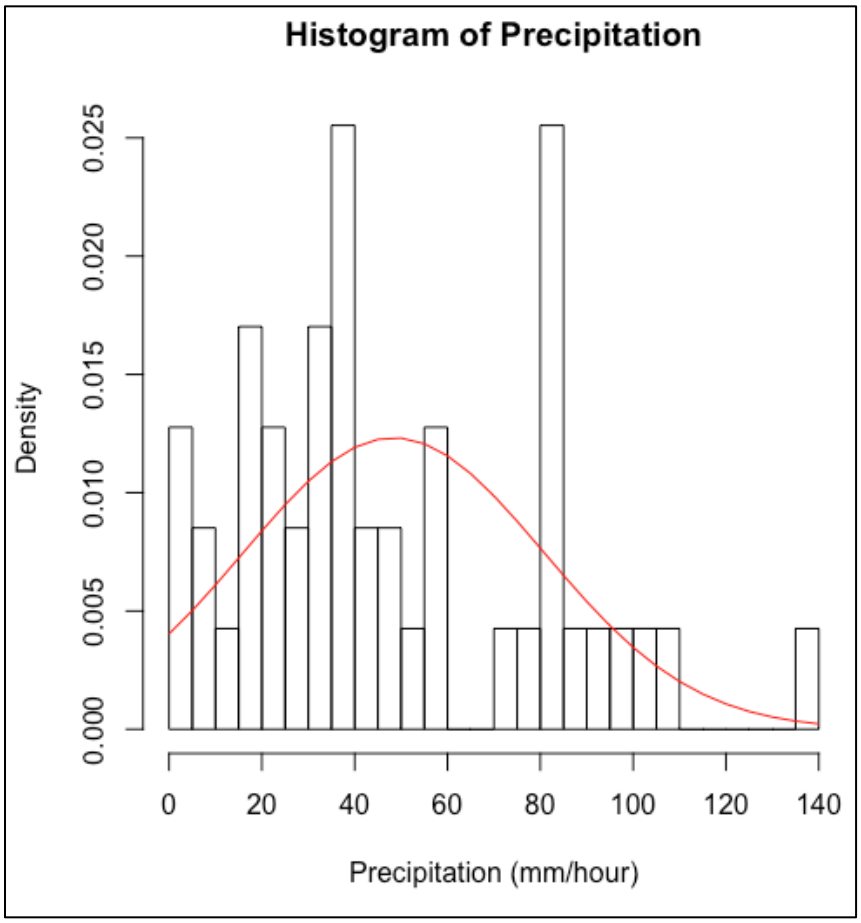

Figure 7.3: Annual maximum precipitation occurring over a 24-hour period in January from 1964 to 2010 in the Cusco-Pisac region, sorted by density of occurrence and fitted with a normal distribution (red line)

Table 7.1: Design storm modeled from the Cusco-Pisac region hundred-year storm

i	t_i (min)	P_i (mm)	P_i (in)
1	15	23.7	0.93
2	30	37.0	1.46
3	45	38.0	1.50
4	60	25.0	0.98

VII.B. Runoff Curve Number Method

To calculate the quantity of runoff generated by the design storm created in the previous section, the NRCS Runoff Curve Number method was used. This method is one of the most widely used to determining runoff volumes for small watersheds. It relies on one main

parameter, curve number (CN), which is a metric used to determine how much precipitation is available as direct runoff during a storm event. CN is chosen from tables that relate land use and soil type to an integer value that represents the perviousness of the ground surface. Larger CN values indicate a more impervious ground surface, and by result, more direct runoff. The full NRCS CN tables are listed for reference in Appendix XI.C.

To calculate runoff using this method, first, the land cover and hydrologic soil type on site were determined. Next, CN values from the tables in Appendix XI.C were assigned to the land cover classes and soil types on site. For each CN, the potential maximum retention (S) was calculated using Equation 7.1.

$$S = \frac{1000}{CN} - 10$$

Equation 7.1

Using the design storm created in the previous section, the excess precipitation (P_e), which is the amount of precipitation available as direct runoff, was calculated using Equation 7.2,

$$P_{e_i} = \frac{(P_i - 0.2S)^2}{P_i + 0.8S}$$

Equation 7.2

where P_i is the depth of precipitation (in inches) at some time t_i, and P_{e_i} is the depth of excess precipitation (in inches) available from that amount P_i.

In the following sections, the steps listed above are described in more detail as they are applied to calculate the runoff generated by the design storm at Saqsaywaman.

VII.B.1. Land Cover Classification

Current Land Cover

The current land cover on site was grouped into five classes: short grasses, tall grasses, small trees and shrubs, compacted dirt, and impermeable clay (Figure 7.4). Small trees and shrubs cover 48.8% of the site area. They are mainly located on the east and south faces of the site. Short grass covers 32.1% of the site area and is mainly located where original or reconstructed terraces have been maintained. Some of the short grass areas also contain roughly 10% exposed stone (Lohr, 2014), which makes up terrace retaining walls and other foundational remains, but this amount of stone was not large enough to affect runoff calculations and so was not considered its own land cover class. Tall grass covers 11.5% of the site area and is located in

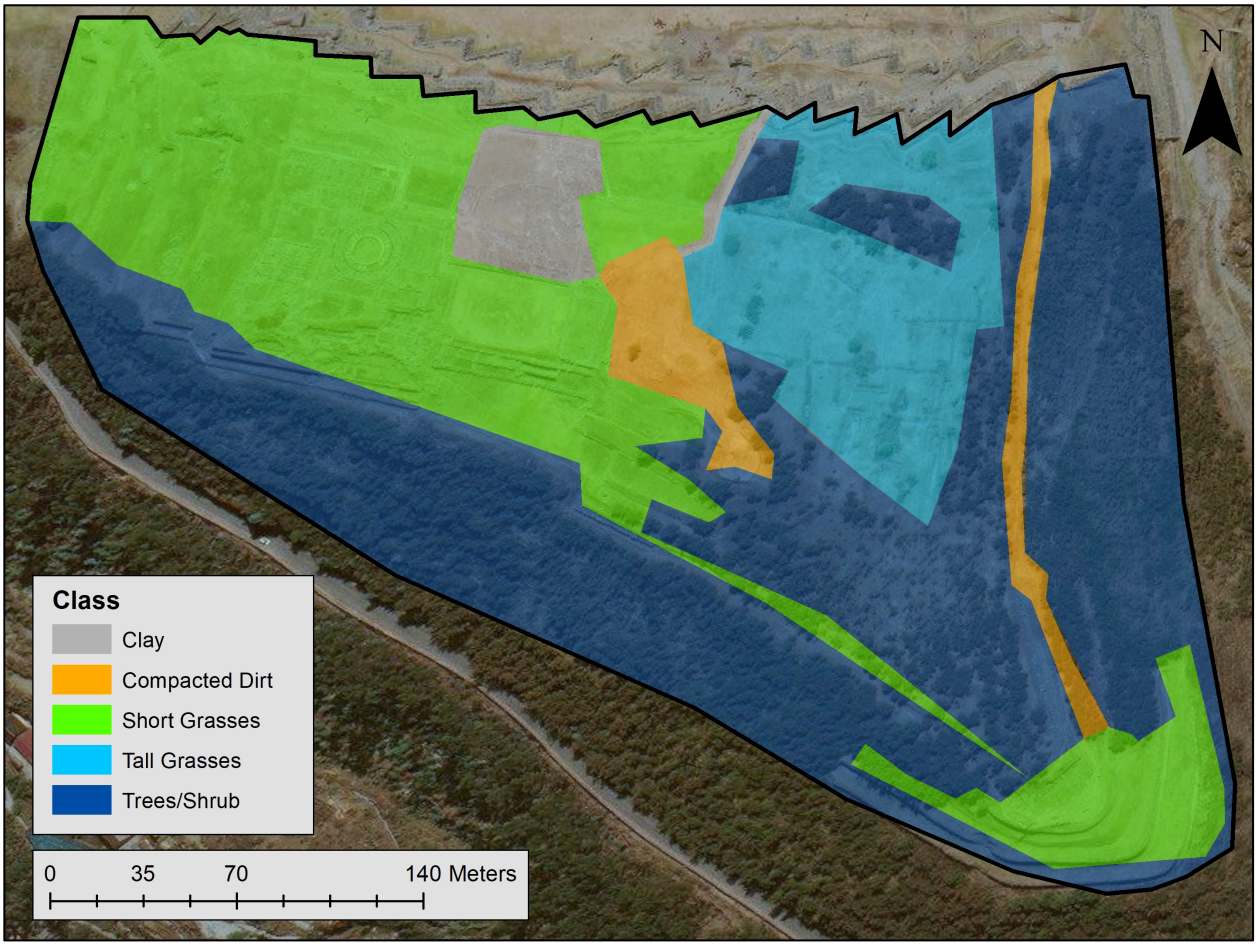

Figure 7.4: Current land cover at Saqsaywaman

the northeast area of the site. Grasses that were at least 3 to 4 inches tall were considered tall grasses (Lohr, 2014). Compacted dirt covers 4.5% of the site area and is located in the areas of the site that are open to tourists and receive a high volume of foot traffic. Impermeable clay covers 3.1% of the site area and is located in two places on site – the path leading up to the Mirador lookout point and the clay cover above the third Great Wall.

Inca-Era Land Cover

During the rule of the Incas, the land cover at Saqsaywaman probably would have looked different than it does today. There was no empirical evidence left on site to indicate what the original land cover was. However, valid assumptions about the original land cover can be made using other better-preserved Incan sites as examples and using archeological and historical observations as justification.

At other Incan sites near Saqsaywaman, there tended to be two main types of land cover: short grass and residential areas. I assumed that Saqsaywaman originally had both of those land cover types, as well as a third type: gravel. I assumed that gravel covered all ceremonial terraces at Saqsaywaman, while non-ceremonial terraces were covered in short grass. Ceremonial terraces were constructed of finely cut stonework, were large in size, and usually had fountains meant for aesthetic display. The use of beautiful stonework and fountains indicated ceremonial importance, because stone and water were sacred to the Inca (Dean, 2010; Dean, 2011; Morrisset, 2016). In contrast, non-ceremonial terraces were constructed of rough or moderately cut stonework, were smaller in size, and were mainly used for purposes of agriculture, drainage, or hillslope stabilization (Hyslop, 1990; Wright et al., 2016). From this definition, the Great Walls were considered ceremonial terraces.

The assumption that all ceremonial terraces at Saqsaywaman were covered in gravel was based off of the discovery that each of the Great Walls were originally covered in 30-50 cm of gravel (Valcarcel, 1934). An observation made by de la Vega led me to assume that the lower three west hill terraces were also originally part of the Great Walls. He wrote that the Great Walls were "in the shape of a half-moon," and at their ends, they met "the other wall of smooth masonry on the side facing the city." (de la Vega, 1966) This implied that the Great Walls might have originally rounded either the northeast or northwest corner of the site to make the "half-moon" shape he described and to make their "ends" connect to a wall on the south side of the site. I assumed that they would have rounded the northwest corner of the site to connect to the south walls, because at the northeast, the three non-ceremonial terraces on the east hill connected with the Great Walls (Squier, 1877). The impressive stonework and size of the well-preserved western terraces further corroborated the assumption that they were originally part of the Great Walls, and therefore would have also been covered in gravel.

I also assumed that one wall on the south hill of the site was a ceremonial terrace. De la Vega described a "wall of smooth masonry" and a "thick, freestone wall" on the side of Saqsaywaman facing the city (1966), which implied that the wall was large in size and constructed of finely cut stonework, indicating that it might have been ceremonial. I assumed that this terrace was the large terrace running through the southeast corner, because of the large size of this terrace and the high ceremonial importance of the Cruz Mo'qo area (Morrisset, 2013; Bauer, 2004) that is located in the southeast corner. Under this assumption, this terrace would also have been covered in gravel.

Last, I assumed that one terrace on the east hill might have also been ceremonial – the terrace that connected the Cruz Mo'qo to the Great Walls. A uniquely large port in the second

Great Wall sat at the north end of this terrace (Figure 7.5). I assumed that this port's purpose was mainly ceremonial because it was carved out of finely cut stonework and, unlike the other ports in the Great Walls, directed water south instead of north, routing water towards the ceremonial Cruz Mo'qo area. The terrace connecting the port to the Cruz Mo'qo would have carried water directly from the port to the Cruz Mo'qo, leading to the assumption that the terrace was also ceremonial, and therefore would have also been covered in gravel.

Figure 7.5: Large south-facing port in the second Great Wall (Miksad)

There was no strong indication that any other terraces at Saqsaywaman might have been ceremonial, so I assumed that all of the other terraces were non-ceremonial, and were therefore covered in short grass.

I assumed that the unterraced areas of the tower sector were mainly covered in buildings. As was discussed in Section II.A, de la Vega wrote that this area contained three towers, two of which were residential and one of which was ceremonial. A representation of the remains of building foundations in this area (Figure 7.6) (Alfaro et al., 2014) and the three-dimensional

representation of this area created by Mar & Beltrán-Caballero (from Figure 2.3) showed other small buildings adjacent to the towers in this area. The density of the buildings in these representations led to the assumption that this area's original land cover could most closely be approximated to our modern-day residential land cover.

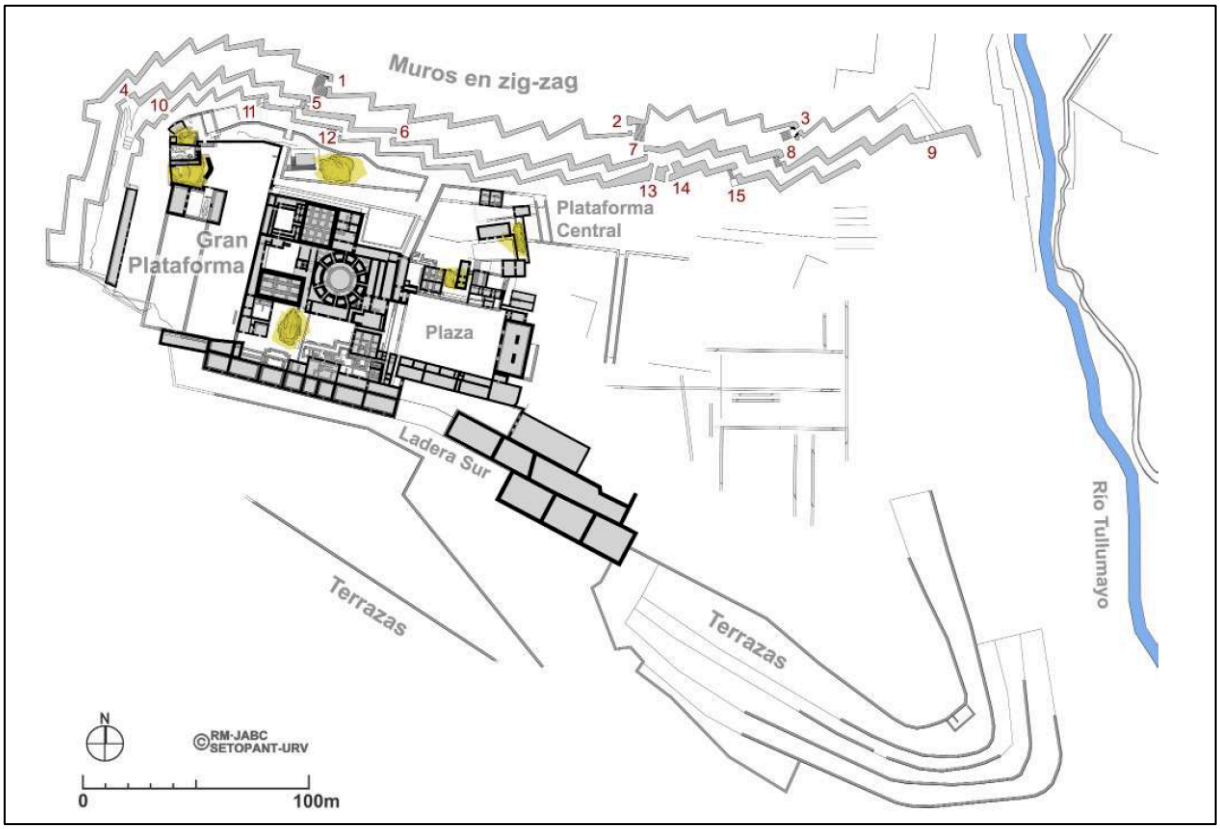

Figure 7.6: Representation of archeological remains in the tower sector (Alfaro et al., 2014)

From the assumptions made above, the proposed original land cover at Saqsaywaman is shown in Figure 7.7. In this representation, short grasses covered 77.2% of the site area, gravel covered 15.0% of the site area, and residential areas covered 7.8% of the site area.

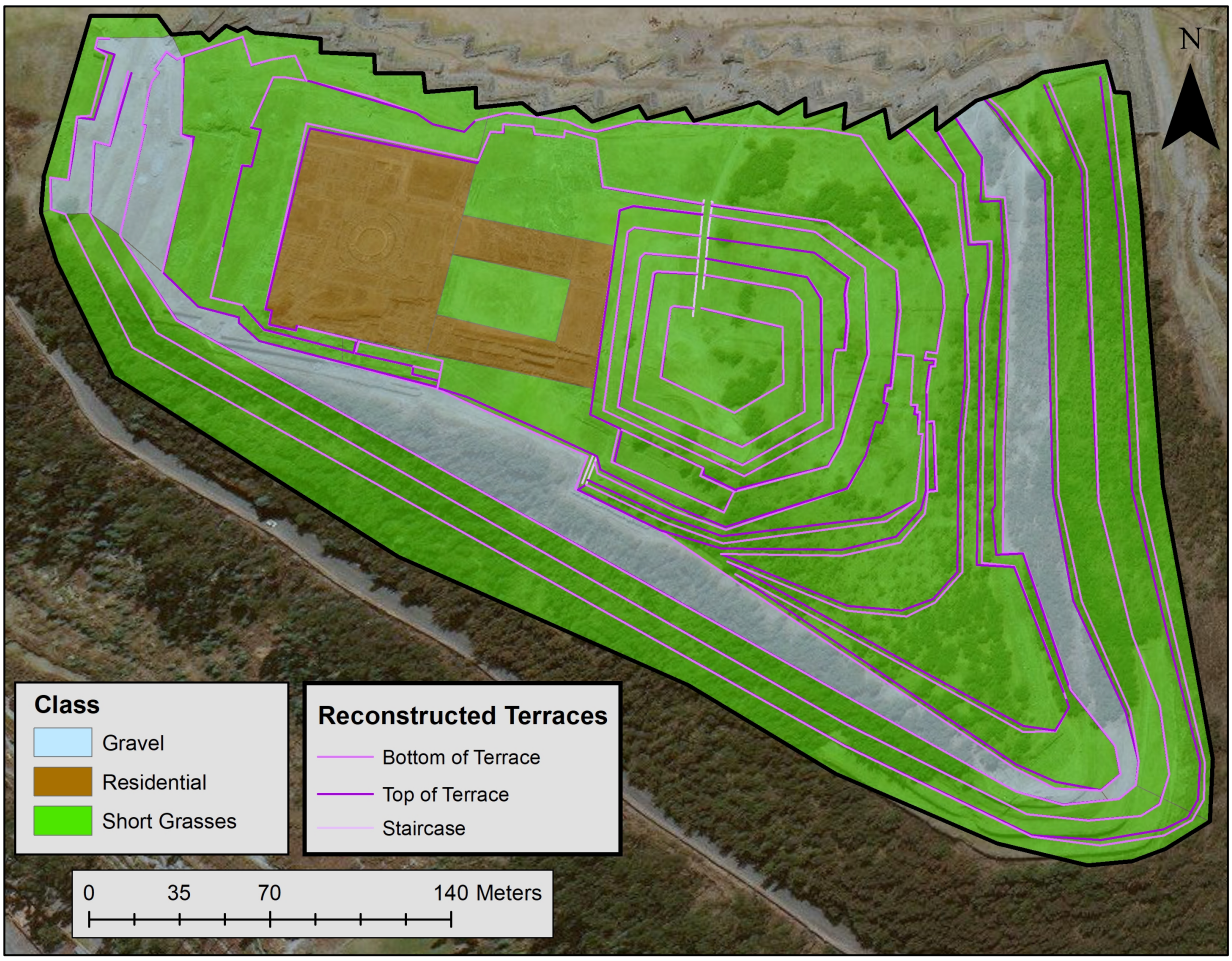

Figure 7.7: Proposed original land cover at Saqsaywaman (overlaid with the proposed terrace system reconstruction for reference)

VII.B.2. Hydrologic Soil Type Classification

A 2007 excavation of the Muyuqmarka and Cruz Mo'qo areas of Saqsaywaman showed that the soils in those areas were mainly clay and clayey silt, which best matched the definition of hydrologic soil group D (INC-Cusco, 2007). Group D soils have "a high runoff potential when thoroughly wet" and "typically have greater than 40 percent clay, less than 50 percent sand, and have clayey textures." (USDA, 2007) There was very limited quantitative data available about the soil types on site besides this excavation report, but visual field inspections showed that the soils were qualitatively similar throughout all areas of the site. For this study, it was assumed that

the whole site is made up of Group D soils, and that the soil type has not significantly changed since the Inca era.

VII.B.3. Assigning Curve Numbers

Current Site Curve Numbers

The land cover classes from Figure 7.4 were assigned CN values from Table 11.1 in Appendix XI.C. The assignments are shown in Table 7.2.

Table 7.2: Current site curve number assignments

Land Cover	**CN Class (from Table 11.1)**	**CN**
Small Trees/Shrubs	Brush: Poor condition	83
Short Grass	Open space: Good condition	80
Tall Grass	Meadow	78
Compacted Dirt	Streets and roads: Dirt	89
Impermeable Clay	Streets and roads: Paved	98

For small trees and shrubs, the CN for "Brush: Poor condition" was chosen because Table 11.1b describes this category as being dominated by brush and having less than 50% ground cover. The trees and shrubs at Saqsaywaman are widely dispersed enough that one can walk through them, and they are frequently heavily trimmed back by the site's maintenance crew.

For short grass, "Open space: Good condition" was chosen because Table 11.1a describes this category as having greater than 75% grass cover, which accounts for the 10% exposed stone that is present in some of the short grass areas.

For tall grass, "Meadow" was chosen because the tall grass areas on site are protected from general walking traffic and are often mowed back by the site's maintenance crew, which fits the description of this category in Table 11.1b.

For compacted dirt, “Streets and roads: Dirt” was chosen because the compacted dirt areas on site are hard-packed enough that they are nearly impermeable, and they bear most of the foot traffic on the site.

For impermeable clay, “Streets and roads: Paved” was chosen because it has the highest CN of all the categories in Table 11.1, and therefore is the most impermeable CN class.

Inca-Era Site Curve Numbers

The land cover classes from Figure 7.7 were assigned CN values from Table 11.1. The assignments are shown in Table 7.3.

Table 7.3: Inca-era site curve number assignments

Land Cover	**CN Class (from Table 11.1)**	**CN**
Short Grass	Open space: Good condition	80
Gravel	Streets and roads: Gravel	91
Residential	Residential: 1/8 acre lot size	92

For the non-ceremonial terraces, “Open space: Good condition” was chosen as the CN class because as was discussed above in Section VII.B.1, these terraces were mainly covered in short grass, which fits Table 11.1a’s description of this class having greater than 75% grass cover.

For the gravel-covered ceremonial terraces, “Streets and roads: Gravel” was chosen as the CN class because gravel-covered roads are most representative of gravel-covered terraces out of all of the classes in Table 11.1.

For the residential areas, the CN class of “Residential districts by average lost size: 1/8 acre or less” was chosen because of the close adjacency of the structural foundations present in these areas.

VII.B.4. Runoff Curve Number Method Results

Using the current site and Inca-era site CN assignments, the maximum potential retention (S) and the excess precipitation (P_{ei}) was calculated for each ith 15-minute period of the hour-long design storm (Table 7.1). These calculations were done using Equations 7.1 and 7.2, and the results are shown in Tables 7.4 and 7.5 below.

Table 7.4: Excess precipitation on current site

CN	S	P_{e1} (in)	P_{e2} (in)	P_{e3} (in)	P_{e4} (in)
83	2.048	0.107	0.354	0.377	0.126
80	2.500	0.064	0.265	0.284	0.079
78	2.821	0.043	0.215	0.231	0.054
89	1.236	0.245	0.598	0.628	0.275
98	0.204	0.726	1.238	1.276	0.776

Table 7.5: Excess precipitation on Inca-era site

CN	S	P_{e1} (in)	P_{e2} (in)	P_{e3} (in)	P_{e4} (in)
80	2.500	0.064	0.265	0.284	0.079
91	0.989	0.314	0.705	0.737	0.348
92	0.870	0.354	0.765	0.798	0.391

VII.C. Mapping Runoff Flow Paths

After the excess precipitation was calculated for the design storm, the runoff flow paths of the excess precipitation were mapped onto the current site topography (from Figure 5.13) and the terraced Inca-era site topography (from Figure 5.11) in ArcGIS. First, contributing area raster maps were generated from the two topographies using the flow accumulation tool in ArcGIS. In a contributing area raster map, the value of each cell is the number of upstream cells that flow into that cell (ESRI). This results in a map that shows where flowing water will accumulate over a three-dimensional surface. In larger areas, contributing area maps are often used to determine

where streams and rivers will form in a watershed. For smaller areas, such as Saqsaywaman, contributing area maps can be used to determine where stormwater runoff will flow. The contributing area maps of Saqsaywaman's current topography and terraced topography are shown below in Figures 7.8 and 7.9, respectively. In the maps, the blue lines color the cells that have at least 100 upstream cells draining into them. This roughly delineates the streamlines that would form on site from runoff during a significant storm event. Each cell has an area of one square meter, so each blue cell has at least 100 square meters of area draining into it. The yellow arrows in Figures 7.8 and 7.9 show the directions of flow of the streamlines.

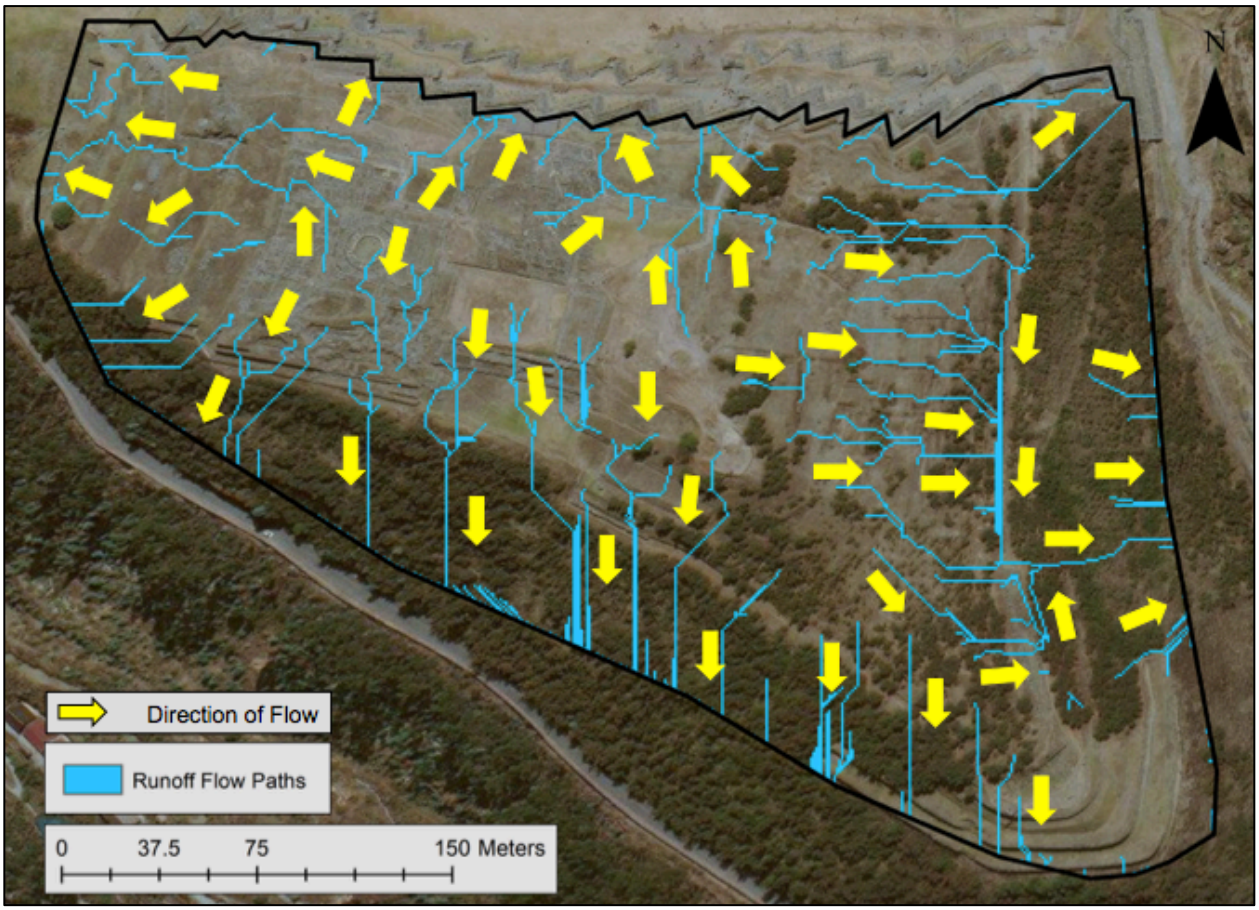

Figure 7.8: Contributing area map of the current site topography

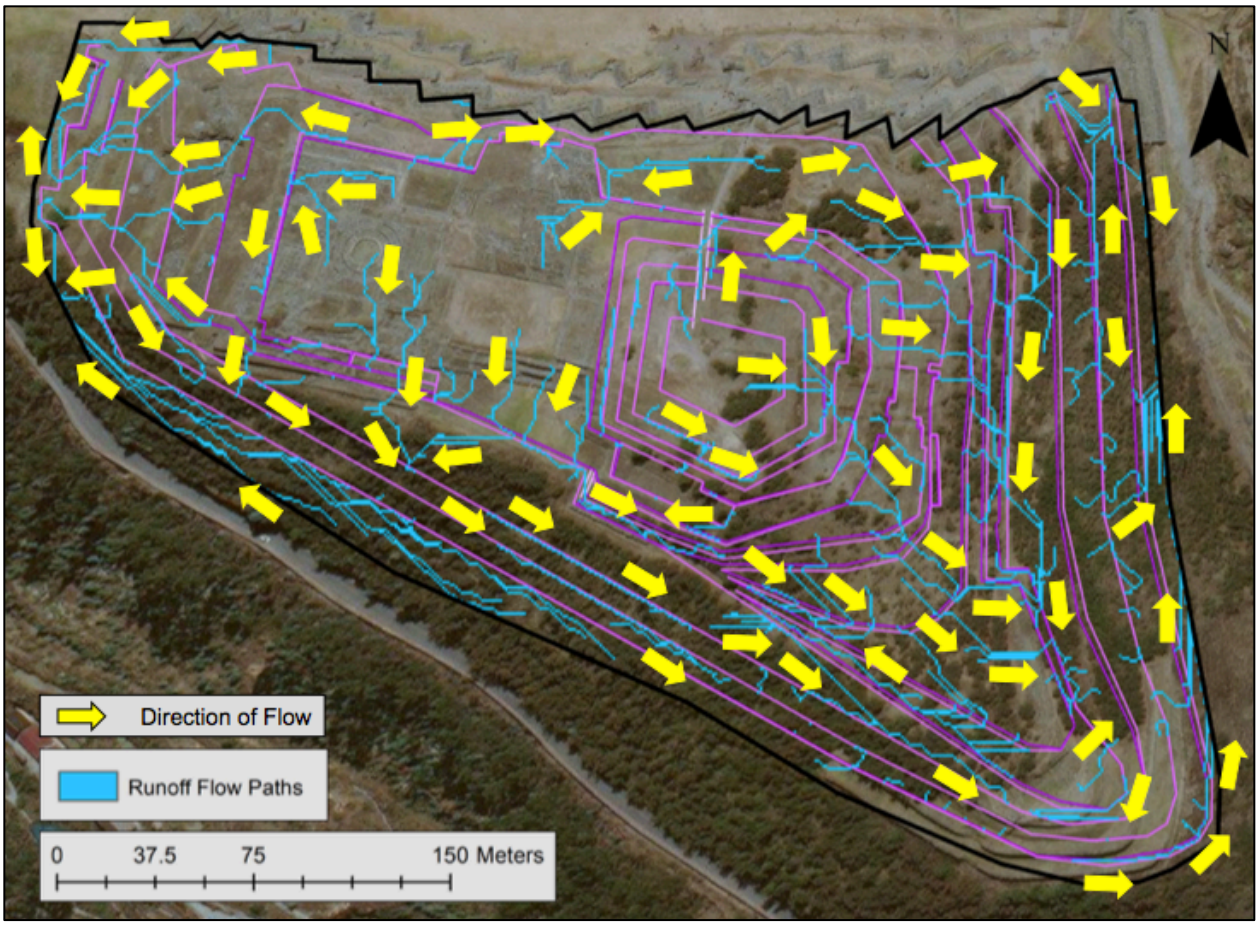

Figure 7.9: Contributing area map of the terraced site topography

Next, we found the volume of runoff that would flow over the site during the design storm event. The volume of runoff is dependent on the quantity of excess precipitation available as runoff in the area of each cell, so the excess precipitation was mapped onto raster maps of the current and terraced versions of the site. Figures 7.10 and 7.11 show the excess precipitation (from Tables 7.4 and 7.5, respectively) available as runoff at each 15-minute time step of the design storm.

These excess precipitation quantities are dependent on CN, which is dependent on the site land cover. Comparing Figures 7.10 and 7.11, we can see that the Inca-era land cover would have allowed less excess precipitation to be available in front of the Great Walls, whereas the

current land cover has the largest amount of excess precipitation directly in front of the Great Walls, due to the clay cover.

The runoff volumes resulting from the excess precipitation was determined using the flow accumulation tool with the excess precipitation maps added as weights to the flow accumulation. Adding the excess precipitation as weights resulted in maps that showed the same

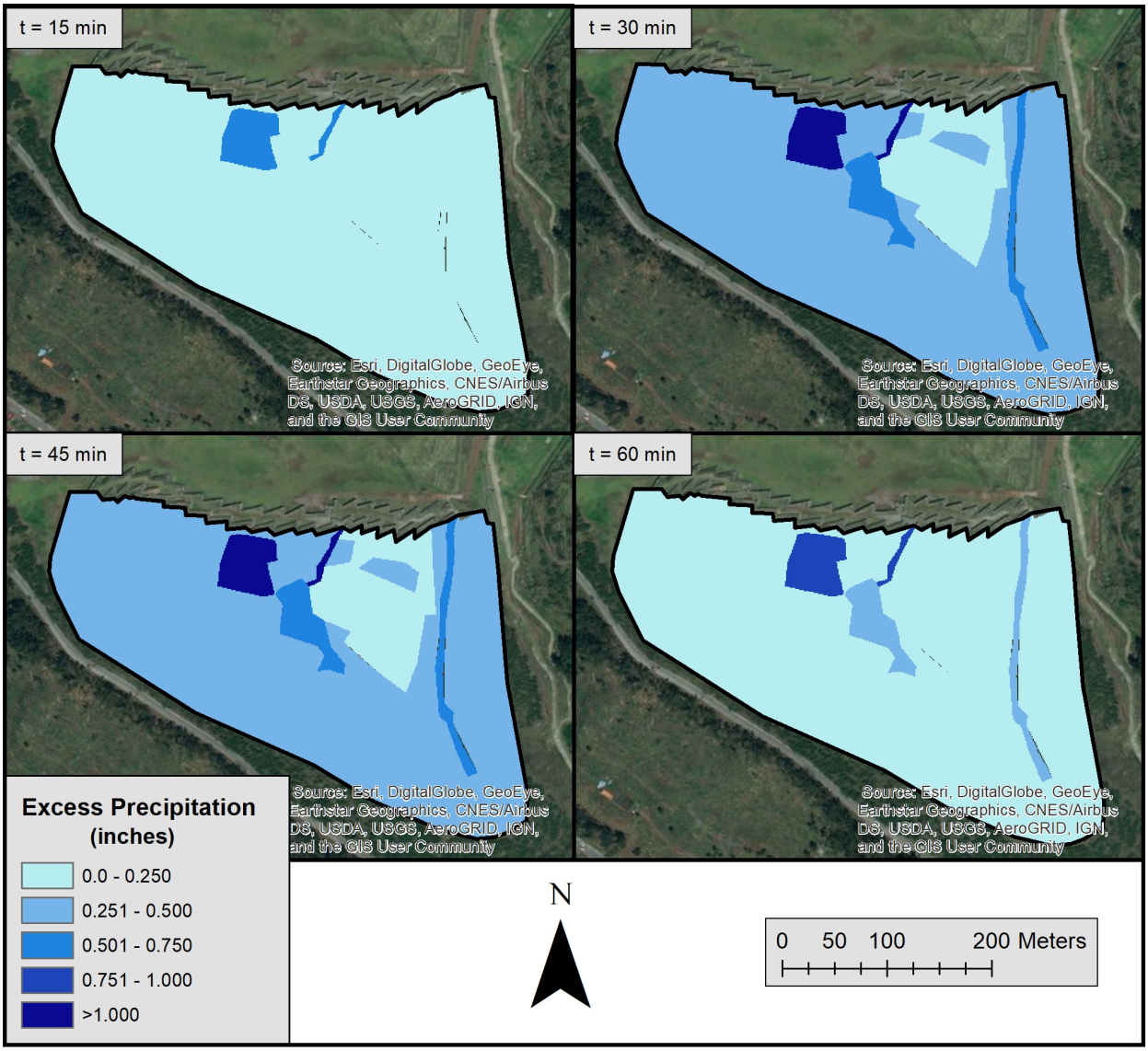

Figure 7.10: Excess precipitation available as runoff during each time step of the design storm for the current land cover

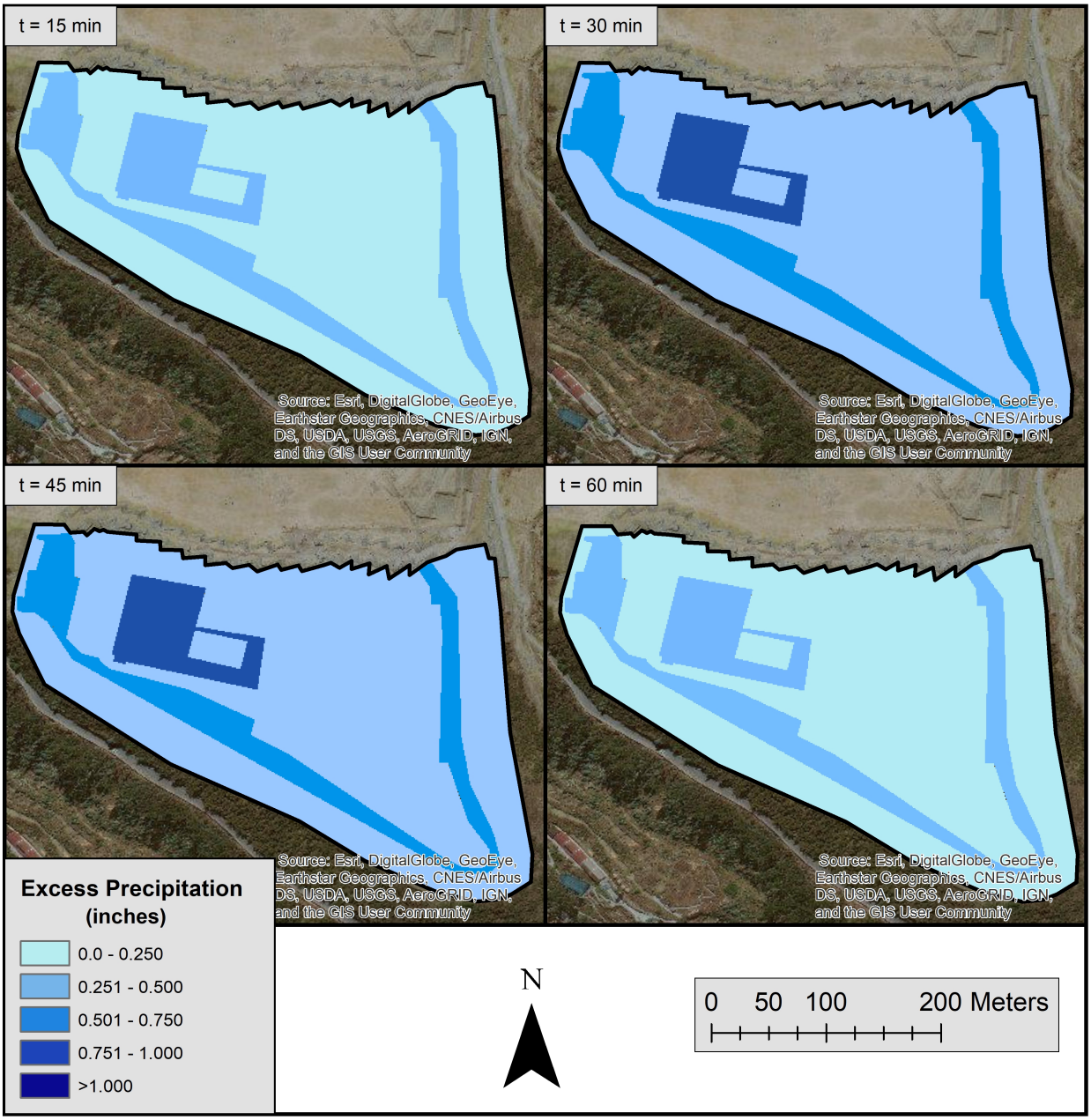

Figure 7.11: Excess precipitation available as runoff during each time step of the design storm for the Inca-era land cover

flow paths as in the contributing area maps, but also showed the quantity of water flowing through the flow paths. The output maps in Figures 7.12 and 7.13 show the flow paths containing flow rates of greater than 100 liters per minute.

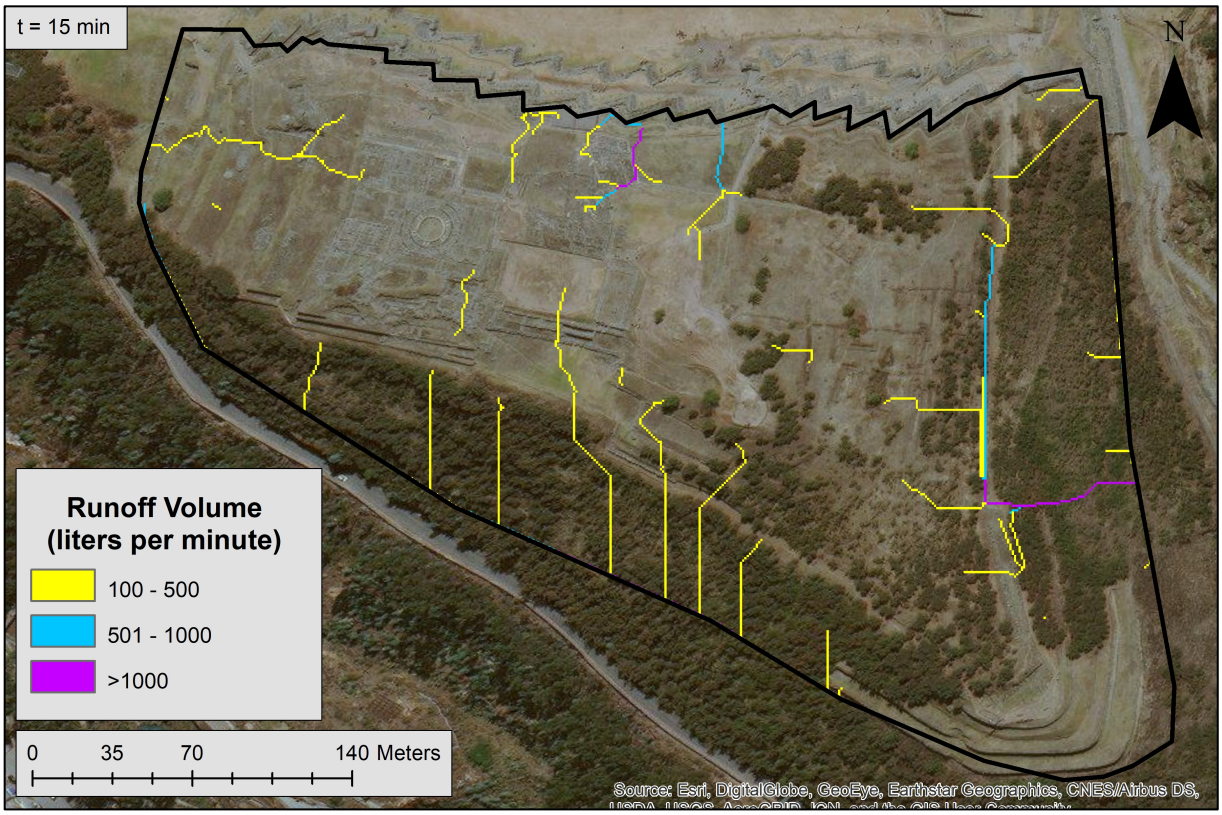

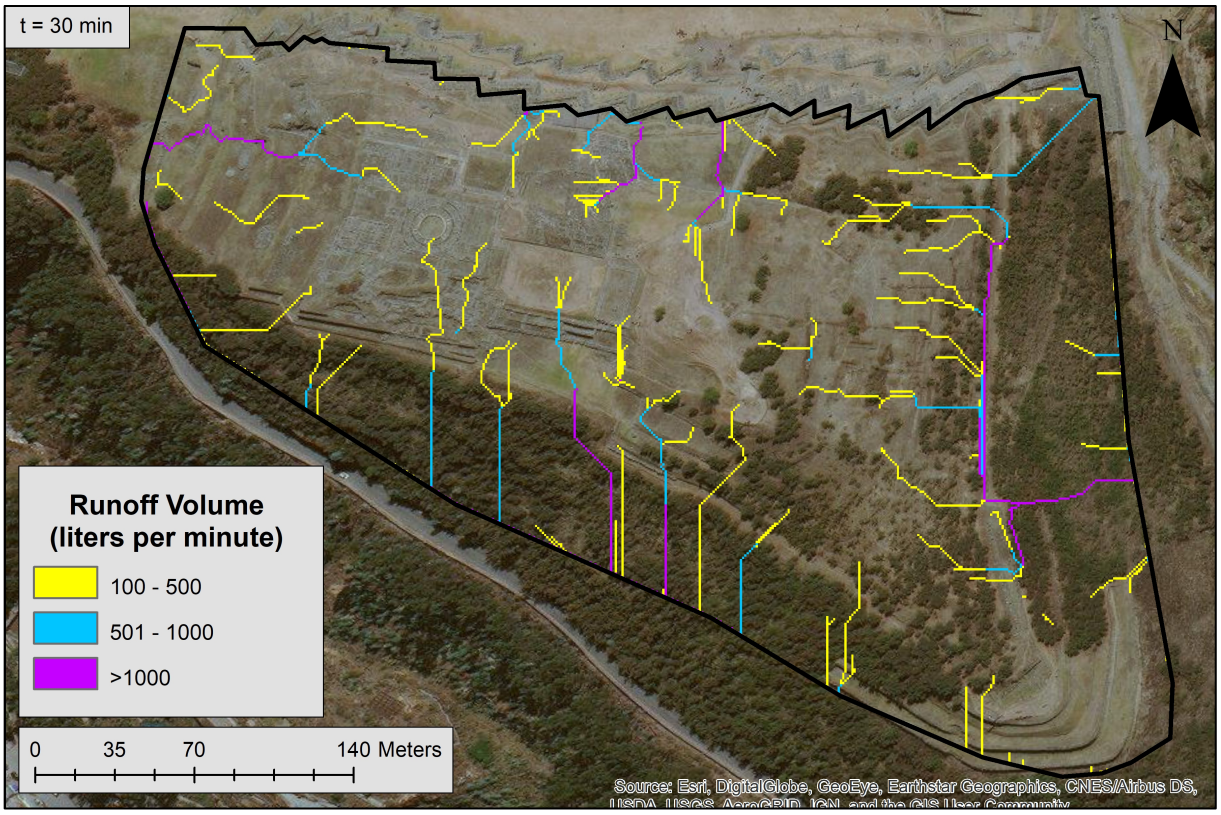

Figure 7.12 (continued on next page): Runoff flow rates during each step of the design storm for current land cover

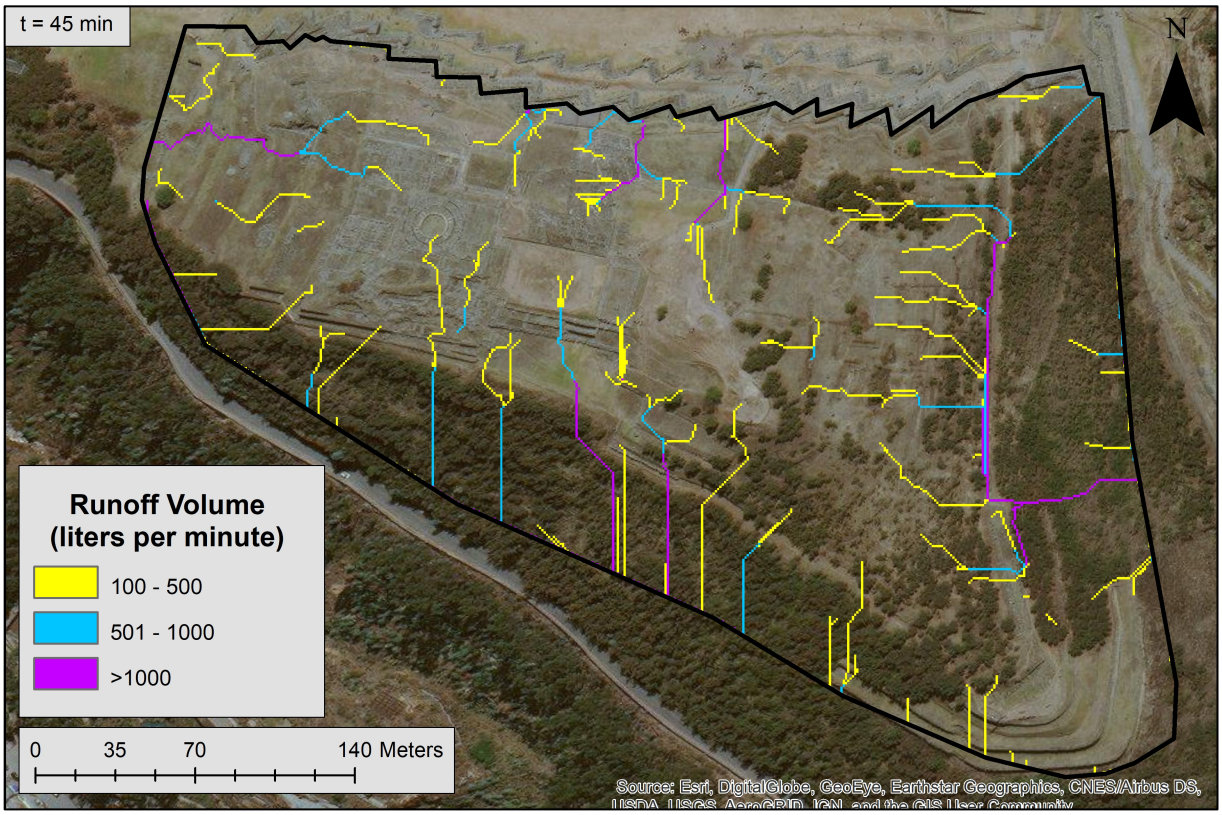

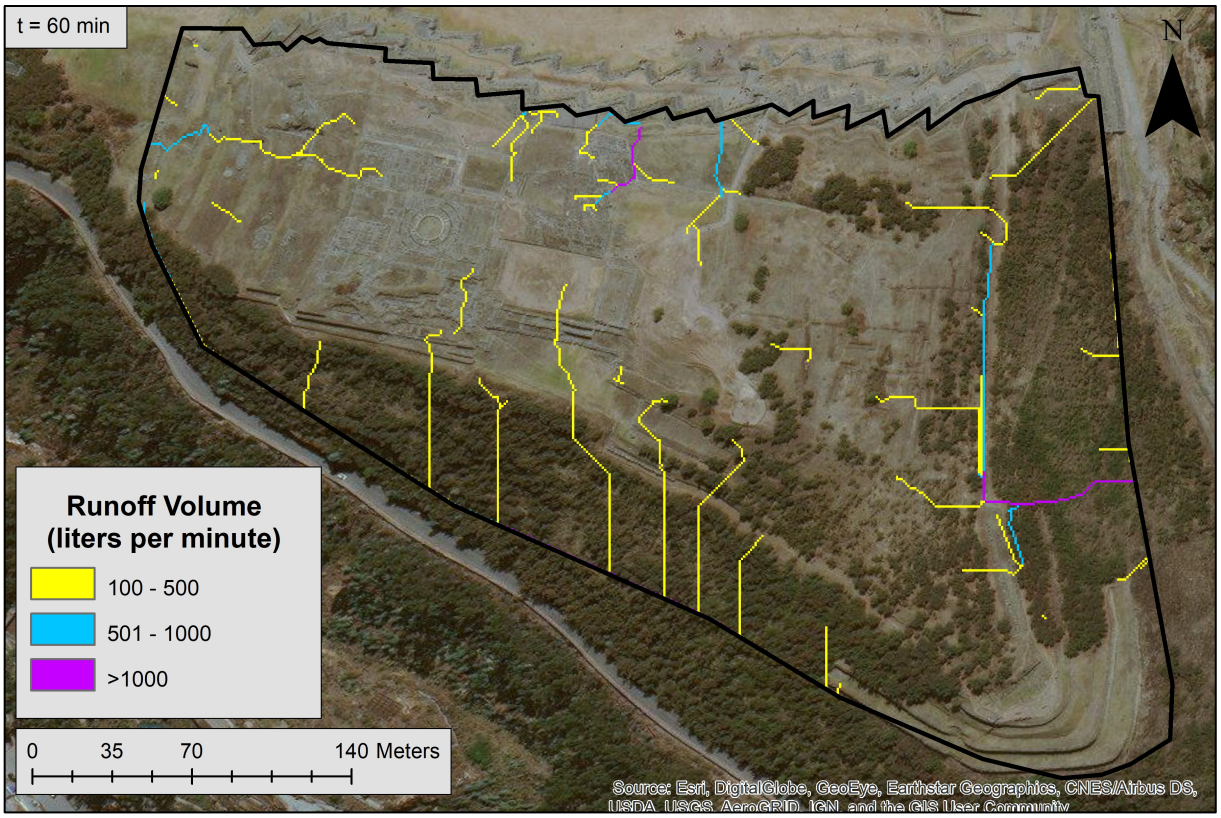

Figure 7.12 (continued from previous page): Runoff flow rates during each step of the design storm for current land cover

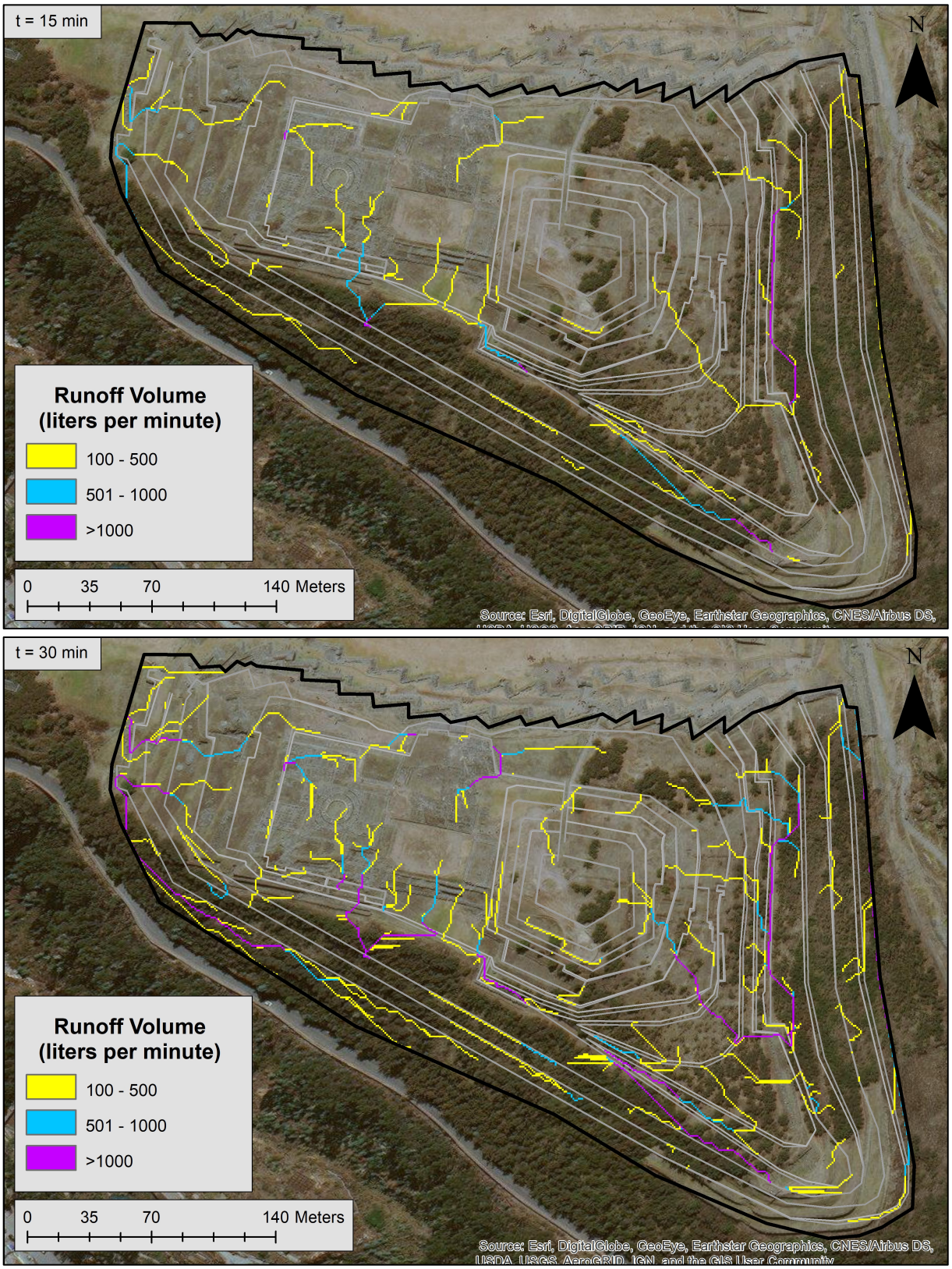

Figure 7.13 (continued on next page): Runoff flow rates during each step of the design storm for Inca-era land cover

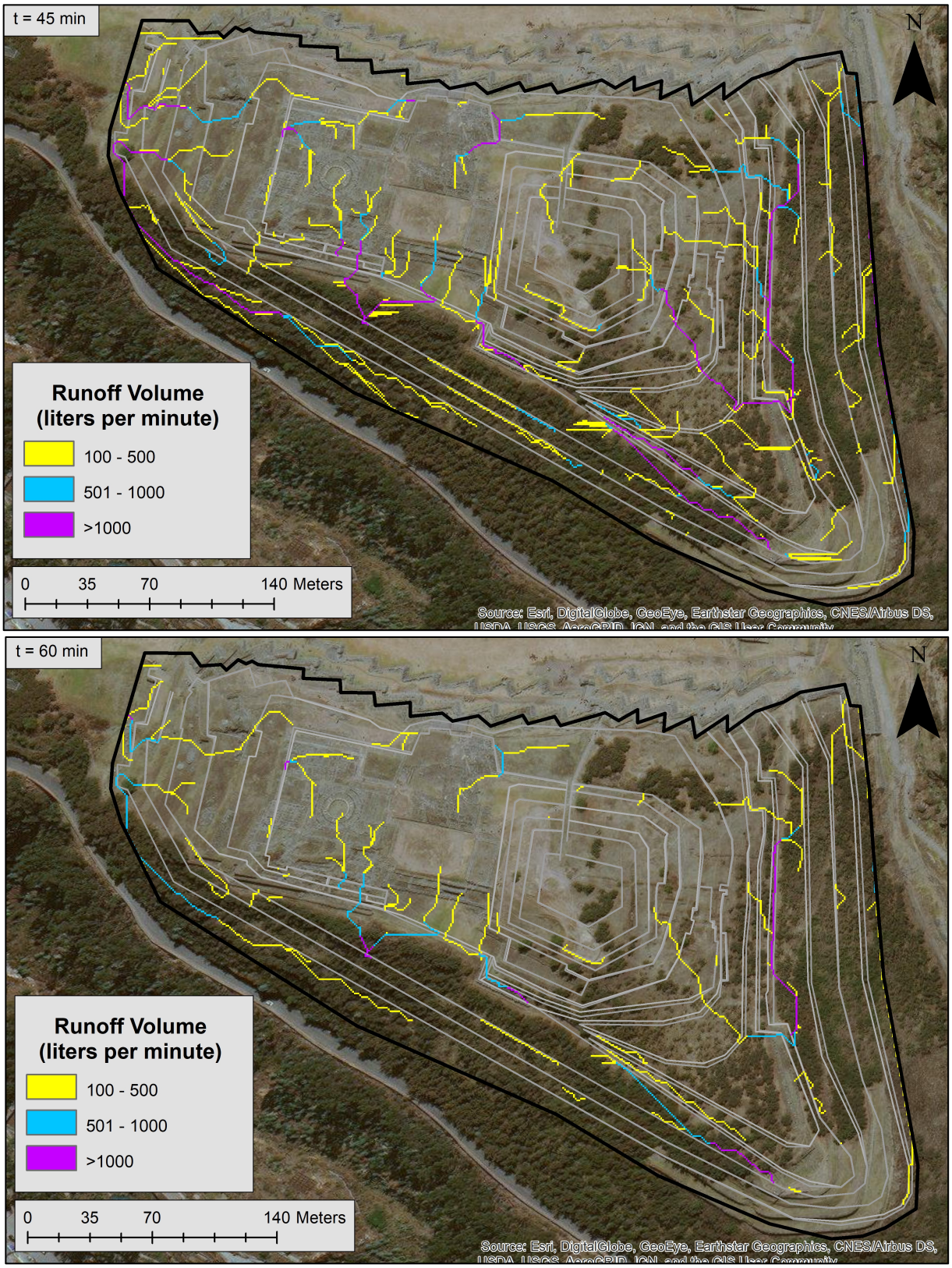

Figure 7.13 (continued from previous page): Runoff flow rates during each step of the design storm for Inca-era land cover

I hypothesized that adding terraces to the topography would protect the Great Walls and would control runoff across the site by redirecting water laterally along the tops of the terraces. This was achieved in some locations. On the current site's flow maps (Figures 7.8 and 7.12), there were multiple streamlines flowing directly into the Great Walls. On the terraced site's flow maps (Figures 7.9 and 7.13), there were almost no streamlines flowing into the walls, and the bulk of the water in that area was redirected to the east or west. On the south hill of the site, water went from flowing directly downhill to flowing along the terraces.

However, there were still several areas where water did not flow laterally along the terraces. In the next section, I will discuss how the proposed hydraulic drainage features would help mitigate this issue.

VII.D. Effect of Proposed Terrace System Drainage Methods on Runoff

I analyzed how the multi-layered draining backfill that was discussed in Section V.C.1 might affect the surface runoff flowing over the edges of terraces in Figures 7.9 and 7.13. This backfill would decrease the amount of excess precipitation on the surface of the site, which would in turn decrease the volume of runoff flowing over the site. It was determined that the backfill had a vertical drainage rate of about 0.425 inches per hour. At this drainage rate, about 51% of excess precipitation from the hundred-year design storm would be converted from surface water to subsurface water by the layered terrace backfill in the non-ceremonial terraces. The non-ceremonial terraces were considered to be all terraces covered in short grass, as was discussed in Section VII.B.1.

To show the runoff that would remain after the maximum amount of excess precipitation was absorbed by the backfill, first, the absorbed precipitation was mapped onto the non-

ceremonial terrace areas of the site in ArcGIS (Figure 7.14). For the drainage rate of 0.425 inches per hours, the absorbed precipitation was 0.106 inches per 15-minute time step of the design storm.

Then, the flow accumulation tool was used, with the map from Figure 7.14 added as a weight to flow accumulation, to show the volume and locations of runoff that would occur because of this absorbed excess precipitation. This absorbed precipitation flow map was then subtracted from the maps in Figure 7.13. The resulting maps (Figure 7.15) show the runoff that would remain after maximum drainage of excess precipitation through the layered backfill.

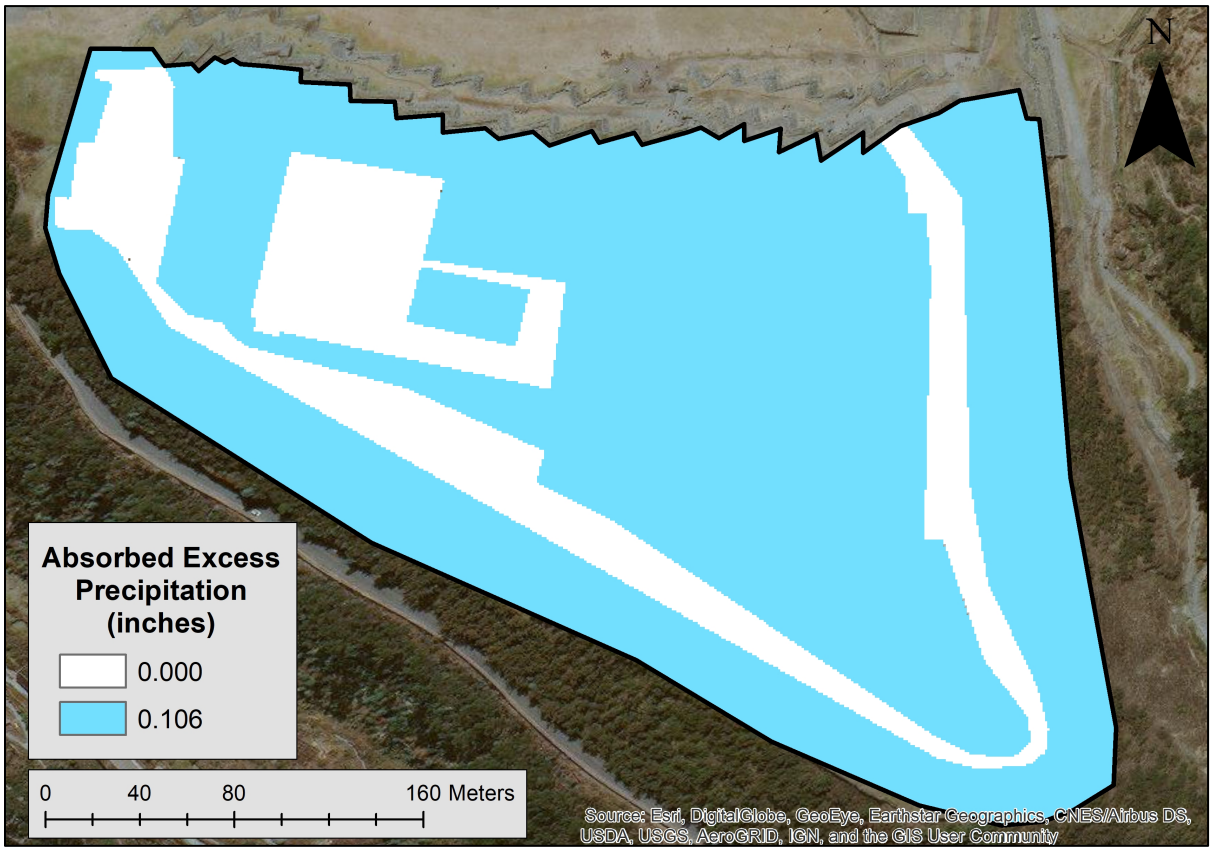

Figure 7.14: Excess precipitation absorbed by non-ceremonial terrace backfill

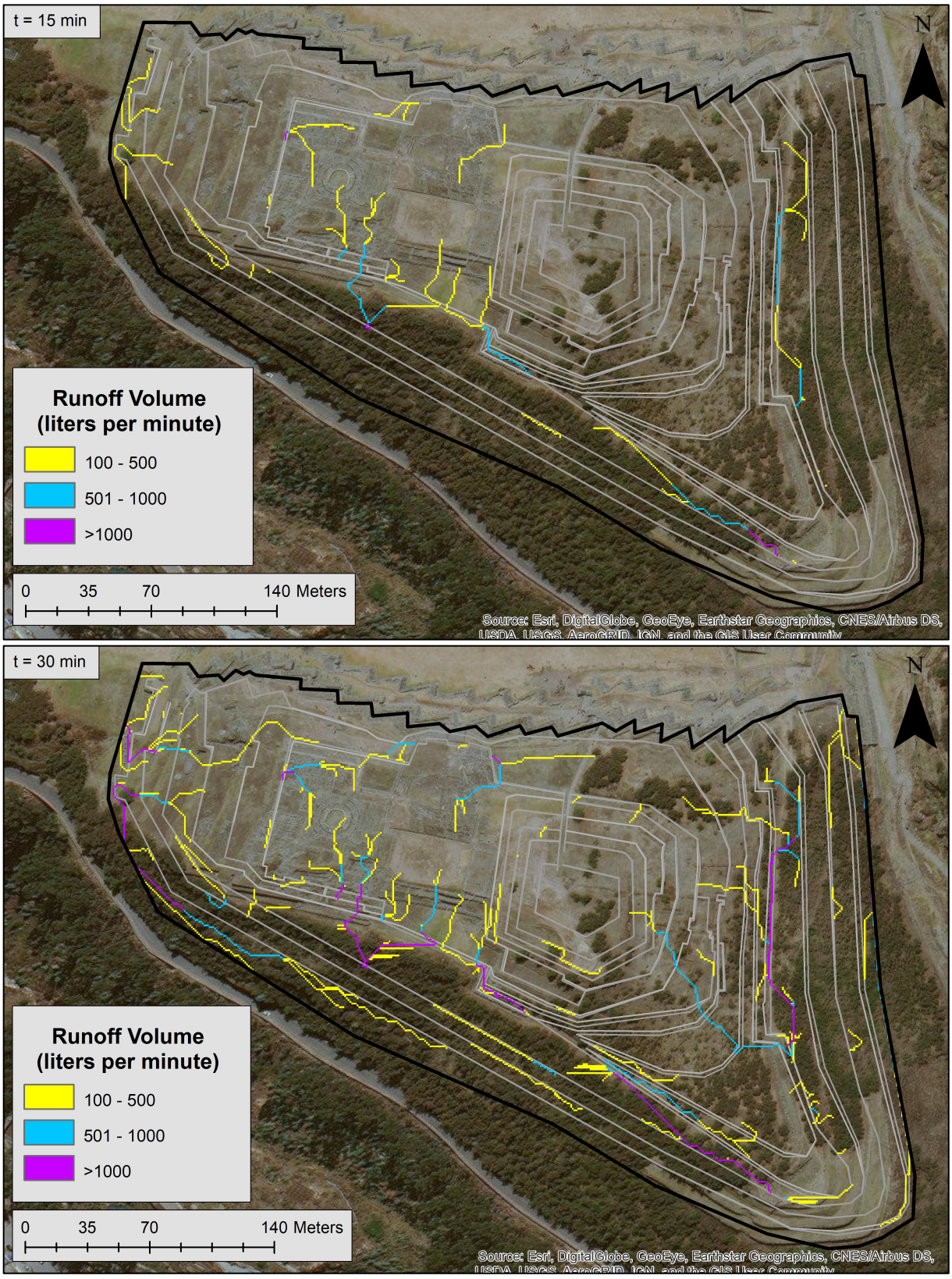

Figure 7.15 (continued on next page): Runoff flow rates during each step of the design storm after maximum drainage through terrace backfill

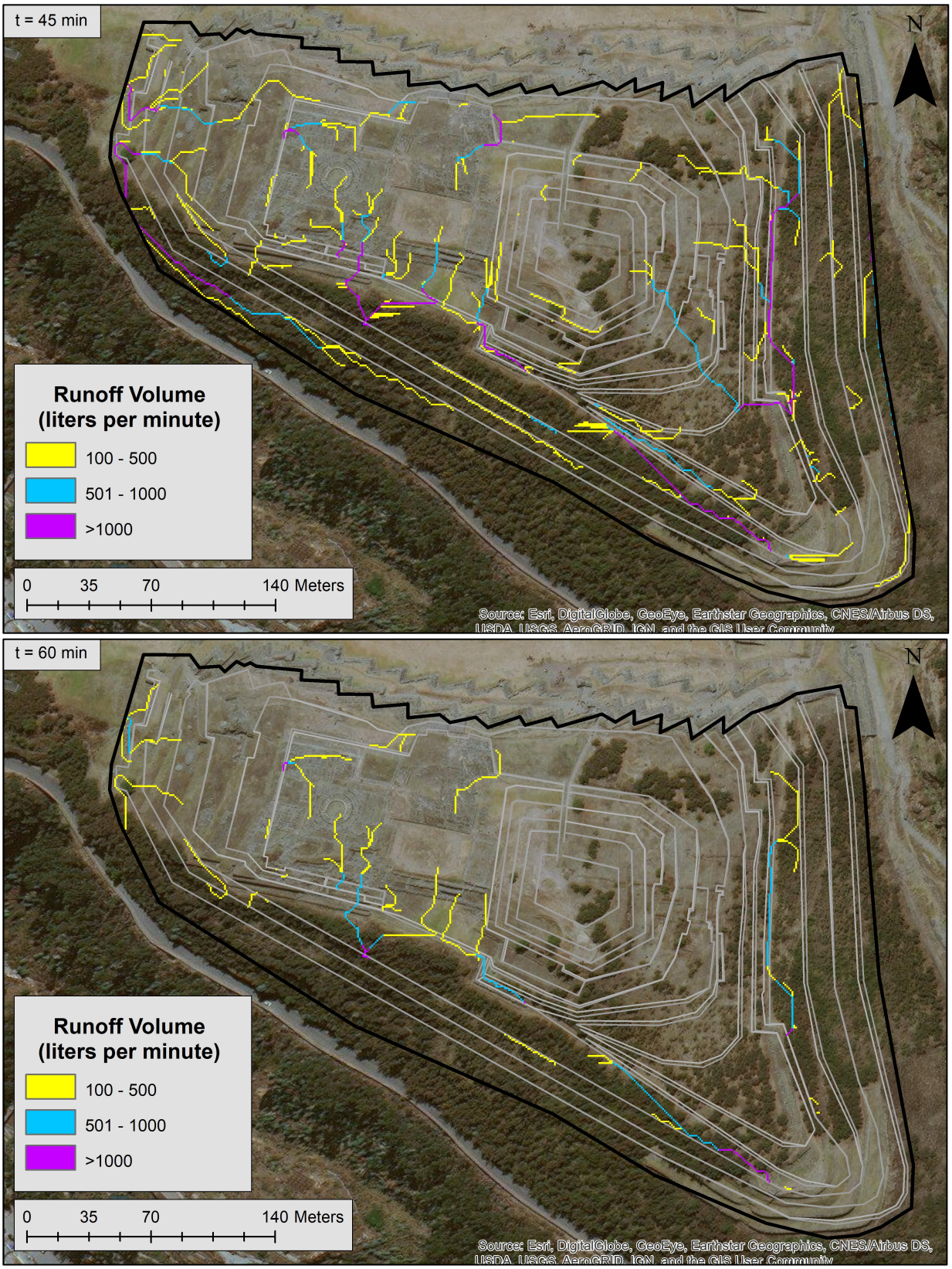

Figure 7.15 (continued from previous page): Runoff flow rates during each step of the design storm after maximum drainage through terrace backfill

Figure 7.15 showed that the volumes of flow were decreased compared to the flow volumes in Figure 7.13. However, there were still places where water was flowing over edges of the terraces rather than laterally along them, as was desired. In the next section, I will discuss how the proposed surface drainage system could have affected that issue.

VII.E. Effect of Proposed Surface Drainage System on Runoff

To model the effect the proposed surface drainage system would have on the runoff at Saqsaywaman, first, the surface drainage system channels were "burned" into the terraced topography in ArcGIS. This caused there to be a discrete, uniform elevation decrease in the topography in the locations of all of the channels. This elevation decrease did not represent the precise channel depths that were calculated in Section VI.B, but it imprints the channel locations so that they will be accounted when flow map calculations are done.

Next, a contributing area map (Figure 7.16) was created using the terraced topography with the imprinted channels. Figure 7.16 shows that the flow paths shifted after the addition of the drainage channels and much of the flow is now confined to the channels. This was the desired effect of the surface drainage system because it allowed stormwater to run off of the site in a controlled manner.

Next, the runoff flow rates during each step of the design storm were mapped onto the terraced topography with the imprinted channels. To do this, the methods from Sections VII.C and VII.D were carried out on this topography to show the cumulative affect all of the drainage features have had on runoff leading up to this point. To recreate those methods, first, the flow accumulation tool was used with the excess precipitation maps from Figure 7.11 added as weights. This created maps showing the runoff flow rates during each step of the design storm.

Next, the effect of the non-ceremonial terrace backfill was incorporated. This was done by subtracting the flow map of the absorbed excess precipitation from the maps of runoff flow rates from the previous step. The resulting maps (Figure 7.17) show the runoff flow rates after incorporating both the well-drained terrace system and the surface drainage system.

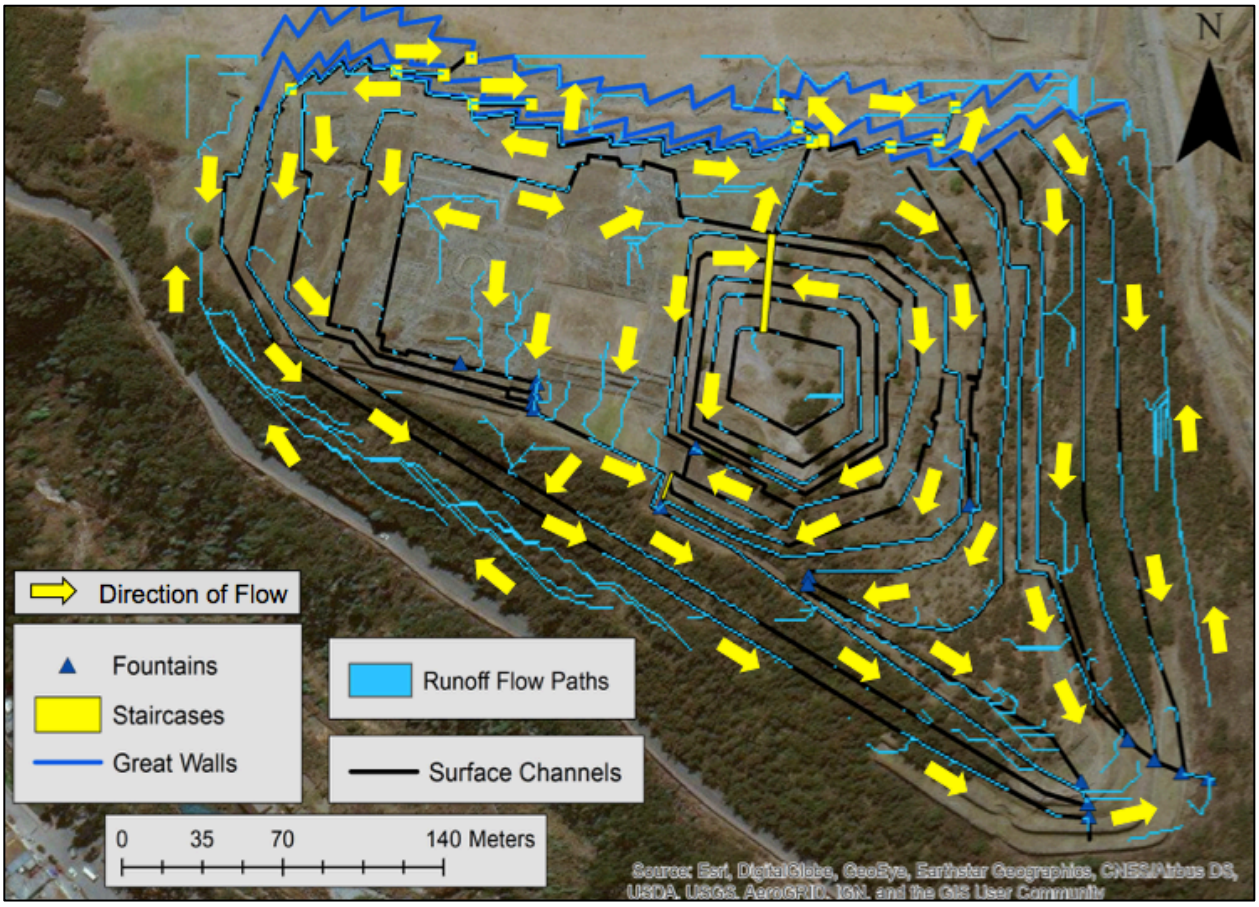

Figure 7.16: Contributing area map of the terraced site topography with the surface drainage system channels implemented

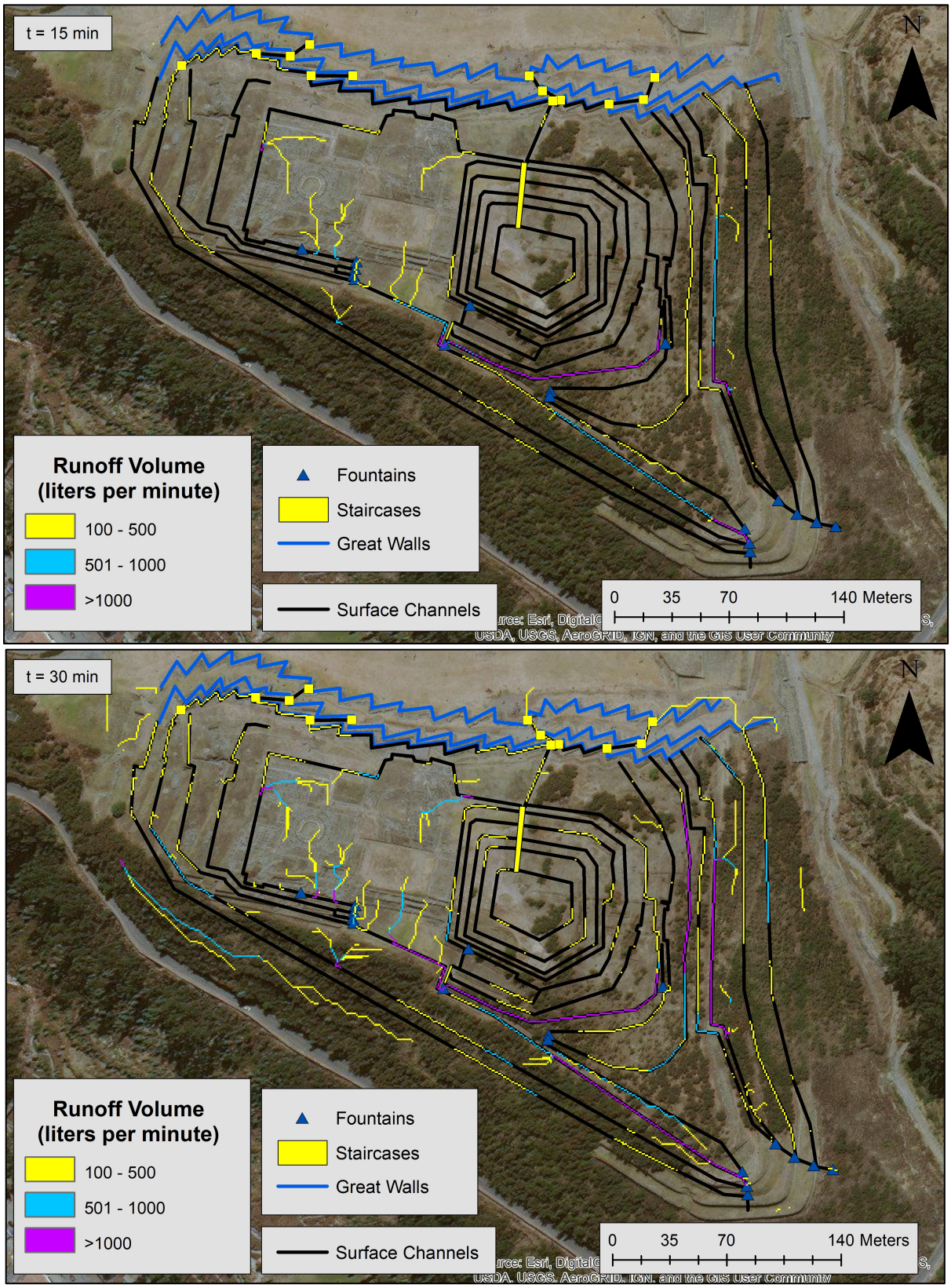

Figure 7.17 (continued on next page): Runoff flow rates during each step of the design storm after implementing the surface drainage system

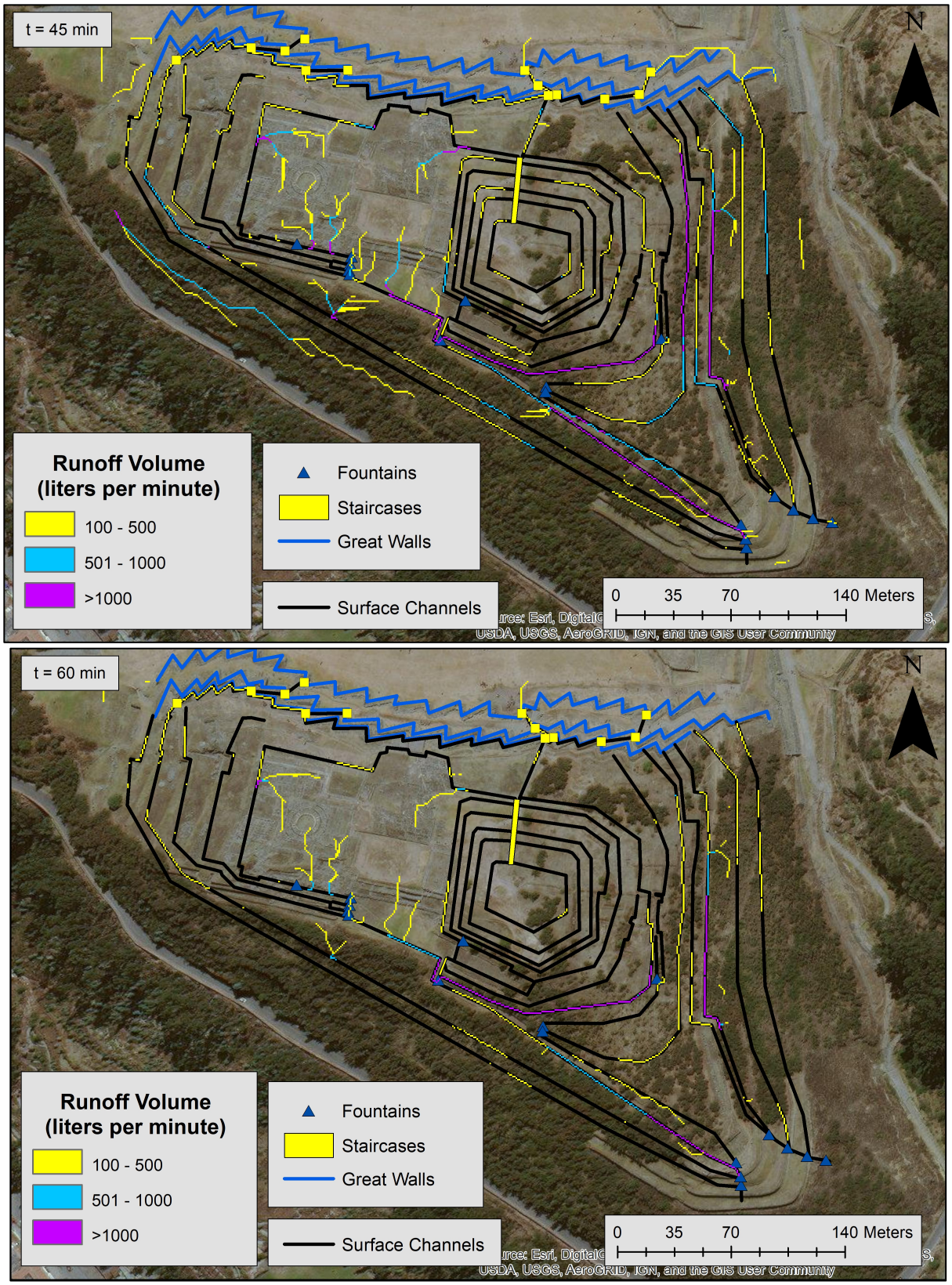

Figure 7.17 (continued from previous page): Runoff flow rates during each step of the design storm after implementing the surface drainage system

VII.F. Discussion of Runoff Analysis

Figures 7.8 and 7.12 show the runoff on the current site. Figures 7.16 and 7.17 show the runoff after the full restoration of the proposed Incan drainage infrastructure. With the implementation of the drainage infrastructure, runoff was not only directed away from the Great Walls and out of the site in a controlled manner, but the volume of surface runoff was also significantly decreased across the site.

In all of the contributing area maps and runoff flow maps, there were some locations where water was flowing in the opposite direction as was desired. On a smaller scale, this occurred in a few localized flow paths that flowed in the opposite directions than were designed. This was most likely due to limitations in the interpolation tool I used to digitally model the three-dimensional surface in ArcGIS. In my assumptions, I stated that the tops of the terraces would be smoothed planes, would slope laterally along the natural elevation decreases of the site, and would slope slightly inward orthogonally. The Spline with Barriers tool was not able to capture all of those stipulations in its interpolation method. It was able to smooth the terrain generally, but was unable to flatten out localized dips and mounds in the terrain, which contributed to the misdirection of some flow paths.

On a larger scale, the flow paths below some of the lowest terraces flowed in the opposite directions than the terraces were designed to flow. Particularly, in the southwest area of the site, water flowed downhill towards the west rather than towards the east as the terraces did. Also, on the lower east hill, water seemed to flow north rather than south as the terraces did. This occurred because there was a discrepancy between the designed terrace elevations and the elevation of the topography into which the terraces were "built". It is unclear whether this topographic difference was representative of the real life terrain or if it was due to limitations in

the interpolation method. It was more likely the latter possibility because we did not collect much topographic data below the lowest terraces on the site. Comparing the spread of topographic data points in Figure 4.1 and the interpolated three-dimensional surface model of the current site in Figures 5.13 and 5.14, we can see that the interpolated surface below the lower east hill terraces and the lower southwest terraces was not based on exact data points, but was instead based on the smoothing methods of the interpolation tool. Until more topographic survey data is collected in those areas, it is unclear how the lower terraces in my design align with the natural topographic contours.

The runoff flow volumes through the channels in Figure 7.17 differed from the flow rates that were used to calculate the channel dimensions in Section VI.B. The flow rates used in Section VI.B were based on an estimate from Tipon's channels, and were used to roughly determine what the channel dimensions might be. The runoff analysis provided flow rates that were closer to what the real life flow rates might be during a hundred-year storm. The channels with one input channel were calculated using the Tipon estimate of 0.0137 m^3/s. In Figure 7.17, the flow rates delineated in the channels were 100 L/min, 500 L/min, and 1000 L/min, which are equal to 0.0167 m^3/s, 0.0083 m^3/s, and 0.0017 m^3/s, respectively. So, for channels with less than 0.0137 m^3/s, or 822 L/min, of water flowing through them, the calculated dimensions from Section VI.B should be adequate to carry the necessary flow. For channels with larger than 822 L/min of flow, the channel dimensions might need to be recalculated to adjust for the larger than expected flow.

VIII. CONCLUSIONS

It was hypothesized that restoring the original Incan drainage infrastructure at Saqsaywaman is a potential way to control stormwater runoff in order to protect the site from further failure. Using field data, archeological evidence, and historical justification, I designed one possible drainage system that could have existed at Saqsaywaman during the Incan Empire. My proposed reconstruction of the drainage infrastructure consisted of two main parts: 1. A well-drained terrace system, and 2. A surface drainage system composed of channels and hydraulic drops.

From my analyses, I reached three main conclusions. First, I demonstrated that changing the land cover and adding a full-site terrace system to the topography could protect the Great Walls by redirecting runoff flow paths laterally to the east and west. Second, I found that implementing a multi-layered draining backfill in the non-ceremonial terraces would transfer 51% of the surface runoff to subsurface runoff for the hundred-year design storm. Third, I showed that a surface drainage system composed of channels and hydraulic drops would control most of the remaining 49% of surface runoff by confining the runoff flow paths to the surface channels and safely directing water out of the site.

To summarize, my proposed drainage system as a whole would protect the Great Walls by decreasing and redirecting the stormwater flowing towards the walls, and it would protect the rest of the site from water-induced damage by controlling and safely removing much of the runoff from the site.

IX. RECOMMENDATIONS

This thesis represents one of the first ever attempts at recreating the original Incan drainage system at Saqsaywaman in its entirety. This design was based on empirical evidence as much as was possible, but due to Saqsaywaman's age and history, there was not enough empirical evidence available from which to build a whole drainage system. For this reason, much of the design was based on assumptions and estimations. Following this study, I recommend that other engineers independently draw their own assumptions and make more attempts at recreating this ancient drainage infrastructure.

As was discussed in Section VII.F, my infrastructure designs and runoff analyses were completed using a computer program, which had some limitations. In order to verify the conclusions that I have drawn, I recommend that my analyses be recreated by other engineers who might go about the modeling process using different methods or using different computer modeling programs.

Further, I recommend that the archeological and historical assumptions I made be further verified by excavations and Andean historians. Although I have made every effort to research the archeological history of Saqsaywaman and synthesize it with my work where appropriate, I am not an archeologist and this thesis is first and foremost an engineering analysis.

Last, I recommend that if the INC chooses to move forward with a full-site restoration of Saqsaywaman using my proposed drainage infrastructure design or a design that is similar, that the restoration should be carried out in two distinct phases: 1. Rebuild terraces and terrace retaining walls into the topography of the site, with the subsurface draining backfill implemented and the land cover changed to the assumed Inca-era land cover, and 2. Implement the surface drainage system of channels and hydraulic drops. The first phase is the most important for

protecting the Great Walls, because I found that the majority of runoff in the area of the walls was decreased and redirected by the land cover change and the well-drained terrace system. It is also important that the phases are done in this order because the surface drainage system alone will not adequately control stormwater. The terraces are the foundation of the whole system, and the success of the surface drainage system is contingent on the terraces being implemented.

X. REFERENCES

Alfaro, C., Matos, R., Beltrán-Caballero, J. A., Mar, R. (2014). *El urbanismo Inka del Cusco: Nuevas aportaciones.* Cusco: La Biblioteca Nacional del Perú No. 2014-17503.

Alva, J., Ortiz, C., Soto, J., & Pérez, A. (2018). The use of non-destructive geophysical survey technology to locate the buried ruins of Saqsaywaman. Universidad Nacional de Ingeniería, Lima, Peru.

ASTM D5777-00(2011)el Standard Guide for Using the Seismic Refraction Method for Subsurface Investigation, ASTM International, West Conshohocken, PA, 2011, https://doi.org/10.1520/D5777-00R11E01.

Bauer, B. S. (2004). *Ancient Cuzco: Heartland of the Inca* (1st ed.). University of Texas Press.

Budhu, M. (2011). *Soil mechanics and foundations* (5th ed.). Hoboken, NJ: John Wiley & Sons, Inc.

Dean, C. J. (2010). *A culture of stone: Inka perspectives on rock.* Durham, NC: Duke University Press.

Dean, C. J. (2011). Inka water management and the symbolic dimensions of display fountains. *RES: Anthropology and Aesthetics.* 59/60: 22-38.

Dean, C. S. (1998). Creating a ruin in colonial Cusco: Sacsahuaman and what was made of it. *Andean Past, 5*(12).

de la Vega, G. (1966). *Royal commentaries of the Incas, and general history of Peru, part one.* (H. V. Livermore, Trans.). Austin, TX: University of Texas Press. (Original work published 1609)

Elger, D. F., Williams, B. C., Crowe, C. T., & Roberson, J. A. (2013). *Engineering Fluid Mechanics* (10th ed.). Hoboken, NJ: John Wiley & Sons, Inc.

Environmental Systems Research Institute, Inc. (ESRI). (n.d.) *ArcGIS 10.5.1 Tool Help.* Retrieved from http://desktop.arcgis.com/en/arcmap/

Gasparini, G., & Margolies, L. (1980). *Inca architecture* (P. J., Trans.). Bloomington, IN: Indiana University Press.

Google earth. (2014). Saqsaywaman, Peru. DigitalGlobe 2014. http://www.google.com/earth

Hyslop, J. (1990). *Inka settlement planning.* Austin, TX: University of Texas Press.

INC-Cusco (2007). Investigaciones arqueologicas del P. A. Saqsaywaman – sector Muyukmarka 2007.

Jarriel, T. (2016). Using 3D terrace modeling to preserve the Incan site of Saqsaywaman (Unpublished Masters of Science thesis). University of Virginia, Charlottesville, VA, United States.

Liberto, T. D. (2016). How can we call something a thousand-year storm if we don't have a thousand years of climate observations?. NOAA, Climate.gov. Retrieved from: https://www.climate.gov/news-features/event-tracker/how-can-we-call-something-thousand-year-storm-if-we-don%E2%80%99t-have-thousand

Lohr, K. (2014). Restoring and preserving the Incan cultural wonder of Saqsaywaman (Unpublished Masters of Science thesis). University of Virginia, Charlottesville, VA, United States.

MacQuarrie, K. (2007). *The last days of the Incas.* New York, NY: Simon & Schuster, Inc.

Mar, R., & Beltrán-Caballero, J. A. (2014). "*El Conjunto Arquelogogico de Saqsaywaman", (Cusco) Una Aproximcion a su Arquitectura,* Revista Espannola de Antropologia Americana.

Mavity, K., Nicholakos, H., & Schmitt, Z. (2017). Locating Inca terraces of Saqsaywaman, Peru to prevent hydrologic damage of ruins: Summer 2016 field survey analysis (Unpublished Bachelors of Science thesis). University of Virginia, Charlottesville, VA, United States.

Miksad, R. W. (Photographer). [Digital]

Mitas, L., & Mitasova, H. (1988). General variational approach to the interpolation problem. *Computers and Math with Applications, 16*(12), 983-992.

Morrisset, S. (2016). Conduits of power: Ritualized displays of water at the Inka site of Saksaywaman. (Unpublished Master in Philosophy dissertation). St. Johns College, Cambridge, England.

O'Neil, G. (2016). Locating Inca terraces at Saqsaywaman to restore the original drainage system and protect the Great Walls (Unpublished Masters of Science thesis). University of Virginia, Charlottesville, VA, United States.

Palma, J. A. R. (Photographer) (2013). [Digital].

Perry, L. B., Seimon, A., & Kelly, G. M. (2014). Precipitation delivery in the tropical high Andes of southern Peru: New findings and paleoclimatic implications. *International Journal of Climatology, 34,* 197-215.

Squier, E. G. (1877). *Peru: Incidents of travel and exploration in the land of the Incas.* New York: Harper & Brothers, Publishers.

Torp, J. (Designer). (2014). Drainage port runoff analysis.

United States Department of Agriculture (USDA). (1986). Urban hydrology for small watersheds. Technical Release 55 (TR-55) (Second ed.). Natural Resources Conservation Service, Conservation Engineering Division.

United States Department of Agriculture (USDA). (2007). Chapter 7: Hydrologic soil groups. Part 630 Hydrology National Engineering Handbook. Natural Resources Conservation Service, Conservation Engineering Division.

Valcarcel, L. E. (1934). Sajsaywaman redescubierto. *Revista del Museo Nacional.*

Wildfire, L., Miksad, R.W., Perez, A., Culotti, A., Beckman, E., Vranich, A., & Wright, K. R. (2011). A paleo-hydrologic analysis of rainfall-runoff and drainage of the incan ruins of Saqsaywaman, Cusco, Peru.

Wright, K. R., & Zegarra, A. V. (2000). *Machu Picchu: A civil engineering marvel.* United States of America: American Society of Civil Engineers.

Wright, K. R. (2006). *Tipon: Water engineering masterpiece of the Inca empire.* United States of America: American Society of Civil Engineers.

Wright, K. R., Oviedo, A. M. G., McEwan, G. F., Miksad, R. W., & Wright, R. M. (2016). *Incamisana: Engineering an Inca Water Temple.* United States of America: American Society of Civil Engineers.

XI. APPENDICES

XI.A. R Code Used to Create Transects in Mirador Area

```
#Creating Transects to Locate Potential Buried Terrace Remains

library(fields)
library(akima)
library("ggplot2")

#Step 1: Load N, E, Z data into R and plot 3D surface
H = read.table(file= "nesurf_ascii.txt", header=F, sep="", nrow=6)
Z = read.table(file = "nesurf_ascii.txt", header=F, sep="", skip=6)
Z1 = as.matrix(Z)

ncols = H[1,2] #number of columns in matrix Z1 = 126
nrows = H[2,2] #number of rows in matrix Z1 = 130
yllcorner = H[3,2] #easting of lower left corner = 177190.5
xllcorner = H[4,2] #northing of lower left corner = 8504525.8
cellsize = H[5,2] #cellsize = 1.0 square meter
Z3 = as.matrix(t(Z1))
Z4 = as.matrix(Z3[,ncol(Z3):1])
y = seq(xllcorner, xllcorner+129*cellsize, cellsize)
x = seq(yllcorner, yllcorner+125*cellsize, cellsize)

Zna = which(Z4 == -9999)
Z2 = replace(Z4, Z4 == -9999, NA)

image.plot(x, y, as.matrix(Z2), useRaster = T, asp = 1,
col=terrain.colors(100), xlab = "Easting (m)", ylab = "Northing (m)")
#original DEM
contour(x, y, Z2, add=T, col="peru")

#Step 2: Create transects that run north to south
transE1 = 177210
lt = which(abs(x - transE1) < 0.5)
if (length(lt) > 1) lt = lt[1]
transelevE1 = Z2[lt,]
plot(y, transelevE1, type = "l", xlab = "Northing (m)", ylab =
"Elevation (m)", main = "Vertical Transect 1")

transE2 = 177215
lt = which(abs(x - transE2) < 0.5)
if (length(lt) > 1) lt = lt[1]
transelevE2 = Z2[lt,]
plot(y, transelevE2, type = "l", xlab = "Northing (m)", ylab =
"Elevation (m)", main = "Vertical Transect 2")

transE3 = 177220
lt = which(abs(x - transE3) < 0.5)
if (length(lt) > 1) lt = lt[1]
transelevE3 = Z2[lt,]
plot(y, transelevE3, type = "l", xlab = "Northing (m)", ylab =
"Elevation (m)", main = "Vertical Transect 3")
```

```
transE4 = 177225
lt = which(abs(x - transE4) < 0.5)
if (length(lt) > 1) lt = lt[1]
transelevE4 = Z2[lt,]
plot(y, transelevE4, type = "l", xlab = "Northing (m)", ylab =
"Elevation (m)", main = "Vertical Transect 4")

transE5 = 177230
lt = which(abs(x - transE5) < 0.5)
if (length(lt) > 1) lt = lt[1]
transelevE5 = Z2[lt,]
plot(y, transelevE5, type = "l", xlab = "Northing (m)", ylab =
"Elevation (m)", main = "Vertical Transect 5")

transE6 = 177235
lt = which(abs(x - transE6) < 0.5)
if (length(lt) > 1) lt = lt[1]
transelevE6 = Z2[lt,]
plot(y, transelevE6, type = "l", xlab = "Northing (m)", ylab =
"Elevation (m)", main = "Vertical Transect 6")

transE7 = 177240
lt = which(abs(x - transE7) < 0.5)
if (length(lt) > 1) lt = lt[1]
transelevE7 = Z2[lt,]
plot(y, transelevE7, type = "l", xlab = "Northing (m)", ylab =
"Elevation (m)", main = "Vertical Transect 7")

#Step 3: Plot transect lines over contour map for reference
image.plot(x, y, as.matrix(Z2), useRaster = T, asp = 1,
col=terrain.colors(100), xlab = "Easting (m)", ylab = "Northing (m)")
#original DEM
contour(x, y, Z2, add=T, col="peru")
xline(transE1, col = "blue")
xline(transE2, col = "blue")
xline(transE3, col = "blue")
xline(transE4, col = "blue")
xline(transE5, col = "blue")
xline(transE6, col = "blue")
xline(transE7, col = "blue")
```

XI.B. R Code Used to Calculate Storm Statistics

```
#Saqsaywaman Storm Statistics

library(readxl)
Historic_Rainfall_in_Pisac_Cusco_Numbers <-
read_excel("~/Documents/Historic Rainfall in Pisac-Cusco Numbers.xlsx")
P = Historic_Rainfall_in_Pisac_Cusco_Numbers

precip = P[,2]
bins = seq(0, 140, 5)
avg = mean(precip)

h5 = hist(precip, breaks = bins, freq = F, include.lowest = T, xlab =
"Precipitation (mm/hour)", main = "Histogram of Precipitation")
sd5 = sd(precip)
g5 = dnorm(bins, avg, sd5)
lines(bins, g5, col="red")

p = qnorm(.99, avg, sd5) #calculates hundred-year storm
p = qnorm(.50, avg, sd5) #calculates average storm
```

XI.C. NRCS Runoff Curve Number Reference Tables

Table 11.1a: Runoff curve numbers for urban areas (USDA, 1986)

Cover description: Cover type and hydrologic condition	Average percent impervious area [2]	Curve numbers for hydrologic soil group: A	B	C	D
Fully developed urban areas (vegetation established)					
Open space (lawns, parks, golf courses, cemeteries, etc.) [3]:					
Poor condition (grass cover < 50%)		68	79	86	89
Fair condition (grass cover 50% to 75%)		49	69	79	84
Good condition (grass cover > 75%)		39	61	74	80
Impervious areas:					
Paved parking lots, roofs, driveways, etc. (excluding right-of-way)		98	98	98	98
Streets and roads:					
Paved; curbs and storm sewers (excluding right-of-way)		98	98	98	98
Paved; open ditches (including right-of-way)		83	89	92	93
Gravel (including right-of-way)		76	85	89	91
Dirt (including right-of-way)		72	82	87	89
Western desert urban areas:					
Natural desert landscaping (pervious areas only) [4]		63	77	85	88
Artificial desert landscaping (impervious weed barrier, desert shrub with 1- to 2-inch sand or gravel mulch and basin borders)		96	96	96	96
Urban districts:					
Commercial and business	85	89	92	94	95
Industrial	72	81	88	91	93
Residential districts by average lot size:					
1/8 acre or less (town houses)	65	77	85	90	92
1/4 acre	38	61	75	83	87
1/3 acre	30	57	72	81	86
1/2 acre	25	54	70	80	85
1 acre	20	51	68	79	84
2 acres	12	46	65	77	82
Developing urban areas					
Newly graded areas (pervious areas only, no vegetation) [5]		77	86	91	94
Idle lands (CN's are determined using cover types similar to those in table 2-2c).					

[1] Average runoff condition, and $I_a = 0.2S$.

[2] The average percent impervious area shown was used to develop the composite CN's. Other assumptions are as follows: impervious areas are directly connected to the drainage system, impervious areas have a CN of 98, and pervious areas are considered equivalent to open space in good hydrologic condition. CN's for other combinations of conditions may be computed using figure 2-3 or 2-4.

[3] CN's shown are equivalent to those of pasture. Composite CN's may be computed for other combinations of open space cover type.

[4] Composite CN's for natural desert landscaping should be computed using figures 2-3 or 2-4 based on the impervious area percentage (CN = 98) and the pervious area CN. The pervious area CN's are assumed equivalent to desert shrub in poor hydrologic condition.

[5] Composite CN's to use for the design of temporary measures during grading and construction should be computed using figure 2-3 or 2-4 based on the degree of development (impervious area percentage) and the CN's for the newly graded pervious areas.

Table 11.1b: Runoff curve numbers for cultivated agricultural lands (USDA, 1986)

Cover description			Curve numbers for hydrologic soil group			
Cover type	Treatment [2]	Hydrologic condition [3]	A	B	C	D
Fallow	Bare soil	—	77	86	91	94
	Crop residue cover (CR)	Poor	76	85	90	93
		Good	74	83	88	90
Row crops	Straight row (SR)	Poor	72	81	88	91
		Good	67	78	85	89
	SR + CR	Poor	71	80	87	90
		Good	64	75	82	85
	Contoured (C)	Poor	70	79	84	88
		Good	65	75	82	86
	C + CR	Poor	69	78	83	87
		Good	64	74	81	85
	Contoured & terraced (C&T)	Poor	66	74	80	82
		Good	62	71	78	81
	C&T+ CR	Poor	65	73	79	81
		Good	61	70	77	80
Small grain	SR	Poor	65	76	84	88
		Good	63	75	83	87
	SR + CR	Poor	64	75	83	86
		Good	60	72	80	84
	C	Poor	63	74	82	85
		Good	61	73	81	84
	C + CR	Poor	62	73	81	84
		Good	60	72	80	83
	C&T	Poor	61	72	79	82
		Good	59	70	78	81
	C&T+ CR	Poor	60	71	78	81
		Good	58	69	77	80
Close-seeded or broadcast legumes or rotation meadow	SR	Poor	66	77	85	89
		Good	58	72	81	85
	C	Poor	64	75	83	85
		Good	55	69	78	83
	C&T	Poor	63	73	80	83
		Good	51	67	76	80

[1] Average runoff condition, and I_a=0.2S

[2] Crop residue cover applies only if residue is on at least 5% of the surface throughout the year.

[3] Hydraulic condition is based on combination factors that affect infiltration and runoff, including (a) density and canopy of vegetative areas, (b) amount of year-round cover, (c) amount of grass or close-seeded legumes, (d) percent of residue cover on the land surface (good ≥ 20%), and (e) degree of surface roughness.

Poor: Factors impair infiltration and tend to increase runoff.

Good: Factors encourage average and better than average infiltration and tend to decrease runoff.

Table 11.1c: Runoff curve numbers for other agricultural lands (USDA, 1986)

Cover description		Curve numbers for hydrologic soil group			
Cover type	Hydrologic condition	A	B	C	D
Pasture, grassland, or range—continuous forage for grazing. [2]	Poor	68	79	86	89
	Fair	49	69	79	84
	Good	39	61	74	80
Meadow—continuous grass, protected from grazing and generally mowed for hay.	—	30	58	71	78
Brush—brush-weed-grass mixture with brush the major element. [3]	Poor	48	67	77	83
	Fair	35	56	70	77
	Good	30 [4]	48	65	73
Woods—grass combination (orchard or tree farm). [5]	Poor	57	73	82	86
	Fair	43	65	76	82
	Good	32	58	72	79
Woods. [6]	Poor	45	66	77	83
	Fair	36	60	73	79
	Good	30 [4]	55	70	77
Farmsteads—buildings, lanes, driveways, and surrounding lots.	—	59	74	82	86

1 Average runoff condition, and $I_a = 0.2S$.

2 ***Poor:*** <50%) ground cover or heavily grazed with no mulch.
Fair: 50 to 75% ground cover and not heavily grazed.
Good: > 75% ground cover and lightly or only occasionally grazed.

3 ***Poor:*** <50% ground cover.
Fair: 50 to 75% ground cover.
Good: >75% ground cover.

4 Actual curve number is less than 30; use CN = 30 for runoff computations.

5 CN's shown were computed for areas with 50% woods and 50% grass (pasture) cover. Other combinations of conditions may be computed from the CN's for woods and pasture.

6 ***Poor:*** Forest litter, small trees, and brush are destroyed by heavy grazing or regular burning.
Fair: Woods are grazed but not burned, and some forest litter covers the soil.
Good: Woods are protected from grazing, and litter and brush adequately cover the soil.